SYNTHESIS AND CHARACTERIZATION OF POLYSTYRENE CLAY NANOCOMPOSITES

A THESIS SUBMITTED TO
THE GRADUATE SCHOOL OF NATURAL AND APPLIED SCIENCES
OF
MIDDLE EAST TECHNICAL UNIVERSITY

BY

GÜLSÜM ÖZDEN

IN PARTIAL FULFILLMENT OF THE REQUIREMENTS
FOR
THE DEGREE OF MASTER OF SCIENCE
IN
CHEMICAL ENGINEERING

JULY 2004

Approval of Graduate School of Natural and Applied Sciences

_____

Prof. Dr. Canan Özgen
Director

I certify that this thesis satisfies all the requirements as a thesis for degree of Master of Science.

_____

Prof. Dr. Timur Doğu
Head of the Department

This is to certify that we have read this thesis and that in our opinion it is fully adequate, in scope and quality, as a thesis for the degree of Master of Science.

_____

Prof. Dr. Ülkü Yılmazer
Supervisor

Examining Committee Members

Prof. Dr. Güngör Gündüz	(METU,CHE)	_____
Prof. Dr. Ülkü Yılmazer	(METU,CHE)	_____
Prof. Dr. Teoman Tinçer	(METU,CHEM)	_____
Prof. Dr. Zuhal Küçükyavuz	(METU,CHEM)	_____
Assoc. Prof. Dr. Göknur Bayram	(METU,CHE)	_____

I hereby declare that all information in this document has been obtained and presented in accordance with academic rules and ethical conduct. I also declare that, as required by these rules and conduct, I have fully cited and referenced all material and results that are not original to this work.

Name, Lastname : Gülsüm Özden

Signature :

ABSTRACT

SYNTHESIS AND CHARACTERIZATION OF POLYSTYRENE CLAY NANOCOMPOSITES

Özden, Gülsüm

M.S., Department of Chemical Engineering

Supervisor: Prof. Dr. Ülkü YILMAZER

July 2004, 102 pages

This study was undertaken to prepare polystyrene (PS)/montmorillonite (MMT) nanocomposites by different methods, including melt intercalation, in-situ polymerization and masterbatch methods. The in-situ polymerization method consisted of dispersing the styrene monomer into the galleries of MMT followed by subsequent polymerization. The PS/MMT nanocomposites formed by melt intercalation method were prepared on a twin-screw extruder. The masterbatch method was in fact a two-step process. As the first step, a high clay content composite of polystyrene (masterbatch) was prepared by in-situ polymerization, and then the prepared masterbatch was diluted to desired compositions with commercial polystyrene in a twin-screw extruder.

The structural, thermal and mechanical properties of the nanocomposites were examined. X-Ray diffraction (XRD) analysis showed that the d-spacing of the in-situ formed nanocomposites containing 0.73 and 1.6 wt. % organoclay increased from 32.9 Å to 36.3 and 36.8 Å respectively, indicating intercalation while the d-spacing of the other prepared materials remained nearly unchanged compared to pure organoclay. At low clay content, (<1 wt. %), in-situ formed nanocomposites showed the best improvement in mechanical properties including tensile, flexural, impact strength and Young's modulus. In all the three methods, the addition of organoclay increased the Young's modulus compared to neat resin, but the maximum

improvement was 88.5 %, obtained at 0.73 wt. % organoclay in the in-situ formed material. In-situ polymerization method did not prove to be efficient at high clay loadings in terms of mechanical properties.

At high clay loadings, the effects of the three methods on promoting mechanical properties were not significantly different from each other. The glass transition temperature increased from 105.5 $^{\circ}$C in the pure polystyrene to 108.4 $^{\circ}$C in the in-situ formed nanocomposite at 0.73 wt % organoclay due to the restricted mobility of the polymer chains within the organoclay layers.

ÖZ

POLİSTİREN KİL NANOKOMPOZİTLERİNİN SENTEZ VE ÖZELLİKLERİNİN BELİRLENMESİ

Özden, Gülsüm

Yüksek Lisans, Kimya Mühendisliği

Tez Yöneticisi: Prof. Dr. Ülkü Yılmazer

Temmuz 2004, 102 sayfa

Bu çalışma, polistiren (PS)/montmorillonit (MMT) nanokompozitlerini, eriyik halde karıştırma, yerinde polimerleştirme ve yoğun bileşimli karışım kullanma yöntemlerinden oluşan üç farklı yöntemle elde etmek amacıyla yürütülmüştür. Yerinde polimerleştirme yöntemi, stiren monomerinin kil tabakaları arasında dağıtıldıktan sonra polimerleştirilmesini içermektedir. Eriyik halde karıştırma yönteminde ise nanokompozitler, aynı yönde dönen çift vidalı ekstruderde hazırlanmıştır. Yoğun bileşimli karışım kullanma yöntemi esas olarak iki basamaktan oluşmaktadır. İlk olarak yerinde polimerleştirme yöntemi ile yüksek kil içerikli polistiren karışımı hazırlanmıştır. Daha sonra, hazırlanan karışım ticari polistirenle çift vidalı ekstruderde istenilen yüzdelere seyreltilmiştir.

Nanokompozitlerin yapısal, ısıl ve mekanik özellikleri incelenmiştir. X-ışını kırınımı analizi sonuçları, yerinde polimerleştirme yöntemiyle hazırlanmış, ağırlıkça % 0.73 ve % 1.6 oranında modifiye edilmiş kil içeren nanokompozitlerin bazal boşluklarının, sırasıyla 32.9 Å' dan 36.3 ve 36.8 Å' a genişlediğini diğer malzemelerde ise saf kile kıyasla sabit kaldığını göstermiştir. Düşük kil içeriğinde (< %1), yerinde polimerleştirme ile hazırlanan nanokompozitlerde çekme, esneme, darbe dayanımı ve Young modülü gibi mekanik özelliklerde saf polimere kıyasla en iyi gelişme gözlemlenmiştir. Üç yöntemde de, kilin eklenmesi Young modülünü saf polistirene göre arttırmıştır, fakat en çok artış (% 88.5) yerinde polimerleştirme ile

sentezlenmiş, ağırlıkça % 0.73 kil içeren malzemede gözlenmiştir. Yerinde polimerleştirme yöntemi mekanik özellikler açısından, yüksek kil içeriğinde verimli olmamıştır.

Yüksek kil oranlarında, üç yöntemin mekanik özellikleri geliştirmedeki etkisi belirgin olarak birbirinden farklı olmamıştır. Saf polistirenin camsı geçiş sıcaklığı, yerinde polimerleştirme ile hazırlanmış ağırlıkça % 0.73 kil içeren nanokompozitte, polimer zincirlerinin kil tabakaları arasında kısıtlanan hareketine bağlı olarak $105.5^{o}C$' tan $108.4^{o}C$' a yükselmiştir.

Anahtar Sözcükler: polistiren, montmorillonit, yoğun bileşimli karışım, nanokompozit

Dedicated to my family…

ACKNOWLEDGEMENTS

TABLE OF CONTENTS

LIST OF TABLES

TABLE

xv

LIST OF FIGURES

CHAPTER I

INTRODUCTION

The history of composite materials dates back to early times but only in the 1950's did these materials gain an accelerated reputation with the introduction of polymer based composites. Composites are the combinations of two or more materials in which a reinforcing material is embedded in a matrix material in a controlled manner to obtain a material with improved properties.

Today most of the composites are polymer based owing to the versatile properties offered by polymeric materials. Polymers have been filled with mineral fillers, metals and fibers in order to promote several properties like mechanical properties, thermal stability or flammability. The resulting materials however, may show the deficiency of an intense interaction at the interface between the constituents, yielding to imperfections. Structural perfection can be more easily reached if the reinforcing elements get smaller, i.e., their dimensions are at the atomic or molecular level [1].

Nanoscience focuses on the study of materials in which some novel unique properties originate from an internal structure possessing dimensions with at least one dimension in the nanometer (10^{-9}m) range. In polymer nanocomposites, one of the challenges is to disperse the nano-sized fillers homogeneously in a polymer matrix. The forementioned dispersion of these nano-sized fillers creates a large interfacial area differentiating the nanocomposites from traditional composites and filled plastics.

The crystalline structure of some clays, especially smectite clays, is layered and amenable to forming nanocomposites because of the weak bonding between layers. The layers themselves are nano-sized in thickness with the other dimensions being such that aspect ratios in the range of 50-1000 can be obtained [2].

1

Montmorillonite (MMT), a smectite type of clay with a layer thickness of about 1 nm is particularly useful. MMT carries a negative charge neutralised by various cations usually sodium and calcium residing in the interlayers [3]. In its pristine state, MMT is quite hydrophilic which is a problem impeding its homogeneous dispersion in the polymer matrix. An essential prerequisite for the successful formation of a polymer nanocomposite is making the clay organophilic prior to use. This is achieved by a simple cation exchange process.

Conventionally, there are three methods to synthesize polymer nanocomposites. They are in-situ polymerization, melt intercalation and solution methods.

This study focuses on a new approach i.e., masterbatch method to synthesize polystyrene-MMT nanocomposites in addition to melt intercalation and in-situ polymerization methods. A concentrated mixture of clay (masterbatch) was prepared first by polymerizing styrene that contains high quantities of organoclay. The organoclay used is montmorillonite modified with a quaternary ammonium salt (Cloisite 15A). The prepared masterbatch was subsequently diluted with addititonal neat PS in a twin-screw extruder and materials containing low clay content were obtained. Nanocomposites were also prepared by the melt intercalation and in-situ polymerization methods. All of the specimens were prepared by injection molding prior to characterization. The properties of the materials prepared by melt intercalation, in-situ polymerization and masterbatch methods are compared at the same clay content.

X-Ray diffraction (XRD) and Scanning Electron Microscopy (SEM) analyses were performed in order to investigate the extent of dispersion of the filler in the matrix. The glass transition temperature of the nanocomposites was determined by Differential Scanning Calorimetry (DSC). Tensile, flexural and impact tests were performed to characterize the mechanical properties of the nanocomposites.

CHAPTER II

BACKGROUND

2.1 Polymer Composites

Worldwide materials have been combined with each other to produce new materials that exhibit the positive characteristics of both of their components. The concept of composites originated from the continuous and intense desire to tailor the structure and properties of materials. A composite material is created by combining two or more materials to provide discernible improvement of properties. In a composite, substantial volume fraction of high strength, high stiffness reinforcing elements are embedded in a matrix phase. The final properties of composites are a function of the properties of the constituent phases, their relative amounts, as well as the geometry of the dispersed phase (i.e., shape of the reinforcing components and size, their distribution and orientation) [4].

Matrix materials are generally polymers, ceramics or metals. The polymer matrices also called resins are by far the most common due to the versatility of their properties such as light weight, easy processing and corrosion resistance [5].

2.1.1 Matrix

The matrix in a polymer composite serves both to maintain the position and orientation of the reinforcement and protects them from adverse environmental effects [6]. In addititon, it helps to distribute the applied load by acting as a stress-transfer medium [4]. The polymer matrices can be of two types differing in their respective intermolecular structures.

2.1.1.1 Thermosets

In a thermoset polymer, the molecules are chemically joined together by crosslinks, forming a rigid, three-dimensional network structure. Once these crosslinks are formed during polymerization reaction (curing), the polymer cannot be remelted and reshaped by the application of heat and pressure [7]. Thermosetting polymers are the most frequently used matrix materials in polymer-based composites production mainly because of the ease of their processing [4]. In the case of thermosets, it is possible to achieve a good wet-out between the fibers and matrices, since the starting materials for the polymerization are low molecular-weight liquid chemicals with very low viscosities [7]. Thermosets are usually more rigid than thermoplastics and also exhibit generally higher temperature performance, however they usually require much longer processing times [8].

2.1.1.2 Thermoplastics

In a thermoplastic polymer, there is no chemical bond between long chain molecules. They are held by weak intermolecular bonds such as van Der Waals or hydrogen bonds [9]. Thermoplastics are heat softenable, heat meltable and reprocessable [4]. The most important advantages of thermoplastics over thermosets are their high impact strength and fracture resistance which in turn imparts excellent damage tolerance characteristics to the composite material [7].

It is therefore obvious that in the choice of thermoplastic versus thermoset resin, several trade-offs and compromises must be made considering the application area of the material.

2.1.2 Reinforcement

The main functions of the reinforcing material in a composite are to carry the load and provide structural properties like stiffness, strength and thermal stability [5]. The classification of reinforcing materials mainly depends on their aspect ratios. The reinforcements can be fibers, particles or whiskers. Each has its own unique

application although fibers are the most commonly selected type in composites and have the greatest influence on properties [8].

2.2 Nanocomposites

The essence of nanotechnology is the ability to work at the molecular level to create large materials possessing unique properties that are not shared by conventional composites. A nanocomposite is defined as a composite wherein the dispersed particle has at least one dimension in the nanometer range (10^{-9}m). Major differences in behavior between conventional composites and nanocomposites result from the fact that the latter have much larger interface area per unit volume leading to unique phase morphology [2].

2.2.1 Polymer-Layered Silicate Nanocomposites

Polymer layered silicate nanocomposites are polymer matrices containing low levels of dispersed platey minerals with at least one dimension in the nanometer range. Polymer nanocomposites have their origin in the pioneering research conducted at Toyota Research Laboratories with the successful synthesis of a nylon 6-clay nanocomposite [10]. The principal expolitable properties that layered silicates can bring to a polymer composite include increased stiffness, thermal and oxidative stability and reduced flammability. The main attraction is that, because of the high surface area and aspect ratio, these benefits are potentially obtainable at much lower volume fractions than with most other fillers [3]. In the last decade, nanocomposites based on different types of polymers including thermosets and thermoplastics have been produced.

2.2.2 Clays

Inorganic particles have been widely used as reinforcement materials for polymers. Special attention has been paid to clays in the field of nanocomposites.

Two particular characteristics of clays are exploited in nanocomposite preparation. The first is the fact that the very fine particles yield to very large specific surface areas and the second is the ability to modify their surface chemistry through the exchange reactions [11]. Clay minerals are not nanometer-sized themselves but can produce nanometer-sized filler. Clay minerals are called layered silicates because of the stacked structure of 1 nm thick silicate layers with a variable interlayer distance [10]. Clays are composed of clay minerals fundamentally containing silicon, aluminum or magnesium, oxygen and hydroxyl with various associate cations according to the species. These ions and OH groups are organized into two-dimensional structures called sheets. Sheets may be of two types: tetrahedral and octahedral [12]. The structural variations among the clay minerals can be understood by considering various physical combinations of tetrahedral and octahedral sheets. The layer charge and configuration yield to the classification of different groups of clays.

2.2.2.1 Montmorillonite

Montmorillonite, a smectite type of clay, is one of the most interesting and widely used clays owing to its unique layered structure, cation exchangeability and expandibility [11]. Smectites are 2:1 clay minerals composed of units consisting of two silica tetrahedral sheets with a central alumina octahedral sheet [13]. The minerals of the smectite group have been formed by surface weathering, low temperature hydrothermal processes or alteration of volcanic dust in stratified beds [14].

2.2.2.1.a Morphology

The crystal structure of montmorillonite consists of layers formed by sandwiching an aluminum octahedral sheet between two silica tetrahedral sheets, so that the oxygen ions of the octahedral sheet do also belong to the tetrahedral sheets (Figure 2.1) [15]. The crystal lattice has an overall negative charge because of substitution of alumina for silica in the tetrahedral sheet and iron or magnesium for

alumina in the octahedral sheet. As the surface between the layers is negatively charged it attracts cations such as Fe^{+2}, Ca^{+2} or Na^+. These cations are not bonded to the crystal; they form a positively charged layer between the negatively charged surfaces of the crystals [13].

The silicate layers of MMT are planar, stiff about 1 nm in thickness with high lateral dimensions so that very high aspect ratios are observed in MMT [2]. These layers organize themselves in a parallel way to form stacks with a regular van der Waals gap in between them, called *interlayer* or *gallery*. The sum of the single layer thickness and the interlayer is called *d-spacing* or *basal spacing* [16].
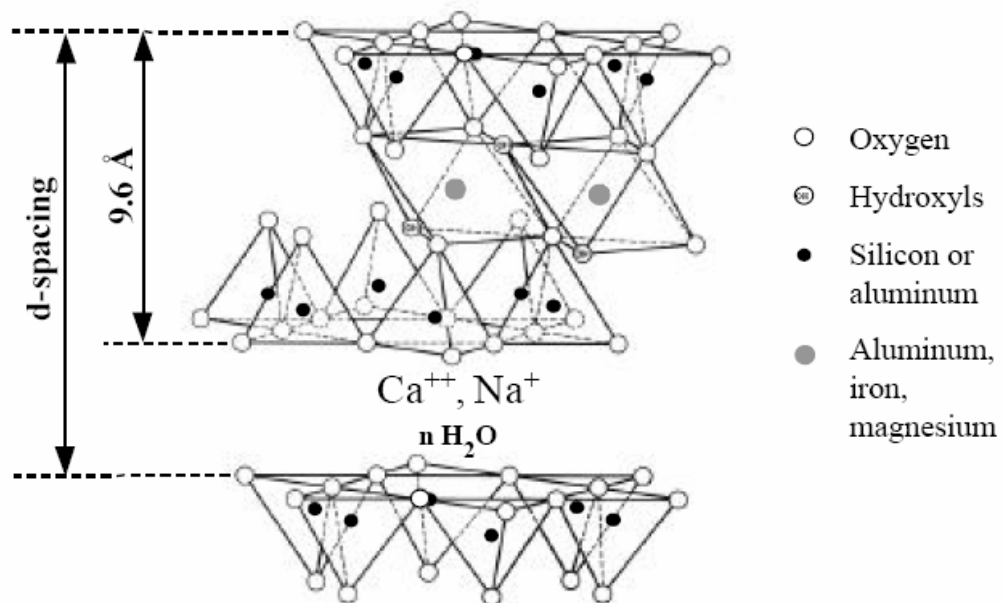
Figure 2.1 Idealized structure of 2:1 layered silicate showing two tetrahedral-site sheets fused to an octahedral-site sheet [16].

2.2.2.1.b Cation- Exchange Process

One important consequence of the charged nature of clays is that they are generally hydrophilic species and therefore naturally incompatible with a wide range of polymer types. To overcome this problem it is often necessary to make the surface organophilic prior to its use [17]. As shown in Figure 2.2, the usual treatment is to

ion-exchange the interlayer cations with an organophilic cation such as an ammonium ion which contains at least one long alkyl chain [18].

Alkylamonnium ions: They are most popular since they can easily be exchanged with the ions situated between the layers. Depending on the layer charge density of the clay, the alkylammonium ions may adopt different structures between the clay layers. Alkylammonium ions reduce the electrostatic interactions between the silicate layers thus facilitate diffusion of the polymer into the galleries [16].
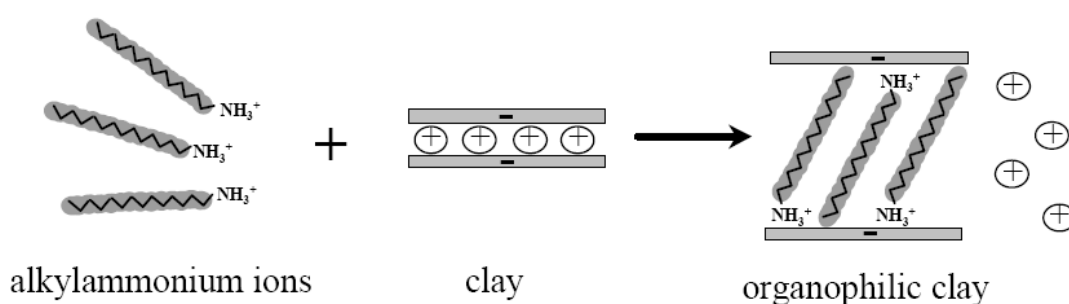
Figure 2.2 Schematic representation of the cation exchange process [16].

The ion-exchange process in smectite clays not only serves to match the clay surface polarity with the polarity of the polymer, but it also expands the clay galleries. In general, the longer the surfactant chain length, the further apart the clay layers will be forced [19]. The ability of clays to retain cations is defined in terms of *cation exchange capacity*. Cation exchange capacity is measured in milliequivalents per 100 g of air-dried clay. The cation exchange capacity of smectite minerals is notably high between 80-150 meq/100g and affords a diagnostic criterion of the group [14].

2.2.2.1.c Synthesis

Several procedures are known so far to synthesize polymer nanocomposites. These include in-situ polymerization, melt intercalation and solution methods.

In-Situ Polymerization Method

In this method, the layered silicate is swollen within the liquid monomer. Polymerization of the monomer occurs in the interlayer of the clay mineral, resulting in an expanded interlayer distance. Polymerization can be initiated by heat or a suitable initiator [16].
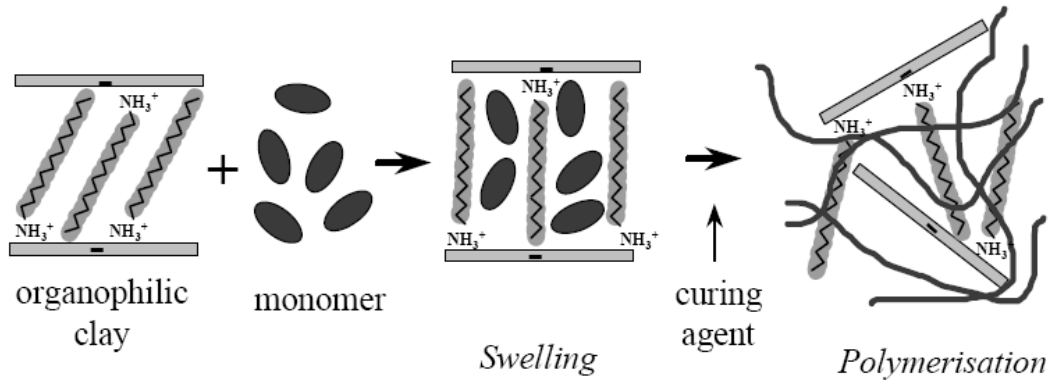
Figure 2.3 Schematic representation of the *in situ* polymerization method [16].

Melt Intercalation Method

The layered silicate is mixed with the polymer matrix in the molten state. If the layer surfaces are sufficiently compatible with the chosen polymer, the polymer can separate the clay layers and form either an intercalated or an exfoliated nanocomposite [15].
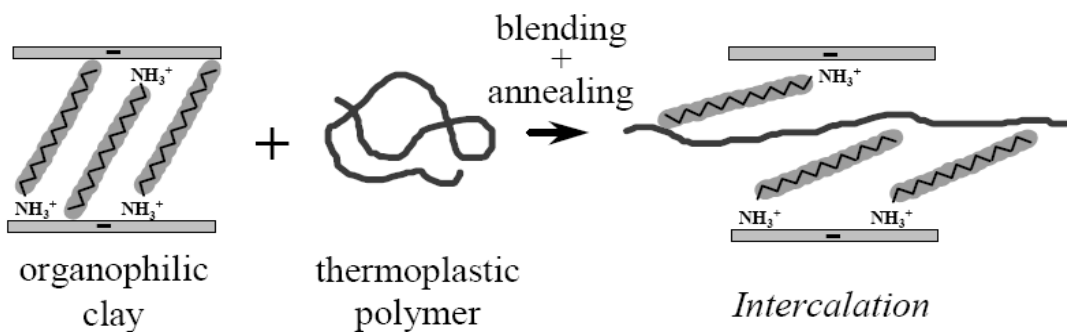
Figure 2.4 Schematic representation of the melt intercalation method [16].

Solution Method

A solvent is used to disperse the organoclay as well as the polymer. Upon removal of the solvent, uniform mixing of polymer and layered silicate is achieved [10].
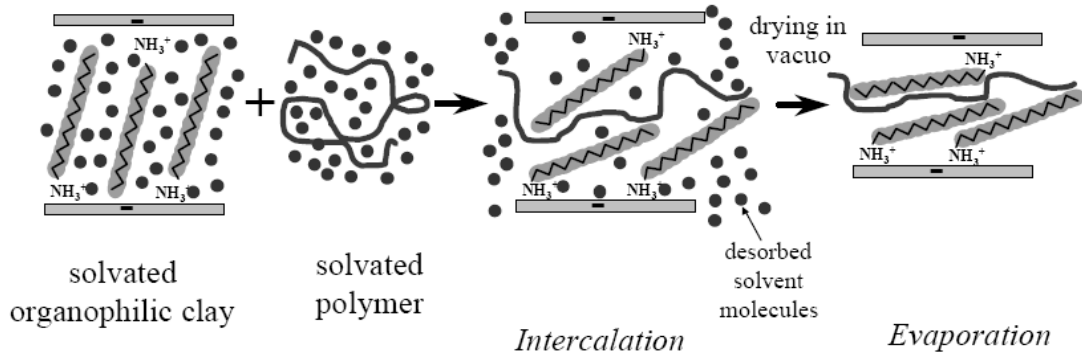
Figure 2.5 Schematic representation of the solution method [16].

2.2.2.1.d Structure

Three main types of structures may be observed at the end of the synthesis methods.

Conventional Composite

In a conventional composite, the clay particles exist in their original aggregated state with no insertion polymer matrix between the layers. An improvement in modulus is normally achieved in conventional clay composite but this reinforcement benefit is usually accompanied with a deficiency in other properties such as strength or elasticity [10].

Intercalated Nanocomposite

Intercalated structures are well-ordered multilayered structures with a fixed d-spacing where the polymer chains are inserted into the gallery space between the silicate layers [20]. An increase in d-spacing is observed but the layers maintain their order.

10

Exfoliated Nanocomposite

In an exfoliated nanocomposite, the individual clay layers are separated and dispersed in a continuous polymer matrix with average distances between layers depending on the clay concentration. Generally, exfoliated nanocomposites exhibit better properties than intercalated ones of the same particle concentration [2].
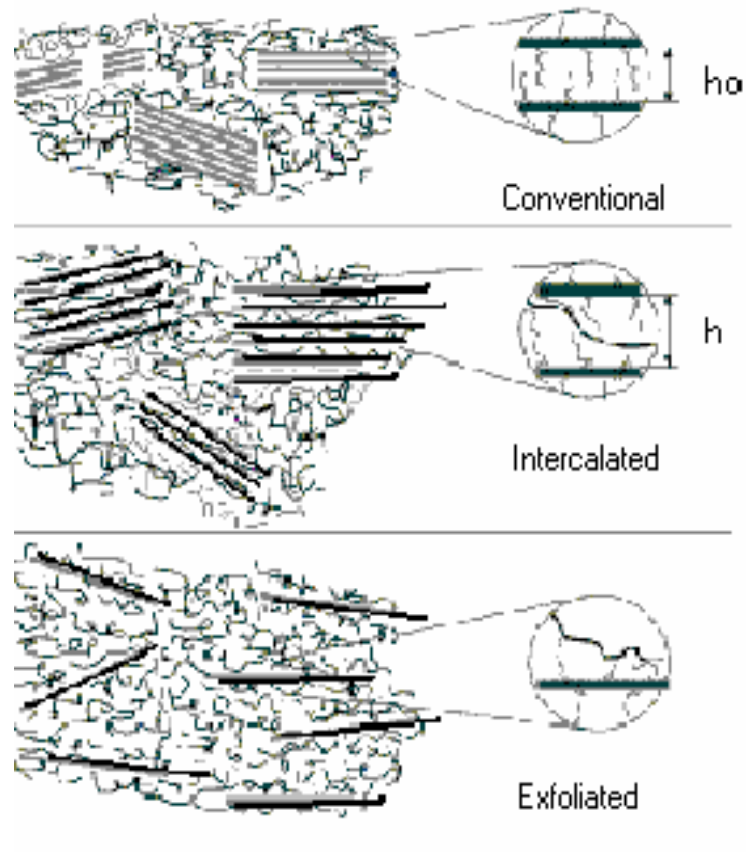
Figure 2.6 Schematic diagrams of the possible nanocomposite structures. Top: the conventional composite where the polymer does not penetrate the stack of silicate layers and the gallery height remains at the pristine value of ho. Middle: The intercalated system, where the polymer chains penetrate into and swells the galleries of the silicate layers to a value h, without destroying the stacking of layers. Bottom: the exfoliated or delaminated system, where individual silicate layers are dispersed in the polymer matrix [21].

2.3 Polystyrene

2.3.1 General Properties and Applications

Polystyrene belongs to the group of standard thermoplastics that also includes polyethylene, polypropylene and polyvinylchloride. Because of its special properties, polystyrene can be used in an extremely wide range of applications [22]. Polystyrene is a versatile polymer whose principal characteristics include transparency, ease of coloring and processing and low cost [23]. Polystyrene is usually available in general purpose or crystal, high impact and expanded grades. It is a linear polymer that in principle can be produced in syndiotactic and atactic forms. The mechanical and rheological behaviour of polystyrene is predominantly determined by its average molecular weight; the strength improves with increasing chain length but the melt viscosity increases as well making processing difficult [22].

The general purpose polystyrene (GP-PS) is atactic and as such amorphous. The GP-PS is a clear rigid polymer resistant towards a large number of chemicals. PS has outstanding flow characteristic, and consequently is very easy to process. Its excellent optical properties including high refractive index and good dielectric properties make it useful in optical and insulation applications. However, GP-PS has a number of limitations, including its brittleness, low heat-deflection temperature and poor UV resistance. PS is sensitive to foodstuffs with high fat or oil content; it crazes and turns yellow during outdoor exposure. The applications for all grades of polystyrene include packaging, housewares, toys, electronics, appliances, furnitures and building and construction insulation [23].

2.3.2 Free-Radical Polymerization

Styrene is almost unique in the extent of its ability to undergo spontaneous polymerization simply by heating the monomer without the aid of chemical initiator. Polystyrene was first produced commercially in 1938 by the Dow Chemical Company. The first polymerization process involved loading cans of styrene into an oven and allowing them to spontaneously polymerize to high conversion. Today,

most polystyrene is manufactured via continuous free radical bulk polymerization with the aid of a suitable initiator [24].

Free-radical polymerization is a rapid reaction which consists of the sequence of events, namely initiation, propagation, and termination [25]. Free-radical polymerization is initiated by the action of free-radicals i.e., electrically neutral species with an unshared electron. Free radicals for the initiation are usually generated by the thermal decomposition of organic peroxides or azo compounds [26]. Their effect on polymerization is to increase the rate of reaction and at the same time, to decrease the molecular weight of the polymer. These compounds are readily homolytically cleaved by heat or ultraviolet light to produce free radicals. Benzoyl peroxide is a typical and widely used initiator and it is useful in the temperature range of $60\,^{o}C$-$90\,^{o}C$ [27].

The decomposition process is as follows; [27]

$$I \longrightarrow 2\,R\cdot \text{ (decomposition)}$$

In the schematic reaction steps, (I) denotes initator (R) the radicals and (M) the monomers.

The formed radical attacks styrene to initiate chain growth.

$$R\cdot + M \longrightarrow R_1\cdot \text{ (addition)}$$

The formed product is still a free radical; it proceeds to propagate the chain by adding another monomer unit [26].

$$R_1\cdot + M \longrightarrow R_2\cdot \text{ (propagation)}$$

Growing chains can be terminated in one of two ways. Two radicals may go mutual termination by either a combination or a disproportionation reaction. Termination by

combination results in higher molecular weight polstyrene than any of the other termination modes [27].

$$R_n\cdot + R_m\cdot \longrightarrow P_{n+m} \text{ (combination)}$$

$$R_n\cdot + R_m\cdot \longrightarrow P_n + P_m \text{ (disproportionation)}$$
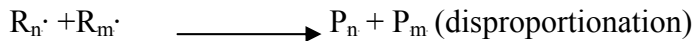
2.4 Extrusion

Extrusion is one of the most widely used ways of fabricating plastic products. It is a processing technique for converting thermoplastic materials in powdered or granular form into a continuous melt, which is shaped into items by forcing it through a die [23]. There are a large number of processes taking place in an extruder, the simplest of which is compounding. Polymers are frequently mixed with additives, colorants, fillers and some other polymers in an extruder [28].

2.4.1 Extruder

The extruder is a versatile machine where plastic pellets are melted and forced through the die to produce the desired form of the product [9]. In the plastics industry, single screw extruders are most common in which a screw rotating in a cylinder creates a pumping action [29]. Various modifications of the single screw design are available.

2.4.1.1 Parts of an Extruder

2.4.1.1.a Screw

Extruder screw is a long cylinder with a helical flight wrapped around it [29]. The function of the screw is to convey the solid pellets forward and convert them into

14

molten polymer in addition to mixing the polymer melt and pumping it through the die [26].

2.4.1.1.b Barrel

The barrel of the extruder is normally a long tube in which the screw is horizontally mounted. It can be made of a bimetallic material to provide resistance against wear and corrosion [23]. Considering economic aspects, more often only a barrel liner is made from these materials. The barrel is equipped with systems for both heat input and extraction [9].

2.4.1.1.c Feed Throat

The feed throat is connected to the barrel; it contains the feed opening through which the plastic material is introduced to the extruder [29].

2.4.1.1.d Die

The die is mounted at the discharge end of the extruder and shapes the polymer extrudate into the desired article. If the extruder is used to compound polymers, the product is usually in cylindirical strands [28].

2.4.1.1 Twin-Screw Extruders

Multiscrew extruders are also in current use for specialized applications in case the single screw designs are inefficient with twin-screw type being the most common [23]. Some advantages of twin-screw over single-screw extruders are lower possible melt temperatures and better mixing [30]. Twin-screw extruder does not subject the polymer to the typically very high shear seen in the single-screw extruder. This is quite important in processing shear-sensitive polymers such as rigid PVC and polymers containing temperature sensitive additives such as antioxidants, fire retardants and foaming agents [28].

Co-Rotating twin screw extruders: If both screws rotate in the same direction, the extruder is called a co-rotating twin screw extruder.

Counter-rotating twin screw extruders: This type of extruder has counter-rotating screws to give a conveying action similiar to a positive displacement pump [30]. A distinguishing feature of twin-screw extruders is the extent that the screws intermesh. The screws can be fully intermeshing, partially intermeshing and non-intermeshing [29].
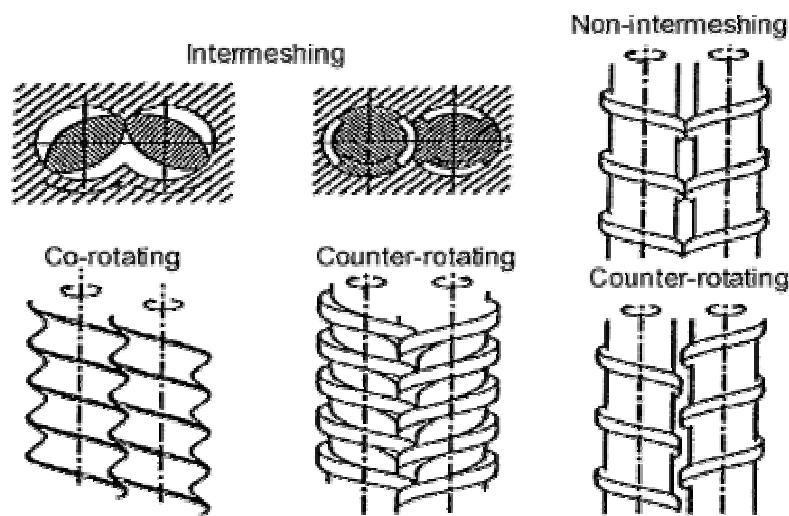
Figure 2.7 Different twin screw designs [31].

2.5. Injection Molding

Injection molding is one of the common processing techniques for converting thermoplastics, recently thermosets, from the pellet or powder form into a variety of useful products. In this process, the material is heated until it melts. The melt is then injected into and held in a cooled mold under pressure until the material solidifes. The mold opens and the product is ejected. The injection unit and the clamp unit are the two principal components to perform the cyclical steps in the injection molding process. The injection unit has two functions: melt the polymer and then inject it into the mold. The clamping unit of an injection molding machine has one main function

16

i.e., to keep the mold closed and under sufficient pressure during the injection of the plastic melt to prevent any plastic from escaping [9].

These mentioned steps during an injection process must be performed under appropriate conditions selected for the polymer (pressure and temperature) that ideally should result in high quality.

Some polymer properties that should be considered during injection molding are thermal properties, polymer melt viscosity and crystallization kinetics [28].

2.6. Characterization

2.6.1 X-ray Diffraction

The application of X-rays to the study of nanocomposites makes possible the determination of detailed information on the state of order or disorder of the material. XRD is used to identify the interlayer spacing in intercalated structures [15].

X-rays are electromagnetic radiation of exactly the same nature as light but of very much shorter wavelength. X-rays are generated when high-speed electrons collide with a metal target. Any X-ray tube therefore contains a source of electrons, a high accelerating voltage and a metal target [32]. The essential feature of diffraction is that the distance between the scattering centers be of the same order of magnitude as the wavelength of the waves being scattered [33]. This requirement follows from Bragg's Law which can be written as;

$$n \lambda = 2d\sin \theta \qquad (2.1)$$

where λ denotes the wavelength of the X-ray radiation used, **d** denotes interlayer spacing and **θ** is the measured diffraction angle. The integer **n** refers to the degree of diffraction. In the case of diffraction, the smallest value of n is 1 [16].

In XRD measurements Bragg's Law is applied such that by using X-rays of known wavelength and measuring θ, the d-spacing is determined [32].

XRD is a versatile method to characterize nanocomposites. The sample preparation is relatively easy and the X-ray analysis can be performed within few hours [16].

2.6.2 Scanning Electron Microscopy

The Scanning Electron Microscope (SEM) is one of the most versatile instruments available for the examination and analysis of the structural characteristics of materials. The primary reason for the SEM's usefulness is the high resolution combined with a great depth of focus. The basic components of the SEM are the lens system, electron gun, electron collector, visual and recording cathode ray tubes and the electronics associated with them [34].

In SEM, the electrons are accelerated by applying high voltage and the electron beam is focused with a series of electromagnetic lenses [35]. As the electron beam scans the specimen surface, the information collected modulates the raster of a cathode-ray tube and each point on the cathode-ray tube raster corresponds to a point on the specimen surface. Although secondary electron transmission is the principal mode of imaging, much information can be gained from x-rays and light photons generated by the electron beam [35]. In SEM, if the specimen is not a good conductor, it should be coated with a thin layer of conducting material. This coating is done by placing the specimen in a high-vacuum evaporator and vaporizing a suitable material to deposit on the specimen. Typical coating materials are gold, silver and aluminum. Specimen preparation for the SEM requires considerably less time than preparing a sample for transmission electron microscope [35].

2.6.3 Differential Scanning Calorimetry

Thermal transitions in polymers are conveniently studied using differential scanning calorimeter DSC [26]. DSC is a technique of nonequilibrium calorimetry in which the heat flow into or away from the polymer is measured as a function of temperature or time [25]. Small samples of polymer placed in a pan, and the reference (usually an empty pan) are heated at a pre-programmed rate to keep the two pans at the same temperature. The difference in power needed to keep both at the

same temperature is amplified and provides the information about thermal transitions [30]. For instance at T_g, the heat capacity of the sample suddenly increases requiring more power (relative to reference) to maintain the temperatures the same. The differential heat flow to the sample (endothermic) causes a drop in the DSC curve [26]. A sample mass of 5-10 mg and a heating rate of 10-40°C are typical conditions [30]. The higher the heating rate the quicker is the measurement, a practically desirable result. However, because polymer chains can not respond instantaneously to the changing temperature at high heating rates, very low heating rates should be used to approach true equilibrium values [26]. Figure 2.8 shows a typical DSC cell.
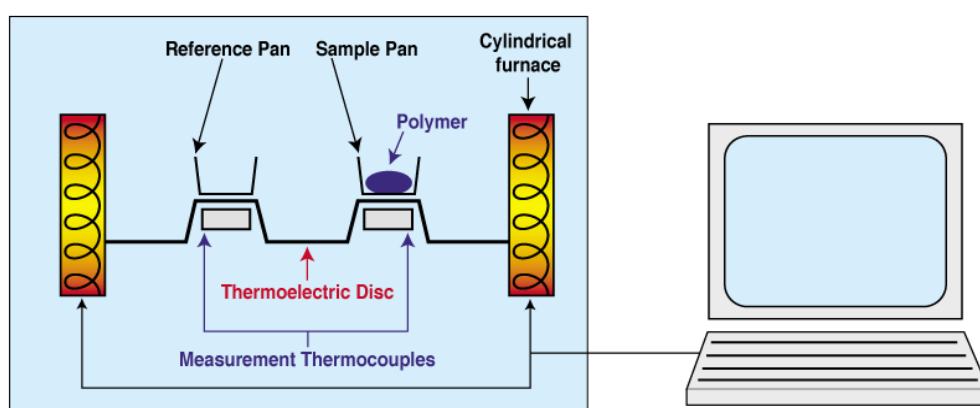
Figure 2.8 Differential Scanning Calorimeter cell [36].

2.6.4 Mechanical Tests

In the selection of a polymer for a specific use, a clear understanding of mechanical properties is essential to obtain the best performance. Many test methods are available to predict the mechanical performance of a polymer under certain conditions. These include tension, compression and shear tests.

2.6.4.1 Tensile Test

In tensile test, the specimen is pulled at a constant rate of elongation and the stress required for this deformation is measured simultaneously. The test continues

until the center of the specimen fails. Figure 2.9 shows a typical tensile specimen in the form of dogbone as specified in ASTM D638.
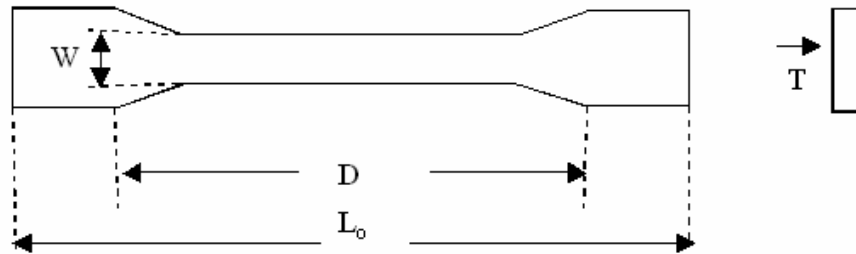
Figure 2.9 Tensile test specimen [37].

In Figure 2.9, D stands for original gage length, L_o for overall length of the specimen, W for gage width and T for thickness of the specimen.

In discussing tensile properties it is of importance to be familiar with some terms.

Stress: Stress is defined as the force per unit area perpendicular or normal to a force.

$$\text{Stress } (\sigma) = F / A_o \qquad (2.2)$$

Strain (engineering): Strain is defined as; $\varepsilon = \Delta D / D$ $\qquad$ (2.3)

where;

D= original gage length

ΔD= the change in gage length due to deformation [28].

Tensile Strength: It is calculated by dividing the maximum load in Newtons by the original cross-sectional area of the specimen (mm^2). The result is expressed in terms of mega Pascal [37].

$$\text{Tensile Strength} = \frac{\text{Force (Load) (N)}}{\text{Cross Section Area } (mm^2)} \qquad (2.4)$$

Young's Modulus: It is also called the tensile or elastic modulus. Young's modulus can be calculated from the initial straight line portion of a stress-strain curve; tensile modulus is the slope of this line [38]. The result is expressed in MPa unit.

$$\text{Tensile Modulus } = \frac{\text{Difference in Stress}}{\text{Difference in Corresponding Strain}} \qquad (2.5)$$

When maximum stress occurs at break, it is designated as tensile strength at break.

$$\text{Tensile Strength at Break (MPa)} = \frac{\text{Load Recorded at Break}}{\text{Cross Section Area (mm}^2)} \qquad (2.6)$$

Tensile Strain at Break: It is the strain measured at the breaking point.

2.6.4.2 Flexural Test

Flexural test is performed to measure the material's resistance to bending. The ASTM D790 test specifies two different test methods with either single or two points loading on a simply supported beam. The test specimen of length L* is placed on two supporting mounts seperated by a distance L. The perpendicular load P is either applied to the beam at the center of the support (Figure 2.10) or in two equal loads of P/2 applied to the beam at distances L/3 from each support. In flexural tests, the load is applied at a constant cross-head rate [28].
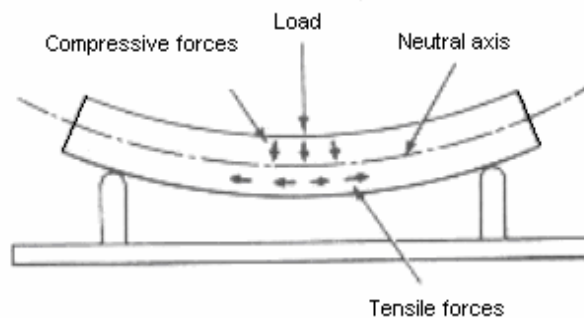
Figure 2.10 The stresses on the sample during flexural testing [39].

Flexural Strength: When a material is subjected to a bending force, the maximum stress developed is called as flexural strength. It is calculated by the following equation:

$$S = \frac{3PL}{2bd^2}$$

$$(2.7)$$

where; S is the stress in the outer fibers at midspan (MPa), P is the load at a given point on the load-deflection curve (N), L is the support span (mm), b and d are the width and the depth of beam tested in mm, respectively.

Flexural Strain at Break: It is the deflection at the breaking point. It is calculated by the following equation:

$$r = \frac{6Dd}{L^2}$$

$$(2.8)$$

where; r is the maximum strain in the outer fibers, D is the maximum deflection of the center of the beam (mm), L is the support span (mm), and d is the depth of the sample (mm).

Flexural Modulus: It is the property used to indicate the bending stiffness of a material. It can be related to the slope of the initial straight-line portion of the stress-strain curve within the elastic region [40].

$$E_b = \frac{L^3m}{4bd^3}$$

$$(2.9)$$

where; E_b shows the modulus of elasticity in bending (MPa), L is the support span (mm), b and d are the width and the depth of beam tested, respectively (mm), and m is the slope of the tangent to the initial straight line portion of the load-deflection curve (N/mm).

2.6.4.3 Impact Test

Impact test gives an idea about the toughness of a material by measuring the energy to break the sample. This energy is measured from the kinetic energy loss of a known weight striking the sample. The most popular impact tests are Izod and Charpy impact tests specified in ASTM D256 [25].

Izod Impact Test: The specimen is held vertical position at the base of the test stand. The pendulum falls through a vertical height and breaks the sample. The specimen can be tested without a notch [28].

Charpy Impact Test: The specimen is supported as horizontal and broken by a single swing of the pendulum with impact line midway between the supports [41]. Impact strength can be calculated by dividing the absorbed energy by the area of the sample.

2.6.5 Melt Flow Index (MFI) Test

The ability of a thermoplastic melt to flow is often measured in a melt index tester. The melt index machine is a simple ram extruder. Plastic is placed in the barrel and heated to the appropriate temperature [29]. When the polymer is molten and free of bubbles, a weight is placed on top of the ram causing the polymer to be extruded out. The extrudate is collected over a measured period of time and weighed. The weight per 10 minutes is reported as the melt flow index [28]. As expected, for polymers high MFI value indicates low viscosity and low molecular weight.

2.7 Previous Studies

Xie et al. [42] prepared polystyrene-clay nanocompsites by suspension polymerization of styrene monomer in the presence of organo-MMT and investigated the effects of organo-MMT concentration and alkyl chain lengths of surfactants on the properties of polystyrene-clay nanocomposites. The optimum organoclay content

to yield the best improvement in thermal properties was 5wt. %. The alkyl chain length of surfactant affected the properties of the nanocomposites as well. With the surfactant possessing the highest chain length, the nanocomposite with the highest glass transition temperature was obtained.

Doh and Cho [17] investigated the effects of various org-MMT structures on the properties of PS-MMT nanocomposites. The nanocomposite containing benzyl-unit similiar to styrene monomer in org-MMT exhibited the highest decomposition temperature. It was concluded that structural affinity between styrene monomer and the organic group of modififed clay is an important factor affecting the structure and properties of the nanocomposites.

Zhang et al. [43] synthesized PS-clay nanocomposites by γ-radiation technique using four different modified clays. Three of the modified clays were reactive while one was non-reactive. With the reactive modified clays, exfoliated structures were obtained whereas with the nonreactive clay intercalated structure was obtained. The thermal properties of nanocomposites prepared by reactive clay were greatly enhanced due to the chemical bond formed between the clay and the chains of polystyrene.

Gilman et al. [20] prepared nanocomposites using modified fluorohectorite and montmorillonite by melt intercalation. TEM image of PS-fluorohectorite confirmed that it is a neatly intercalated structure. TEM image for the PS-MMT nanocomposite showed that it contained both intercalated and delaminated MMT layers. Cone calorimetry results showed that the PS-fluorohectorite had no effect on the peak heat release rate whereas PS-MMT hybrid had a 60% reduction in peak heat release rate compared to pure polystyrene. It was also observed that degree of dispersion of the silicate layers affects the flammability properties of the nanocomposites.

Lepoittevin et al. [44] focused on a new approach; masterbatch route to prepare poly (ε-caprolactone)-montmorillonite nanocomposites. Masterbatch route was simply the combination of in-situ polymerization and melt intercalation methods. At the same clay content, the Young's modulus of the nanocomposites prepared by the masterbatch method was higher than that of the ones prepared by

melt intercalation. By applying the new method, an intercalated structure was obtained even with native Na-MMT rather than a microcomposite.

Fu et al. [45] synthesized PS-clay nanocomposites by direct dispersion of organically modified clay in styrene monomer followed by free-radical polymerization.The organoclay contained a vinyl benzyl group in the structure. The XRD and TEM results revealed that the clay layers were exfoliated in the PS matrix. It was concluded that vinyl benzyl group of the surfactant is effective in exfoliating MMT in PS matrix.

Zhang et al. [44] reported the first example of clay that contains a carbocation and its use to prepare PS-clay nanocomposites. The nanocomposite was prepared by emulsion polymerization and its mixed intercalated-exfoliated structure was established by XRD and TEM. Both the clay and its nanocomposite showed outstanding thermal stability. It was deduced that this new organically-modified clay may be useful for the preparation of materials which must be processed at temperatures which are above the thermal stability limit of the common ammonium-substituted clays.

CHAPTER III

EXPERIMENTAL

3.1 Materials

3.1.1 Organoclay

The filler used in this study was organically treated Na-MMT purchased from Southern Clay products, Texas-U.S.A. The commercial name of the organoclay is Cloisite 15A and it is modified by a quaternary ammonium salt. The cation of the organic modifier is dimethyl, dehydrogenated tallow quaternary ammonium (2M2HT) and the anion is chloride (see Figure 3.1). Its properties are listed in Table 3.1.

$$CH_3 - \overset{\overset{\displaystyle CH_3}{|}}{\underset{\underset{\displaystyle HT}{|}}{N^+}} - HT$$
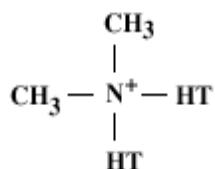
Figure 3.1 Chemical structure of 2M2HT

In Figure 3.1, the HT is hydrogenated tallow (~65% C18, ~30% C16, ~5% C14).

Table 3.1 Manufacturer Data of Cloisite®15A

Properties	Cloisite®15A
Organic Modifier	2M2HT
Modifier Concentration	125meq/100g clay
% Moisture	< 2%
% Weight loss on ignition	43%
Loose bulk, 1bs/ft^3	10.79
Packed bulk, 1bs/ft^3	18.64
Specific gravity	1.66
Color	Off white
Typical Dry Particle Sizes (microns, by volume)	10% less than 2μ 50% less than 6μ 90% less than 13μ
X Ray Results	31.5 Å

3.1.2 Polystyrene

The polystyrene used in this study was purchased from Atofina Chemical Products and its commercial name is Lacqrene®1960N. Its chemical structure is shown in Figure 3.2 and some of its properties are given in Table 3.2.
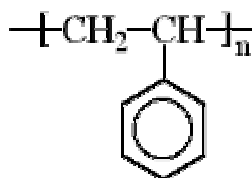
Figure 3.2 Chemical structure of polystyrene

Table 3.2 Properties of Polystyrene

Glass Transition Temperature	~100°C
Bulk Density	0.6 g/cm^3
Water absorption	< 0.1 %
Melt Flow Index(200°C-5kg)	30 g/10min

3.1.3 Styrene

Styrene, the monomer used in polymerization was purchased from Solventaş. Some of its properties are given in Table 3.3 and its chemical structure is shown in the following figure.
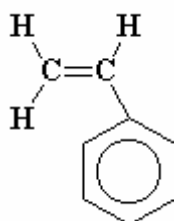
Figure 3.3 Chemical structure of styrene

Table 3.3 Properties of styrene

Molecular Weight(g/mol)	104.15
Boiling Point Temperature(°C)	145
Freezing Point Temperature(°C)	-31.6
Specific gravity	0.91

3.1.4 Benzoyl Peroxide

Benzoyl peroxide was used as the initiator for styrene polymerization. Its chemical structure and general properties are given in Figure 3.4 and Table 3.4, respectively.
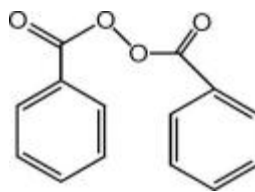
Figure 3.4 Chemical structure of benzoyl peroxide

Table 3.4 General Data for Benzoyl Peroxide

Formula	$C_4H_{10}O_4$
Molecular Weight	242.23 (g/mol)
Melting Point	104-106°C.

3.2 Experimental Procedure

3.2.1 Melt Intercalation Method

As a first step, the polystyrene (PS)-Montmorillonite (MMT) nanocomposites were prepared by melt compounding in a co-rotating twin-screw extruder (Thermoprism TSE 16 TC, L/D = 25). Organoclay was dried overnight in vacuum oven at 120°C prior to its use to avoid the effects of moisture. During processing, the screw speed and the barrel temperature were kept constant at 350 rpm and 200°C respectively. Polystyrene pellets were fed from the main feeder whereas the organoclay was fed from the side feeder. The extruder was calibrated carefully in order to obtain nanocomposites containing 0.73%, 1.6%, 2.4% and 3.36% by weight organoclay. The extrudate was cooled and ground prior to injection molding.

3.2.2 In-Situ Polymerization Method

Before preparation of the nanocomposites, pure polystyrene was synthesized at 90°C with the aid of benzoyl peroxide as the initiator. The polymerization time was approximately 3 hours and the initiator concentration was 0.43% by weight. The conditions were selected in order to obtain polystyrene with a melt flow index value which is same as that of the commercial polystyrene.

Synthesis of nanocomposites by in-situ polymerization basically involved the dispersion of organoclay in styrene followed by free-radical polymerization initiated by the addititon of benzoyl peroxide. Styrene monomer containing the desired amount of organoclay was mechanically mixed for 30 minutes at room temperature. In order to obtain better dispersion, the mixture was further mixed in an ultrasonic bath for 30 minutes. The benzoyl peroxide was then added to the mixture to initiate the polymerization which took place at 90°C for three hours. The composites obtained at the end of polymerization were casted into aluminum molds and kept overnight in an oven at 120°C to complete polymerization and remove the remaining styrene. Then the products were ground and subsequently injection molded.

3.2.3 Masterbatch Method

This new method was in fact a route involving the in-situ polymerization and melt intercalation methods. A concentrated mixture of clay and polystyrene (masterbatch) with high clay loading (21%) was prepared. The masterbatch was prepared polymerizing styrene that contains high amount of clay following the identical procedure reported for the in-situ polymerization process e.g. the polymerization temperature and time were kept constant. Highly viscous polymer was poured into aluminum molds and kept at 120°C overnight. The masterbatch was ground before extrusion.

At the second stage of the masterbatch method, the masterbatch in the form of granules was diluted with commercial polystyrene to desired compositions in a co-rotating twin-screw extruder.

The neat polystyrene was fed from the primary feeder and masterbatch was fed from the side feeder. Finally, the extrudate was ground once more before the injection molding process and nanocomposites with low clay loadings were obtained.

3.3 Sample Preparation

3.3.1 Injection Molding

The specimens for mechanical characterization were prepared by injection molding using a laboratory scale injection-molding machine (Microinjector, Daca Instruments). Figure 3.5 is the schematic view of injection molding machine. During molding; barrel temperature (210°C), mold temperature (30°C), injection pressure (8 bars) and cycle time (1.5 min.) were identical for the preparation of each sample.
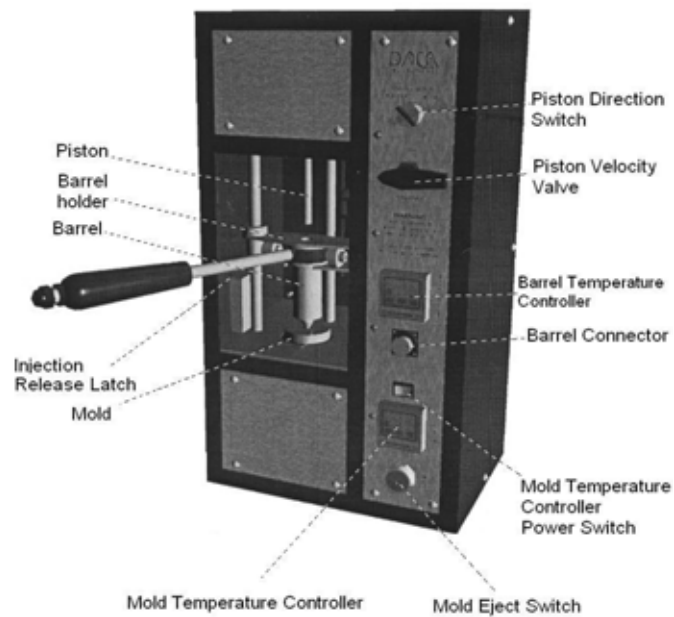
Figure 3.5 Schematic representation of injection molding machine

3.4 Characterization

3.4.1 Morphological Analysis

3.4.1.1 Scanning Electron Microscopy (SEM) Analysis:

Impact fractured surfaces were examined by a JEOL JSM-6400 Scanning Electron Microscope. The fracture surfaces of impact samples were covered with a thin layer of gold to obtain a conductive surface. The SEM photographs were taken at x250 and x3500 magnifications.

3.4.1.2 X-Ray Diffraction (XRD) Analysis:

The nanocomposites were analyzed by using a Philips PW3710 based X-Ray diffractometer. Diffractometer, equipped with CuK anode radiation source operated at a generator tension of 40 kV and a generator current of 55 mA. The diffraction patterns were collected at a diffraction angle 2θ from $1°$ to $10°$ at a scanning rate and step size of $3°$/min and $0.02°$, respectively. The samples for the X-ray diffraction analysis were in the forms of pieces.

3.4.2 Mechanical Analysis

All mechanical tests were performed at room temperature with at least 7 samples for each composition. The standard deviation was calculated in addition to average values.

3.4.2.1 Tensile Test

Tensile tests were performed following the procedure specified in ASTM 638-M 91a (Standard Test Method for Tensile Properties of Plastics) by using a Lloyd 30K Universal Testing Machine.

The shape and dimensions were consistent with Type M-I and the extension rate was 8mm/min. The shape of the tensile specimen is illustrated in Figure 2.9. Tensile strength, Young's modulus, and strain at break values were reported for each specimen. The distance between the grips (D), width (W), and thickness (T) were 80, 7.5 and 2.15 mm respectively.

3.4.2.2 Flexural Test

Test Method-I Procedure A of ASTM D790M-92 (Standard Test Methods for Flexural Properties of Unreinforced and Reinforced Plastics and Electrical Insulating Materials) on rectangular specimens was applied for analysis of flexural behavior. The flexural specimens had the identical shape and dimensions as the tensile specimens. The rate of the cross-head motion was 1.938 mm/min corresponding to a strain rate of 0.01 mm/mm.min and the support span was 50 mm.

3.4.2.3 Impact Test

Pendulum Impact Tester of Coesfeld Material Test was used for Charpy Impact Test. The tests were performed according to the test Method-I Procedure A in ASTM D256-91a (Standard Test Method for Impact Resistance of Plastics). The sample dimensions were 50, 7.5, and 2.15 mm for length, width and thickness respectively.

3.4.3 Thermal Analysis

3.4.3.1 Differential Scanning Calorimetry (DSC) Analysis:

Differential scanning calorimeter (DSC) analyses were performed using a General V4.1.C DuPont 2000. The measurements were carried out in the temperature range of 20-140°C with a heating rate of 20°C/min under nitrogen atmosphere. Changes in T_g values were examined for each composition to see the effect of clay content and type of the method used for composite preparation.

3.4.4 Flow Characteristics

3.4.4.1 Melt Flow Index (MFI) Test

Melt Flow Index Test was performed according to the procedure identified in ASTM D1238-79, condition type T using a Coesfeld Melt Flow Indexer. The conditions were 5 kg load and 200°C. The MFI values were recorded as grams/10 min (g/10min).

CHAPTER IV

RESULTS AND DISCUSSION

4.1 Morphological Analysis

4.1.1 Scanning Electron Microscopy (SEM)

In order to observe the effect of organoclay addition on the morphology of the prepared composites, impact fractured surfaces of the prepared composites were analyzed by means of Scanning Electron Microscopy mainly focusing on the fracture mechanism. The SEM micrographs are presented at x250 and x3500 magnifications.

The fracture mechanism of a polymer is an important subject of interest related to the structure of the material. When a load is applied to a polymer, the weak regions form cracks and voids at the molecular level. These voids can be detected by small-angle X-ray scattering when they reach a size of about 20 to several hundred Angstrom units and the structure can be observed directly by SEM [47].

Figures 4.1 and 4.2 show the impact fractured surfaces of the commercial and synthesized polystyrene respectively. As seen, the two micrographs look similar regarding the smooth lines of crack propagation.

As seen in Figures 4.1 and 4.2 brittle polymers such as polystyrene have straight propagation lines rather than zigzagged or tortuous lines. In such polymers, because of the homogeneous structure, there are not any barriers to stop the crack propagation. The collinear position of the crack lines with respect to one another enhances further growth so that the two cracks coincide and turn into a single crack bringing about fracture with only a small amount of energy [38].

Figures 4.3, 4.4, 4.5 and 4.6 are the micrographs of the in-situ formed materials at different clay contents. It is observed from Figures 4.3 through 4.5 that the crack propagation lines are rather tortuous and enhance the formation of a porous structure upon failure.

35

From a structural standpoint, in the case of well-dispersed polymer layered silicates, many non-linear cracks are formed simultaneously and these non- linear cracks will tend to grow until they interfere with each other. At these points, the stress fields at the tips of the crack lines interact to hinder further growth by reducing the stress at the tips of the cracks. The impact strength of a polymeric material is closely related to the crack formation at the molecular level. If many tortuous cracks are formed during the fracture process, more energy should be absorbed to break the material [38]. This phenomenon explains the highest impact strength obtained for the in-situ formed material at 0.73 wt. % clay content. For the in-situ formed materials, at the highest clay loading linear crack propagation lines are seen but these lines are closer to each other when compared to neat resin. Generally, as the distance between the crack lines is smaller the material can endure higher stresses. At 3.36 wt. % clay loading the porous structure is still maintained (Figure 4.6 b).

Figures 4.7, 4.8, 4.9 and 4.10 reveal the impact fractured surfaces of melt blended composites with increasing clay content respectively. It is evident that the inclusion of clay into the polymer matrix brings about some roughness to the crack propagation path. Among the melt intercalated structures, the nanocomposite containing 1.6 wt. % organoclay exhibits the roughest fracture surface.

Figures 4.11, 4.12, 4.13 and 4.14 correspond to the micrographs of the composites prepared by the masterbatch method at 0.73, 1.6, 2.4 and 3.36 wt. % clay contents respectively. In Figure 4.11 (b) very small circular crack lines are observed. At the lowest clay content (0.73 wt. %), the fracture surface of the material prepared by the masterbatch method has a rather rougher surface compared to the melt intercalated material; this observation confirms the higher impact strength of the material prepared by the masterbatch method.

Through the examination of the SEM micrographs, fracture surfaces of some materials are similar and they are not quite distinguishable from each other. For more accurate and precise analysis of the morphology, Transmission Electron Microscopy (TEM) analysis must be performed as well. Since the TEM has higher resolution, more detailed information about the dispersion of the clay layers can be obtained by TEM analysis.
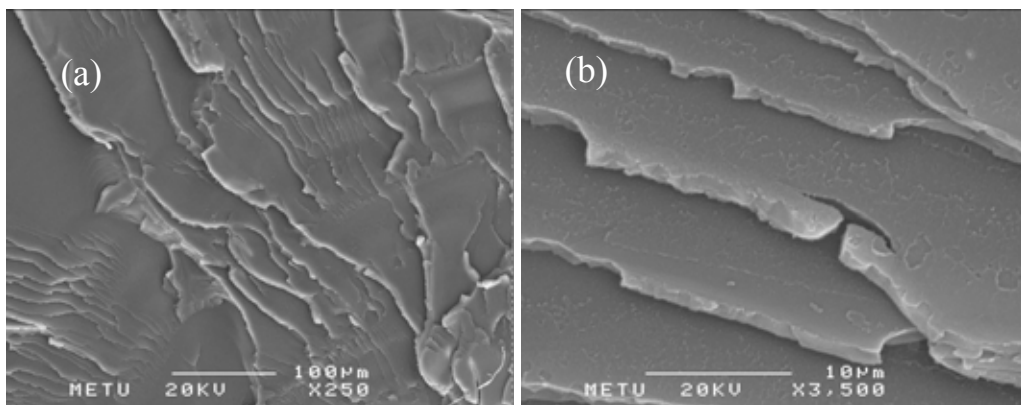
Figure 4.1 SEM micrographs of the commercial polystyrene at (a) 250 (b) 3500 magnifications.
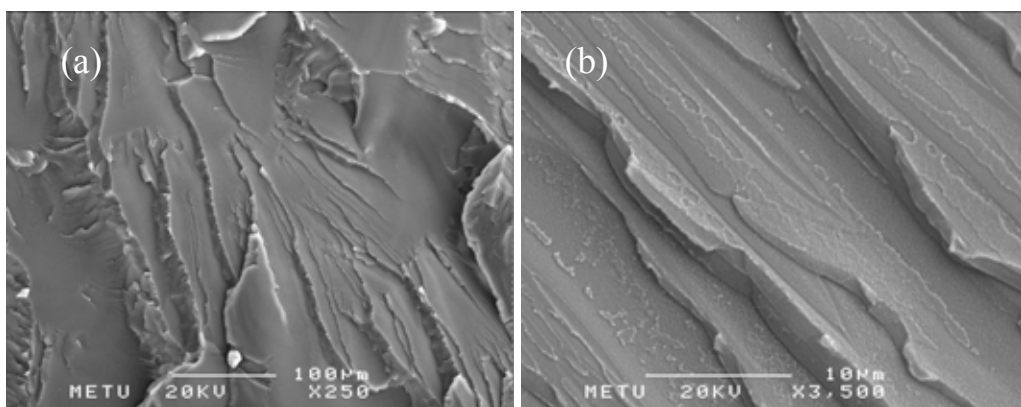
Figure 4.2 SEM micrographs of the synthesized polystyrene at (a) 250 (b) 3500 magnifications.
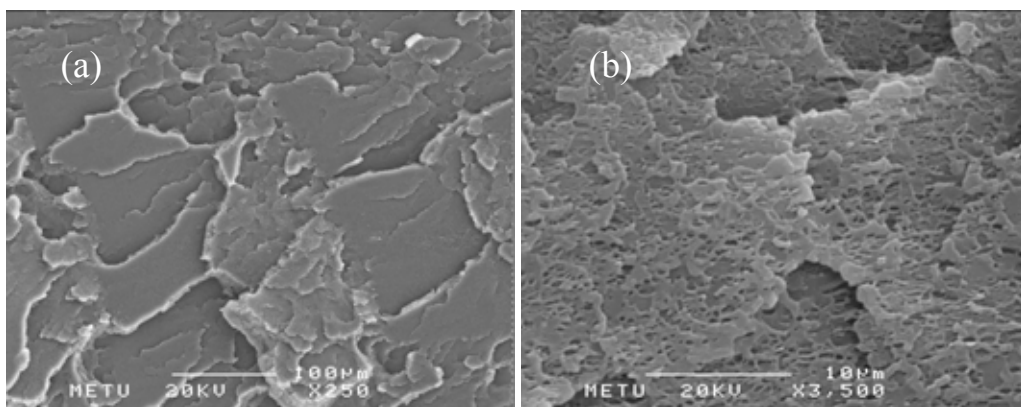
Figure 4.3 SEM micrographs of the nanocomposite prepared by in-situ polymerization method containing 0.73 wt. % MMT at (a) 250 (b) 3500 magnifications.
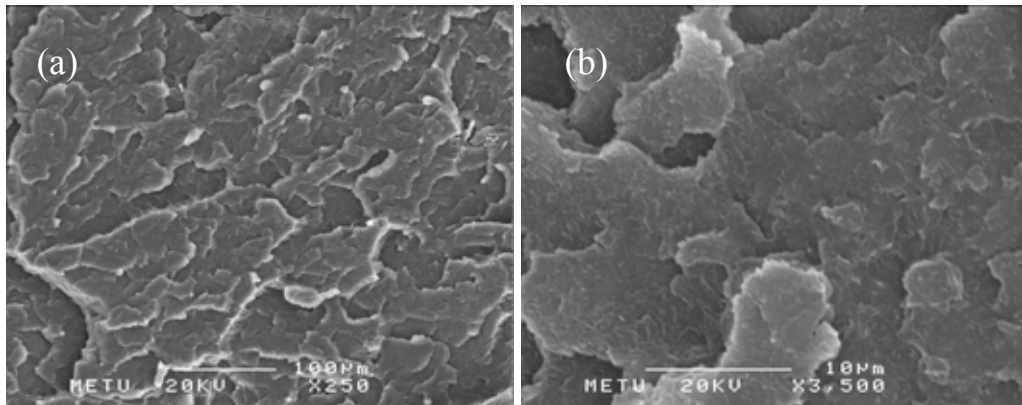
Figure 4.4 SEM micrographs of the nanocomposite prepared by in-situ polymerization method containing 1.6 wt. % MMT at (a) 250 (b) 3500 magnifications.
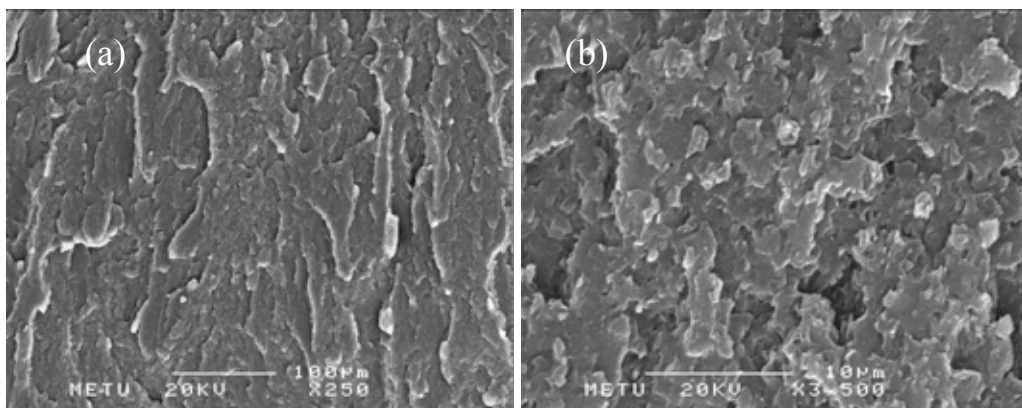
Figure 4.5 SEM micrographs of the nanocomposite prepared by in-situ polymerization method containing 2.4 wt. % MMT at (a) 250 (b) 3500 magnifications.
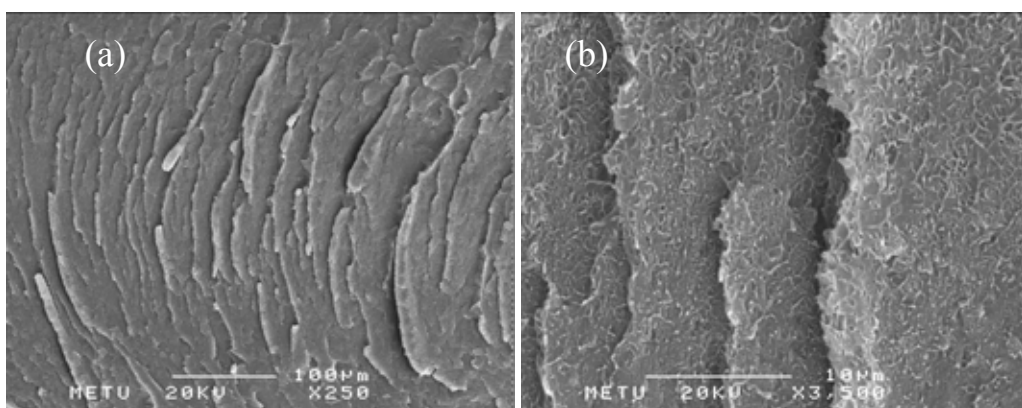
Figure 4.6 SEM micrographs of the nanocomposite prepared by in-situ polymerization method containing 3.36 wt. % MMT at (a) 250 (b) 3500 magnifications.
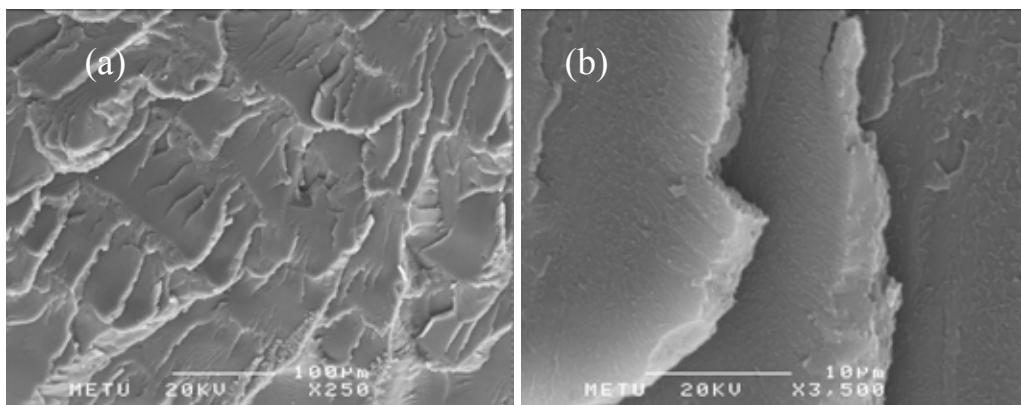
Figure 4.7 SEM micrographs of the nanocomposite prepared by melt intercalation method containing 0.73 wt. % MMT at (a) 250 (b) 3500 magnifications.
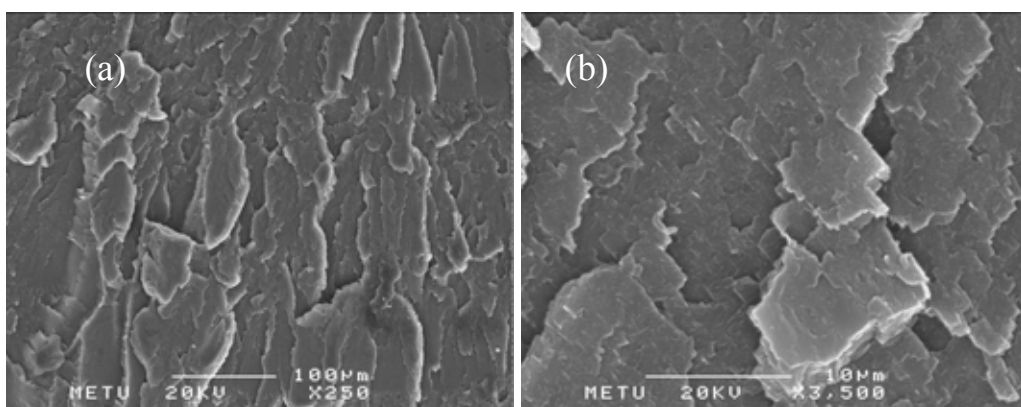
Figure 4.8 SEM micrographs of the nanocomposite prepared by melt intercalation method containing 1.6 wt. % MMT at (a) 250 (b) 3500 magnifications.
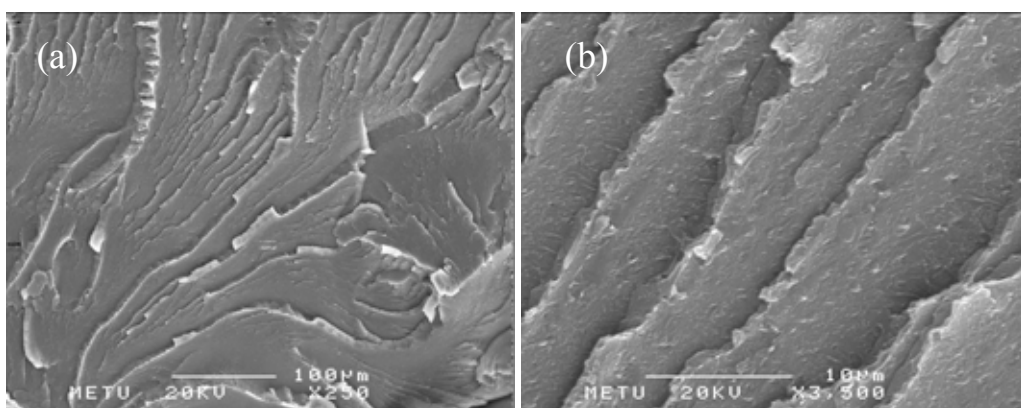
Figure 4.9 SEM micrographs of the nanocomposite prepared by melt intercalation method containing 2.4 wt. % MMT at (a) 250 (b) 3500 magnifications.
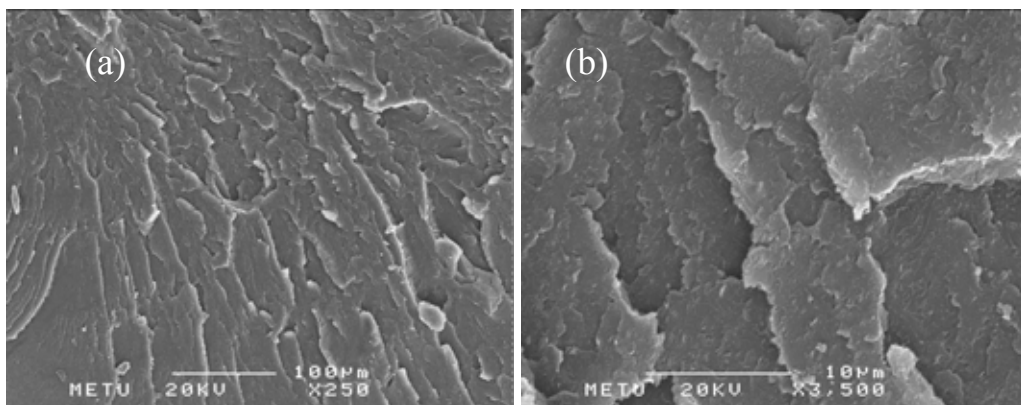
Figure 4.10 SEM micrographs of the nanocomposite prepared by melt intercalation method containing 3.36 wt. % MMT at (a) 250 (b) 3500 magnifications.
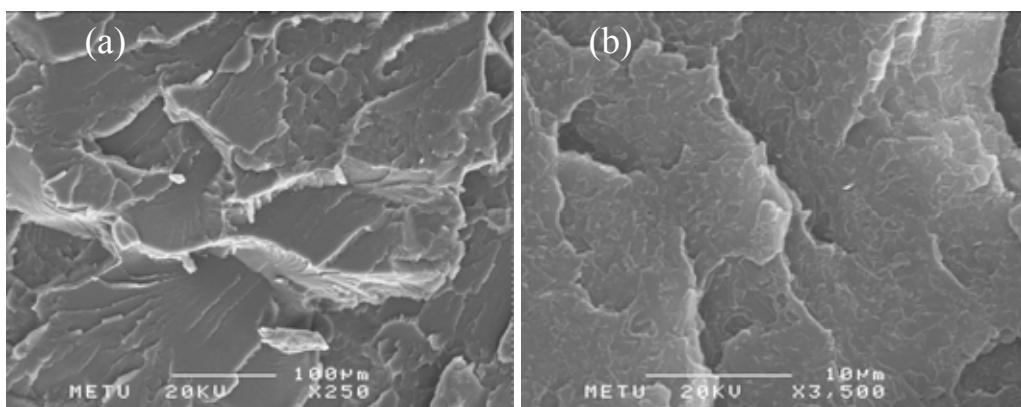
Figure 4.11 SEM micrographs of the nanocomposite prepared by masterbatch method containing 0.73 wt. % MMT at (a) 250 (b) 3500 magnifications.
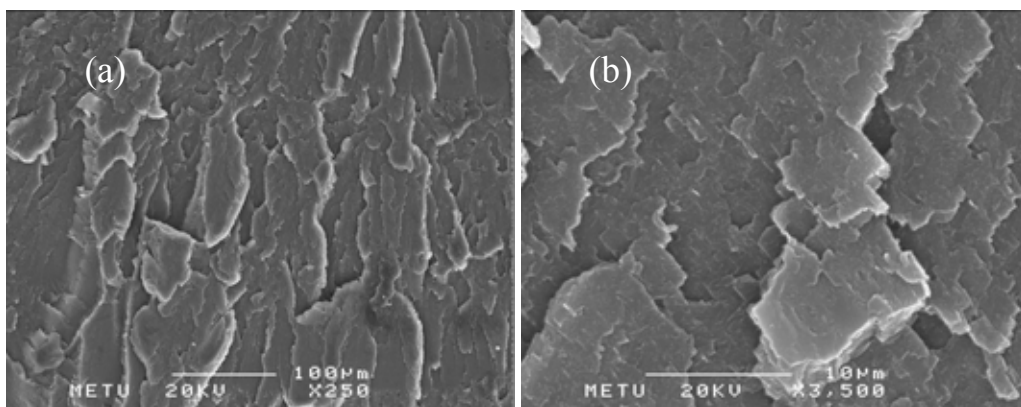
Figure 4.12 SEM micrographs of the nanocomposite prepared by masterbatch method containing 1.6 wt. % MMT at (a) 250 (b) 3500 magnifications.
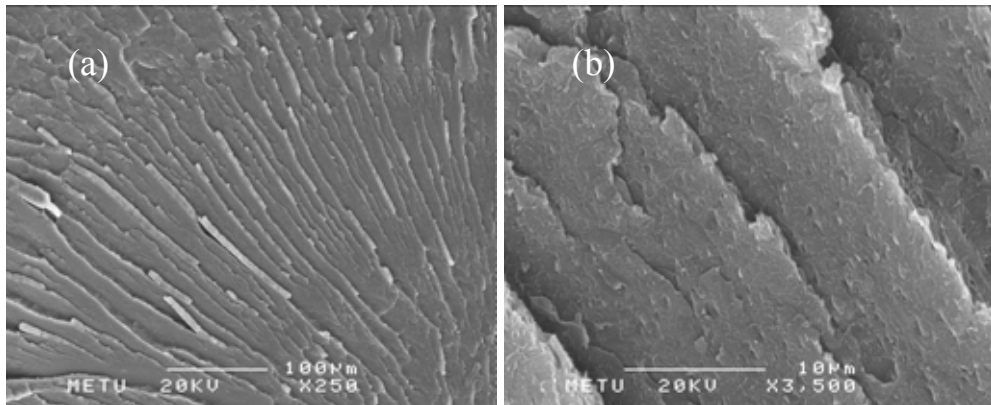
Figure 4.13 SEM micrographs of the nanocomposite prepared by masterbatch method containing 2.4 wt. % MMT at (a) 250 (b) 3500 magnifications.
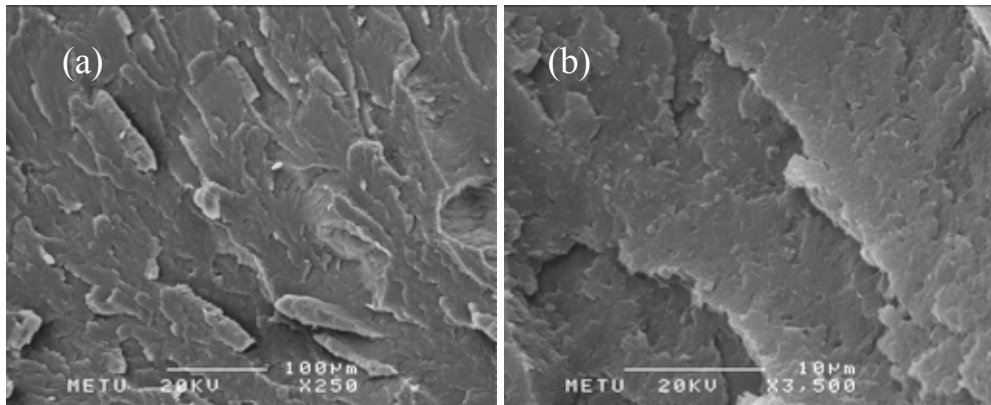
Figure 4.14 SEM micrographs of the nanocomposite prepared by masterbatch method containing 3.36 wt. % MMT at (a) 250 (b) 3500 magnifications.

4.1.2 X-Ray Diffraction Analysis

Table 4.1 d-spacing of the nanocomposites with the corresponding diffraction angles

Organoclay wt. %	Melt Intercalation		In-situ polymerization		Masterbatch	
	d-spacing (Å)	2θ°	d-spacing (Å)	2θ°	d-spacing (Å)	2θ°
0.73	33.02	2.65	36.25	2.43	32.51	2.72
1.6	33.02	2.65	36.78	2.40	32.36	2.74
2.4	33.16	2.64	32.82	2.69	33.02	2.65
3.36	33.51	2.60	33.02	2.65	32.82	2.69
Cloisite 15A d-spacing: 32.94 Å 2θ°: 2.68						

In this study, it is attempted to report the results of the studies on the intercalation of polymers into organoclay layers with regards to their structural, thermal and mechanical properties. XRD patterns provide beneficial information about the d-spacing of the intercalated hybrids by following Bragg's Law: $d=\lambda n/(2\sin\theta)$ at peak positions. The XRD data including d-spacing and peak positions for the modified clay (Cloisite 15A) and the composite materials that are formed by the three methods are shown in Table 4.1. The exemplary diffractograms are presented in Appendix A as well.

The diffractogram of the neat organoclay reveals the basal reflection that is characteristic of the unintercalated repeat distance at d=32.94Å. The basal spacing is in accordance with the value documented in the manufacturer's datasheet.

In nanocomposites, the silicate layers expand to accommodate the polymer chains; thereby make possible the detection of intercalated structures by an increase in d-spacing. In all of the XRD patterns, peaks are clearly seen and it is evident that insertion of polymer chains caused some intercalation but failed to form completely exfoliated structures.

In the diffractograms, some broader peaks with diminishing intensities appear in addition to a dominant sharp peak. The intensities of these secondary and tertiary peaks are not within the limits of accuracy, thus they are not taken into consideration.

42

However, they may in part be explained by the existence of clay layers with different spacings.

An increase in d-spacing is observed for the in-situ formed materials at 1.6 and 0.73 weight % clay loadings with the reflection shifting progressively towards lower angles. This is probably due to the diffusion of the propagating chains within the silicate sheets expanding the galleries. The change in gallery size is small compared to the gallery size of pure clay, since Cloisite 15A has sufficient interlayer spacing permitting the polymerization without further expansion [17]. It should be noted that beyond a certain d-spacing the interlayer attractive forces may not be able to hold the clay layers parallel to each other. Thus, exfoliation would start at high d-spacings. This may be the case for the in-situ formed nanocomposites at 0.73 and 1.6 wt. % organoclay. The in-situ polymerized nanocomposites do not reveal an increase in d-spacing at high clay loadings. This may partially be ascribed to the clay particles remaining as agglomerates. Considering the original high d-spacing of the clay, it is also possible that some intercalation within the clay layers may have occurred without causing a significant increase in d-spacing.

The well-ordered structure of MMT is preserved in the materials prepared by melt intercalation and masterbatch methods. The d-spacings of the materials prepared by the two methods are almost the same as the neat organoclay within practical error limits. In nanocomposites, a decrease in the degree of coherent layer stacking (i.e. a more ordered system) results in peak broadening and intensity loss [10]. Even if some structures seem to have identical d-spacing values, the state of order or the amount of intercalation may be different, distinguishing the structures from each other since they have different peak width and intensities. The XRD analysis alone is not sufficient to detect the amount of intercalation.

4.2 Thermal Analysis

4.2.1 Differential Scanning Calorimetry

Table 4.2 Effect of organoclay content on the glass transition temperature of the nanocomposites prepared by the three methods.

Organoclay wt.%	Glass Transition Temperature (^{o}C)		
	Melt Intercalation	**In-situ poly.**	**Masterbatch**
0 (neat resin)	104.4	105.6	104.4
0.73	104.8	108.5	101.7
1.6	103.9	98.8 (98.7*)	97.9
2.4	104.8	71.8	97.8
3.36	105.5	71.6	97.6

To investigate the effect of organoclay content on the thermal properties of the prepared materials in terms of their T_g values, Differential Scanning Calorimetry (DSC) analyses for neat resins and PS/MMT composites prepared by the three methods were carried out. The results are presented in Table 4.2 and DSC diagrams are given in Appendix B. All the analyses were performed on the 1st run, but for the in-situ formed nanocomposite containing 1.6 wt. % organoclay, the 2nd run was performed as well. The (*) sign denotes the T_g value observed in the 2nd run. It is evident that the T_g observed for the two runs are almost the same within the practical error limits. As seen in the table, bulk polymerized polystyrene (105.6^{o}C) and commercial polystyrene (104.4^{o}C) have T_g values close to each other.

In Table 4.2, it is observed that the in-situ formed nanocomposite at 0.73 wt. % organoclay exhibits the highest glass transition temperature. Theoretically, T_g is defined as the temperature at which the segmental motion of the polymer chains become significant as the temperature is increased [48]. Considering the definition of T_g, the significant improvement can be ascribed to the confinement of intercalated polymer chains within the silicate sheets that prevents the segmental motion of the polymer chains since the intercalation is confirmed by XRD analysis [49].

The restricted segmental motions within the galleries shift the glass transition temperature to higher values. For the in-situ formed nanocomposites, after certain clay loading the glass transition temperature decreases drastically.

As known, the glass transition of a polymer is known to be dependent on factors like forces between the molecules, stiffness of the chains and molecular weight [26]. Since chain end segments are restricted only at one end, they have relatively higher mobility than the internal segments. At a given temperature therefore, chain ends provide a higher free volume for molecular motion. As the number of chain ends increase (which means a decrease in molecular weight), the available free volume increases and consequently there is a depression of T_g. The effect is more pronounced at low molecular weight; but as the molecular weight increases, T_g approaches an asymptotic value [23].

An empirical expression relating the inverse relations between T_g and number average molecular weight M_n is given as;

$$T_g = T_g^{\infty} - C/x \qquad\qquad (4.1)$$

where; C is a constant, x is the chain length and T_g^{∞} is the asymptotic value of the glass transition temperature at infinite chain length [26].

This equation reflects the increased ease of motion for shorter chains. The decrease in T_g with x is only noticeable at low chain lengths. For most commercial polymers x is high enough so that $T_g = T_g^{\infty}$.

At high clay contents, the clay particles may act as blockers stopping the chain propagation causing a decrease in molecular weight, therefore the observed dramatic decrease in T_g values in the in-situ method can be explained by the effect of lower molecular weight on T_g [42]. The results predict the dominancy of the molecular weight effect in decreasing T_g over the effect of organoclay in increasing T_g. Also, at high clay loadings, the clays tend to form agglomerates; there is not much confinement of the polymer chains within the sheets; that also explains the pronounced decrease of the T_g at high clay loadings. However, this decrease may be relatively independent of the preparation method.

In the case of melt blended nanocomposites, glass transition temperature of the polystyrene matrix slightly increased with the addition organoclay. However, for the melt blended composites, even at the highest clay content (3.36wt. %), the T_g

value was not as high as the T_g of the in-situ formed material at the lowest clay loading (0.73wt. %).

The results of the masterbatch method indicate a decrease in glass transition temperature with increasing clay content. For the masterbatch route, the increase of the clay content is accomplished by introducing more masterbatch. Recalling the experimental procedure, masterbatch was synthesized in the presence of high clay loading; therefore it contains short polymer chains. As the content of the organoclay or masterbatch is increased, the molecular weight is decreased. This logic explains the decrease in the T_g values observed in the masterbatch method as the clay content is increased.

4.3 Flow Characteristics

4.3.1 Melt Flow Index Test

Before synthesizing the nanocomposites, it was aimed to synthesize polystyrene such that its melt flow index would be the same as the melt flow index of commercial polystyrene used since MFI is a property correlated with the molecular weight. Therefore, polystyrene was synthesized at different initiator concentrations in order to match the MFI of the neat resins. Figure 4.15 shows the effect of initiator concentration on the MFI values and the black-bordered bar shows the selected initator concentration. In the figure, it is observed that the MFI increases with increasing initiator concentration. This behavior can be interpreted by the decrease of molecular weight in the presence of more free-radicals in a free-radical polymerization medium.
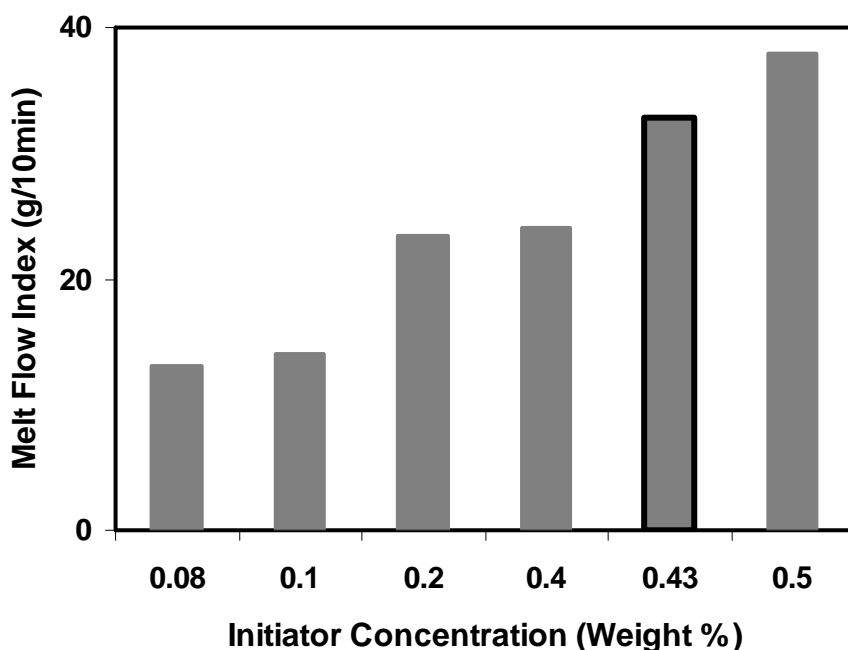
Figure 4.15 Effect of initiator concentration on the melt flow index of polystyrene

Melt Flow Index (MFI) is a measure of the plastic's ability to flow and it is inversely related to melt viscosity. MFI is commonly used to characterize the molecular weight of thermoplastics. Melt flow index of a plastic decreases with increasing molecular weight and increases with decreasing molecular weight [29].

For the MFI measurements, ASTM 1238D procedure were followed, i.e., the polymer was forced to flow through a standard die under 5 kg load at 200°C. MFI results make possible the comparison of the organoclay dispersion effect on each composition since all materials experience the same force and temperature. Table 4.3 exhibits a list of the results expressed in g/10 min.

Table 4.3 Effect of organoclay content on the melt flow index of the nanocomposites prepared by the three methods.

	Melt Flow Index (g/10min)		
Organoclay wt.%	Melt Intercalation	In-situ poly.	Masterbatch
0 (neat resin)	32.9	33.1	32.9
0.73	32.2	28.4	40.6
1.6	29.7	26.0	45.2
2.4	29.4	41.9	46.8
3.36	27.4	88.5	55.1

For the nanocomposites prepared by the melt intercalation method, MFI values decrease with increasing clay content. The clay particles seem to have effects on MFI values from two aspects; (i) The clay particles act as fillers causing an increase in viscosity (ii) The dispersed clay particles further prevent the flow of the polymer chains.

The in-situ polymerized materials on the other hand, reveal a different tendency. It is evident that up to a certain clay loading the MFI values decrease compared to neat resin, however beyond this limit they increase drastically. The polymerization scheme plays a crucial role in observing this effect. Probably at high clay loadings the silicate sheets block the chain propagation. The restricted polymerization within the galleries results in lower molecular weight [42]. The increase in MFI values can be ascribed to the fact that the decrease in molecular weight is dominant over the effect of the clay particles in increasing viscosity.

Effect of organoclay content on the MFI values of the composites prepared by the masterbatch method is exhibited in Table 4.3 as well. It is interesting to report that the MFI values increase with increasing clay content. This may be supported with the phenomena explained for the in-situ formed structures. The masterbatch introduced to the system was synthesized in the presence of high amount of organoclay; consequently, the masterbatch contains short polymer chains. To obtain composites with higher clay content, more masterbatch is introduced to the system. Again, the low molecular weight of the masterbatch matrix is dominant over the filler effect of the clay on changing the MFI values.

4.4 Molecular Weight Determination

Before synthesizing the nanocomposites, it was aimed to synthesize polystyrene such that its molecular weight would approach the molecular weight of the commercial polystyrene. In order to compare the molecular weights of the neat resins, both the number and weight average molecular weights were determined by Gel Permeation Chromatography (GPC) technique. Table 4.4 shows the molecular weight values of the neat resins in addition to the polydispersity index.

Table 4.4 Comparison of the molecular weights of the neat resins

	Commercial polystyrene	Synthesized polystyrene
Weight average molecular weight (M_w)	1.15×10^5	1.30×10^5
Number average molecular weight(M_n)	3.55×10^4	4.44×10^4
Polydispersity index	3.24	2.93

As seen in Table 4.4, the weight and number average molecular weights of the synthesized polystyrene are at the same order of magnitude as the commercial polystyrene. As known, in a bulk free-radical polymerization medium it is hard to control the molecular weight distribution, consequently it is hard to obtain a narrow molecular weight distribution. The main concern is that, the obtained molecular weights for the synthesized polystyrene are within the comparable limits of the commercial polystyrene. Also the results of the Melt Flow Index Test and Differential Scanning Calorimetry are in agreement with the molecular weight analysis, since the glass transition temperature and melt flow index are properties that can be correlated with the molecular weight.

4.5 Mechanical Analysis

In this study tensile, flexural and impact tests were performed to examine the mechanical properties of the synthesized materials. The results of the tests are given in Figures 4.16 through 4.27. The response of the materials prepared by the three methods; melt intercalation (MI), in-situ polymerization (IS) and masterbatch (MB) is compared at 0.73, 1.6, 2.4 and 3.36 weight % organoclay contents.

4.5.1 Tensile Test

The response of a material in a tensile test is well understood by means of a stress-strain curve. The representative stress-strain (%) curves of the commercial polystyrene and synthesized polystyrene are given in Figure 4.16. Stress-strain (%) curves of representative samples from all compositions prepared by the three methods are given in Figures 4.17 through 4.20.

The response of the materials to applied stress distinguishes them as being ductile or brittle. As seen in Figure 4.16 polystyrene exhibits a rapid increase in stress with increasing strain until sample failure, this is the characteristic response of brittle polymers [48]. In Figure 4.16 it is seen that the stress-strain curves of the commercial polystyrene and synthesized polystyrene resemble each other. At low clay loadings (0.73 and 1.6 weight %), the in-situ formed nanocomposites seem to have intercalated and partially exfoliated structures, therefore enduring high limits of stress. At high clay contents, the stress-strain response of the three methods approaches each other. Within the same method, a steeper curve is obtained with the addition of more organoclay as expected, since rigid fillers increase the modulus of the polymers.
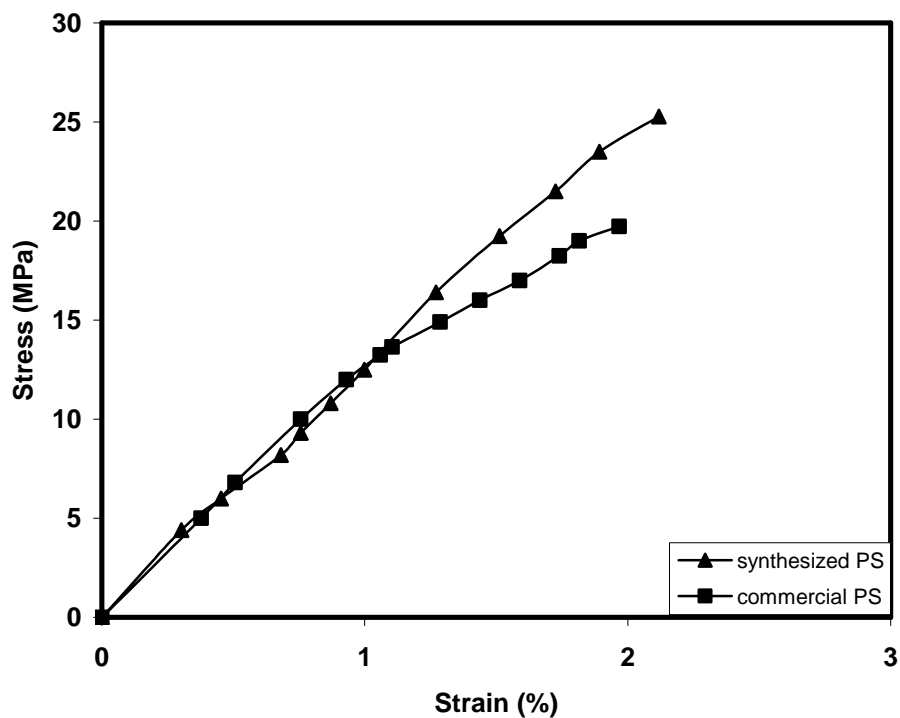
Figure 4.16 Tensile stress-strain (%) curves of the commercial polystyrene and synthesized polystyrene.
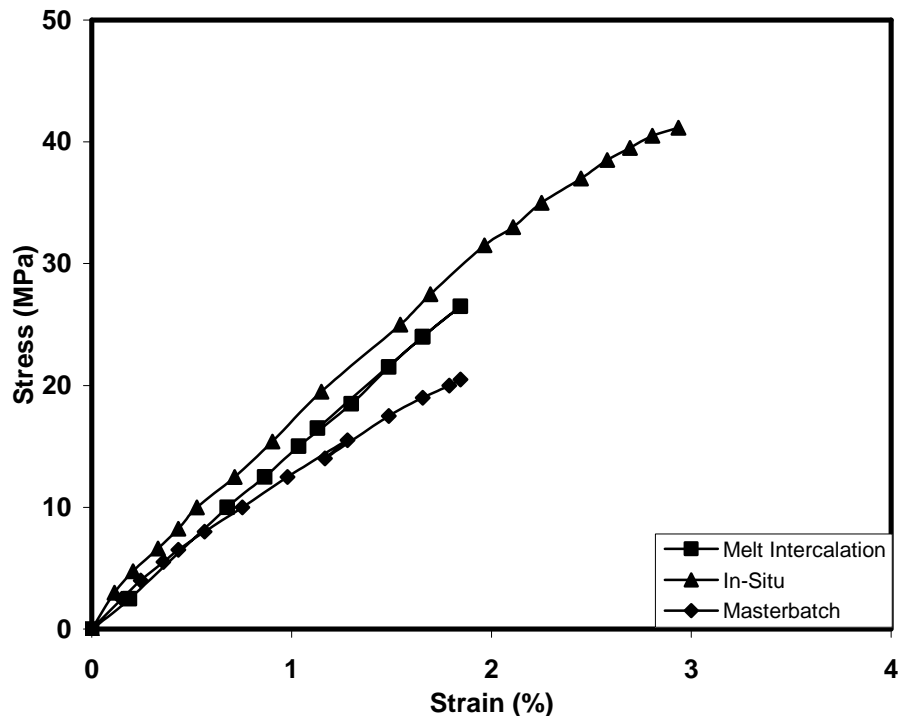
Figure 4.17 Tensile stress-strain (%) curves of the nanocomposites prepared by the three methods containing 0.73 wt. % organoclay.
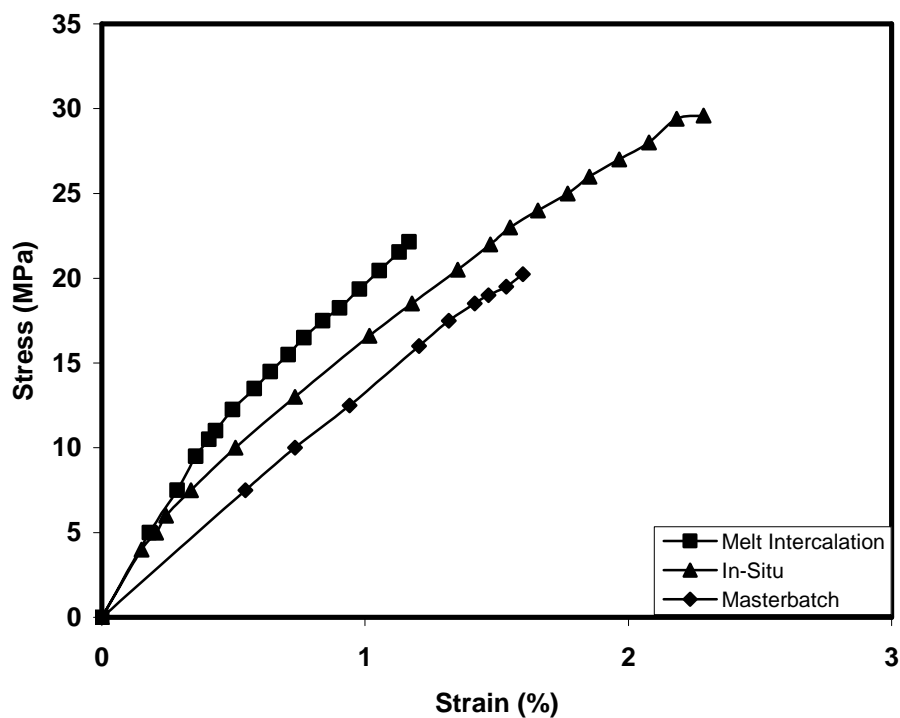
Figure 4.18 Tensile stress-strain (%) curves of the nanocomposites prepared by the three methods containing 1.6 wt. % organoclay.
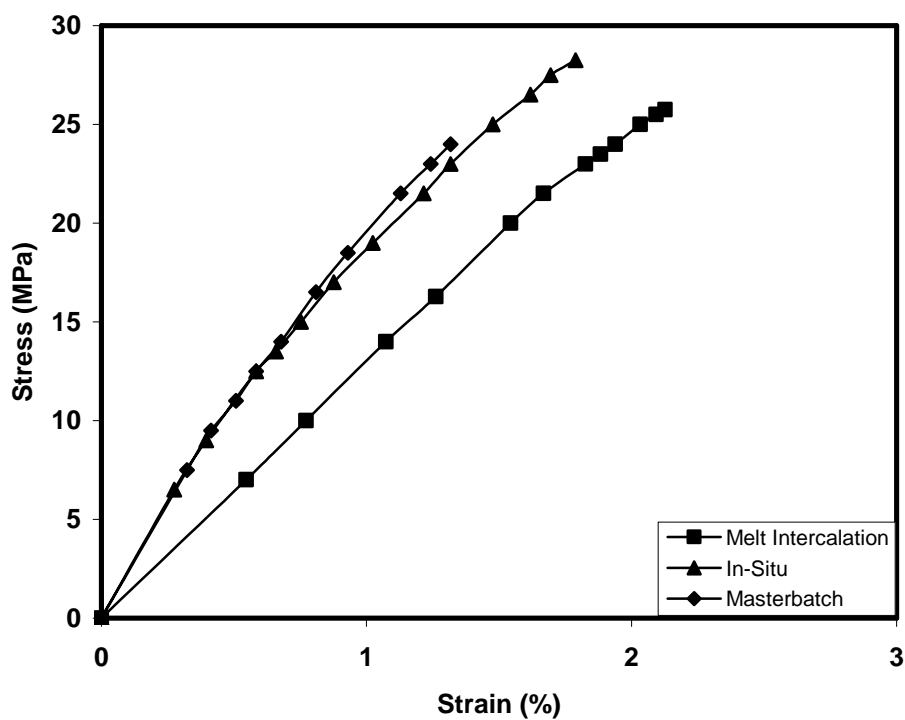
Figure 4.19 Tensile stress-strain (%) curves of the nanocomposites prepared by the three methods containing 2.4 wt. % organoclay.
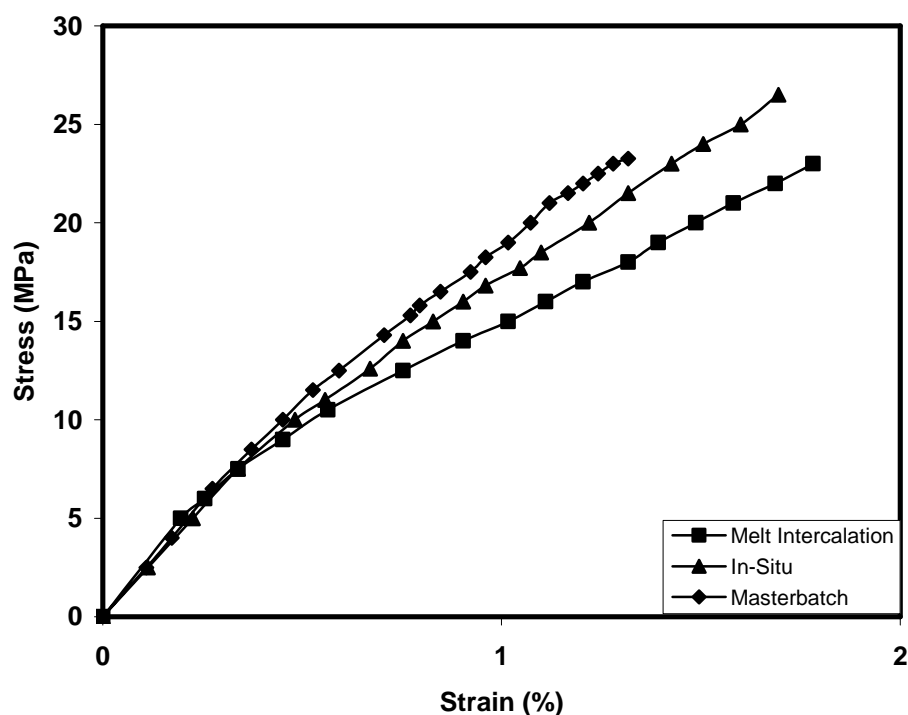
Figure 4.20 Tensile stress-strain (%) curves of the nanocomposites prepared by the three methods containing 3.36 wt. % organoclay.

The tensile properties including Young's modulus, tensile strength and tensile strain at break (%) of all the nanocomposites prepared in this study, together with the values of corresponding virgin polymers are evaluated and the data are presented in Figures 4.21 through 4.23. Table 4.5 is prepared in order to show the improvement obtained in tensile strength with respect to the corresponding neat resin. Figure 4.21 demonstrates the effect of organoclay content on the tensile strength of the nanocomposites prepared by the three methods. It is undeniable that the in-situ formed nanocomposites possess higher tensile strength values compared to the materials prepared by the masterbatch and melt-intercalation methods. The in-situ formed nanocomposite exhibits a maximum value at low clay loading (<1%). The improvement in tensile strength compared to neat resin (50 %) may be ascribed to intercalation of polymer chains into the clay platelets indicating a high level of interaction. Better interaction level facilitates stress transfer to the reinforcement phase yielding sample failure at higher stresses [19].

In-situ formed nanocomposites show a decrease in tensile strength as the amount of clay increases but it still remains at an acceptable level. Particle size has

significant contribution on the tensile strength of the composites related with the interfacial area per unit volume. Particle agglomeration tends to reduce the strength of the material in other words; agglomerates may act as strong stress concentrators. Thereby at high clay loadings the decrease in tensile strength can be attributed to the agglomeration of clay particles [38].

It is known that molecular weight and molecular weight distribution affect the mechanical properties of polymers. The mechanical properties of amorphous polymers improve rapidly up to a critical point then the change levels off after a moderately high molecular weight [48]. In low molecular weight polymers, chain ends may act as imperfections having adverse effects on the stress-strain properties [47]. At high clay loadings, the shielding effect of clay layers blocking the chain propagation may result in low molecular weights. That may in part be a supporting phenomena for the decrease observed in tensile strength. This observation is also supported by the DSC data i.e., at 2.4 and 3.36 wt. % clay contents, the molecular weight of the chains in the matrix is smaller in the in-situ method as indicated by the lower glass transition temperatures observed at these compositions.

It is important to note that, at 0.73 weight % clay loading, the in-situ formed nanocomposite causes almost a 50% increase in tensile strength while the maximum improvement obtained is 15.6% in between the other two methods.

For the most part, the presence of clay does not have a large effect on the tensile strength of the nanocomposites prepared by the masterbatch and melt intercalation methods. At all clay contents, the results of the two methods in terms of tensile strength are close to each other. Considering the steps of the masterbatch method, one would expect for the masterbatch method to show better efficiency in terms of clay dispersion since the clay is dispersed in two stages in masterbatch method. The figures however, exhibit that the masterbatch and melt intercalation methods are close to each other in terms of tensile properties. The deficiency of the masterbatch method may have resulted from the low molecular weight of the prepared masterbatch. This masterbatch was diluted with the commercial PS in the extruder. The nanocomposites prepared by the melt intercalation only have commercial PS at the matrix.

54

The benefit of clay acting as the reinforcing phase increasing modulus (stiffness) is illustrated in Figure 4.22. Table 4.6 exhibits the improvement obtained in tensile modulus of the materials with respect to neat resin. It is observed that in all the three methods, Young's modulus increased at all clay contents compared to neat resin. This is the typical response of the materials reinforced with stiff filler since in a composite the modulus depends on the ratio of the moduli of the two phases [47]. In all the three methods, up to certain clay loading, the Young's modulus increased sharply with increasing clay content, however beyond this point, there appears to be a relatively flat trend. It is worth noting that, for the in-situ formed nanocomposite, the addition of 1.6 wt. % organoclay content caused an approximately 88.5% increase in modulus compared to neat resin. At 1.6 wt. % clay content, the materials prepared by the three methods display their maximum values. The enhancement of modulus is reasonably attributed to the high resistance exerted by the organoclay against the plastic deformation together with the effects of stretching resistance of the polymer chains in the galleries [49].

In the case of modulus, the aforementioned possible chain ends have very little effect on the elastic moduli of hard or brittle materials [47]. At 2.4 and 3.36 wt. % clay contents, for the materials prepared by in-situ method and masterbatch method the chains may be smaller resulting in somewhat smaller modulus. However, below the glass transition temperature the modulus is not very sensitive to the molecular weight. At high clay loadings, two factors compensate each other in changing modulus. The clay particles may form agglomerates destroying the adhesion between the matrix and the filler resulting in a decrease in modulus. On the other hand, the agglomerates still act as fillers which cause an increase in modulus. The flat curve at high clay loadings can be ascribed to these two factors.

For the three methods, change in tensile strain at break with respect to organoclay content is demonstrated in Figure 4.23. Addition of rigid particulate fillers to a polymer matrix decreases the elongations at break since a more brittle structure is obtained. Only in rare instances, if there is a good adhesion between the polymer and the filler the fracture goes from particle to particle rather than following a direct path, the filled polymers have higher elongations at break compared to neat resin [47]. Figure 4.23 is in agreement with the statement i.e., the tensile strain at

break decreases with increasing clay content for the three methods. At 0.73 wt. % and 1.6 wt. % clay content, in-situ formed nanocomposites show an increase in tensile strain at break (%) compared to neat resin. This may be due to the intercalated polymer chains within the silicate sheets leading to a high level of interaction and to the possibility of a partially exfoliated structure at these clay contents. At high clay loadings, for the in-situ formed materials both chain ends and clay agglomerates may act as stress concentrators reducing the elongation at break.
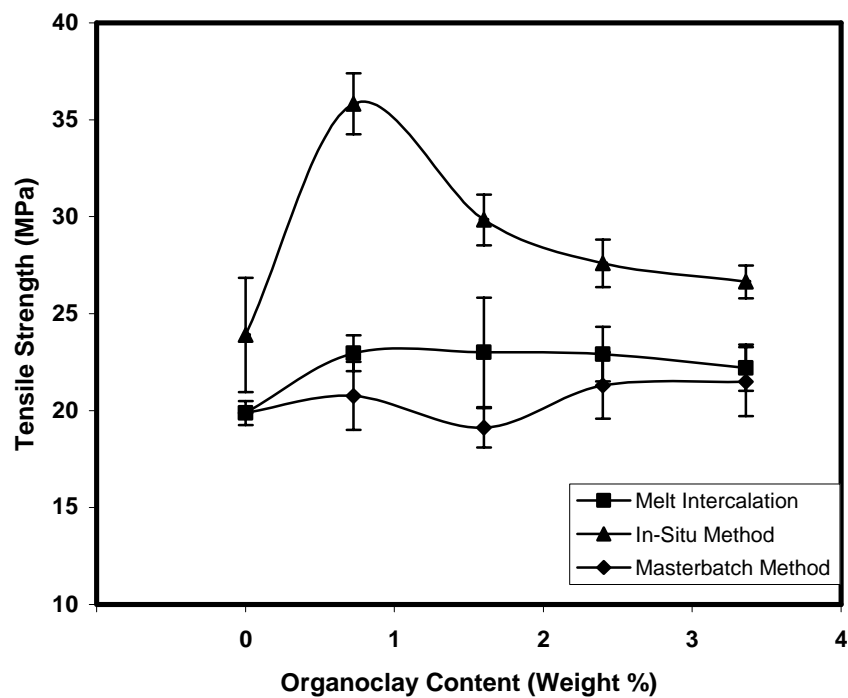
Figure 4.21 Effect of organoclay content on the tensile strength of the nanocomposites prepared by the three methods.
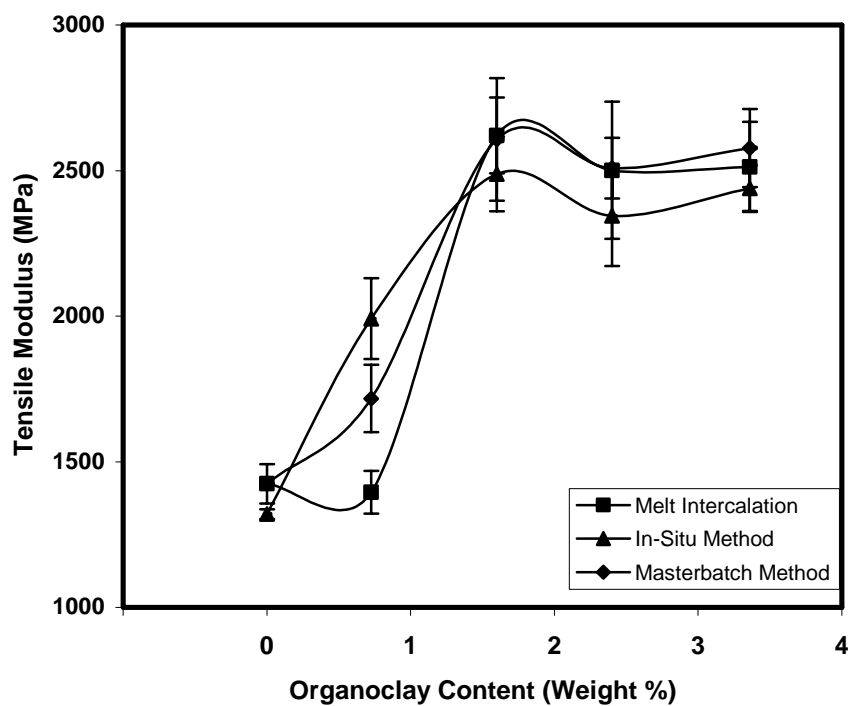
Figure 4.22 Effect of organoclay content on the tensile modulus of the nanocomposites prepared by the three methods.
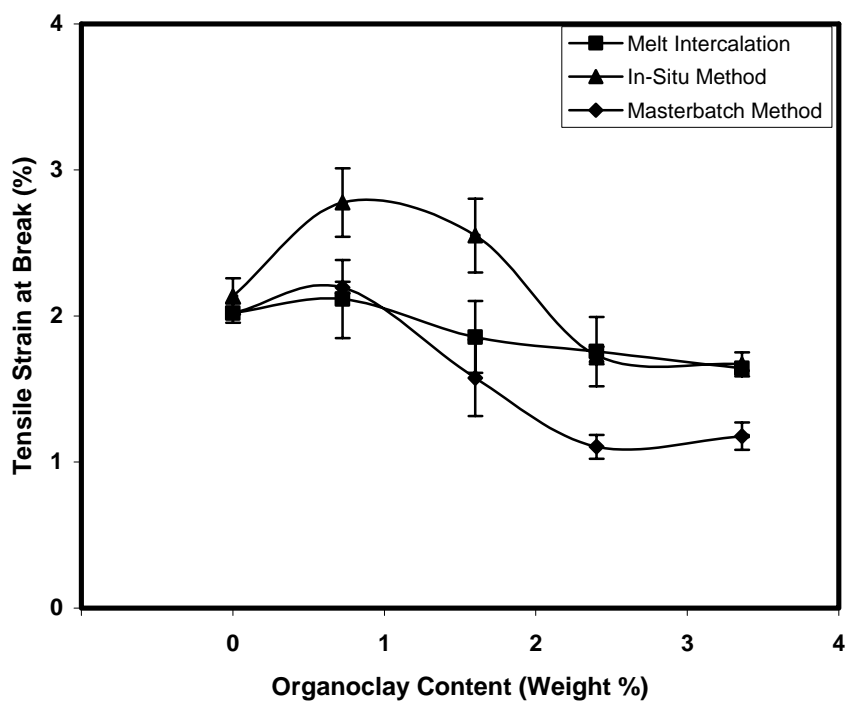
Figure 4.23 Effect of organoclay content on the tensile strain at break (%) of the nanocomposites prepared by the three methods.

57

Table 4.5 % Change of *tensile strength* of the nanocomposites with respect to the method of preparation and organoclay content.

MMT (wt. %)	Method 1 MI (MPa)	% Change wrt to neat resin	Method 2 IS (MPa)	% Change wrt to neat resin	Method 3 MB (MPa)	% Change wrt to neat resin
0 (neat resin)	19.9	0	23.9	0	19.9	1.0
0.73	23.0	15.6	35.8	49.8	20.8	1.0
1.6	23.0	15.6	29.8	24.7	19.1	-4.0
2.4	22.9	15.1	27.6	15.5	21.3	7.0
3.36	22.2	11.6	26.6	11.3	21.5	8.0

Table 4.6 % Change of *tensile modulus* of the nanocomposites with respect to the method of preparation and organoclay content.

MMT (wt. %)	Method 1 MI (MPa)	% Change wrt to neat resin	Method 2 IS (MPa)	% Change wrt to neat resin	Method 3 MB (MPa)	% Change wrt to neat resin
0 (neat resin)	1424	0	1320	0	1424	0
0.73	1595	12.0	1991	50.8	1717	20.6
1.6	2621	84.0	2488	88.5	2607	83.0
2.4	2501	75.6	2345	77.6	2508	76.1
3.36	2513	76.4	2439	84.8	2577	80.1

4.5.2 Flexural Test

Effect of organoclay content on flexural properties of nanocomposites is illustrated in Figures 4.24 through 4.26. Table 4.7 and 4.8 show the % improvement obtained in flexural strength and flexural modulus of the materials compared to neat resin, respectively.

The flexural strength, flexural modulus and flexural strain at break values are higher than the corresponding results obtained from the tensile test. The difference occurs due to the nature of the test since flexural test involves both tension and compression. In a tensile test flaws show up at very small strains but in flexural test the compressive stresses at the upper half of the specimens tend to close cracks rather than open them [38].

The change of flexural strength of the samples with respect to organoclay content shows resemblance to tensile strength change. A maximum value is observed for the in-situ formed nanocomposite at 0.73 weight % clay; 70.6% improvement is obtained for this system compared to neat resin. For the most part, flexural strength decreased with increasing clay content owing to the factors explained in the previous section.

Actually the flexural modulus curves do not show exact behavior of the tensile modulus curves. The flexural modulus of the in-situ formed nanocomposites is lower than the nanocomposites prepared by the other two methods especially at 2.4 and 3.36 wt. % clay contents. These materials have low molecular weight, thus they exhibit lower modulus.

Flexural strain curves look much similar to tensile strain curves in the aspect that the in-situ formed nanocomposites have higher elongations. Flexural strain at break of the in-situ formed materials is much higher in this case compared to the other two methods owing to the intercalated and partially exfoliated structure at low clay contents.

59
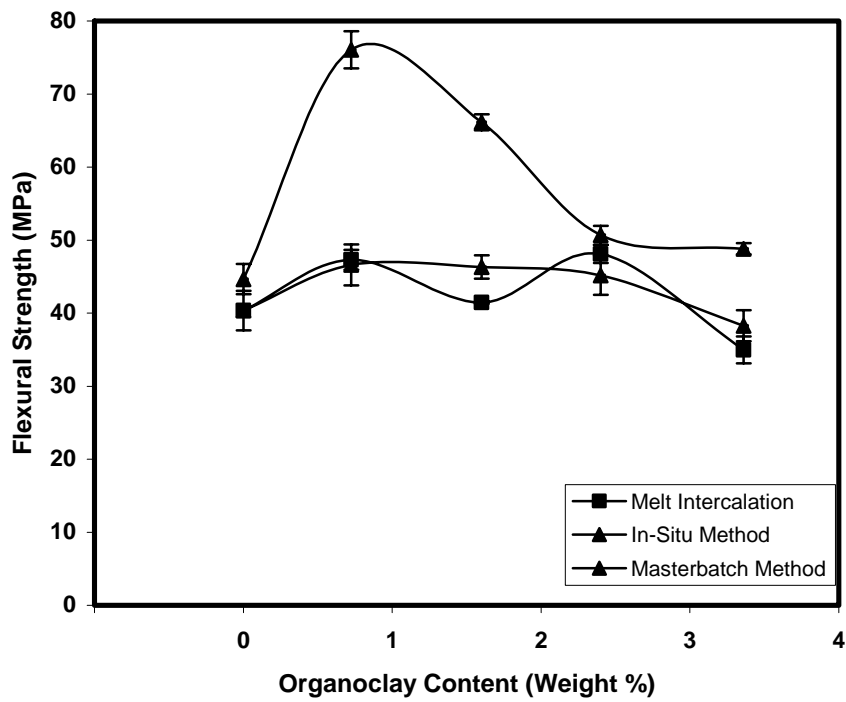
Figure 4.24 Effect of organoclay content on the flexural strength of the nanocomposites prepared by the three methods.
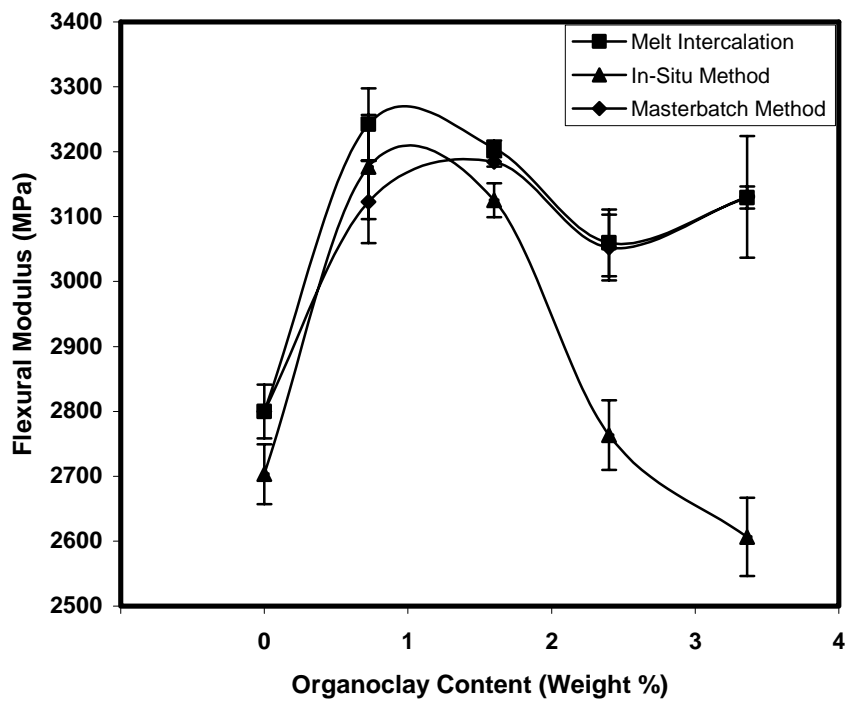
Figure 4.25 Effect of organoclay content on the flexural modulus of the nanocomposites prepared by the three methods.

60
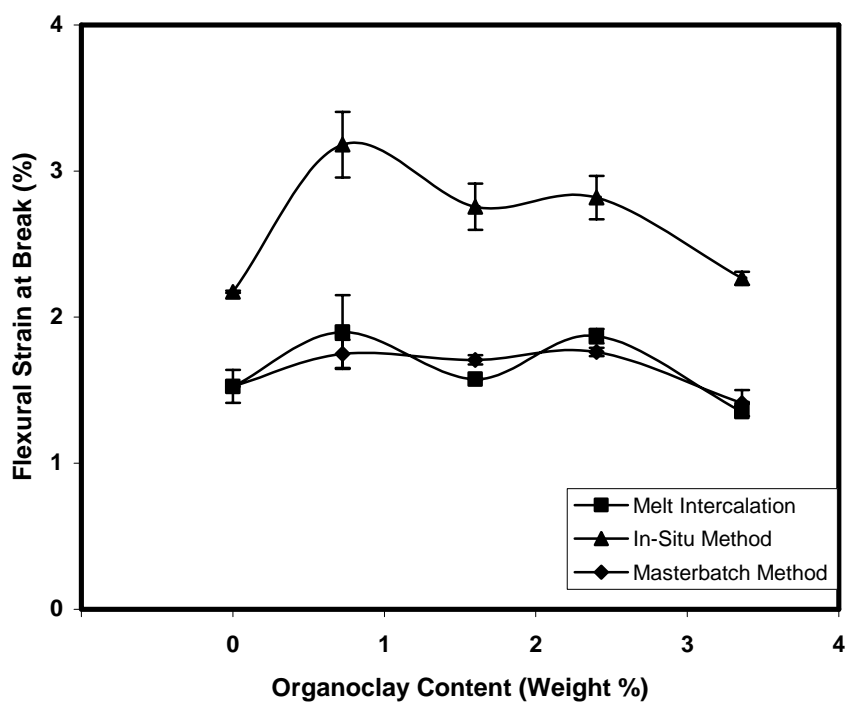
Figure 4.26 Effect of organoclay content on the flexural strain at break (%) of the nanocomposites prepared by the three methods.

Table 4.7 % Change *of flexural strength* of the nanocomposites with respect to the method of preparation and organoclay content.

MMT (wt. %)	Method 1 MI (MPa)	% Change wrt to neat resin	Method 2 IS (MPa)	% Change wrt to neat resin	Method 3 MB (MPa)	% Change wrt to neat resin
0 (neat resin)	40.4	0	44.7	0	40.4	0
0.73	47.3	17.1	76.1	70.6	46.6	15.3
1.6	41.4	2.5	66.1	48.2	46.3	14.6
2.4	48.1	19.1	50.7	2.3	45.1	11.9
3.36	35.0	-13.4	48.8	9.4	38.2	-5.2

Table 4.8 % Change of *flexural modulus* of the nanocomposites with respect to the method of preparation and organoclay content

MMT (wt. %)	Method 1 MI (MPa)	% Change wrt to neat resin	Method 2 IS (MPa)	% Change wrt to neat resin	Method 3 MB (MPa)	% Change wrt to neat resin
0 (neat resin)	2800	0	2703	0	2800	0
0.73	3242	15.8	3176	17.5	3123	11.5
1.6	3205	14.5	3125	15.6	3184	13.7
2.4	3060	9.3	2763	2.2	3052	9.0
3.36	3129	11.8	2606	-3.6	3130	11.8

4.5.3 Impact Test

The effect of organoclay content on the impact strength of the nanocomposites for the three methods is shown in Figure 4.27 and the % improvements obtained compared to corresponding pure resins are given in Table 4.9.

Impact strength of a material is related with its toughness and can be determined by the area under the stress-strain curve. In general brittle polymers, like general purpose polystyrene have low impact strength values [48]. As seen in Table 4.9 the impact strength values (kJ/m^2) obtained for the PS based systems are not significantly high.

Rigid fillers in a rigid polymer generally decrease the impact strength of a polymer [47]. Figure 4.27 confirms this statement, for the PS-MMT nanocomposites impact strength decreased mostly with increasing clay content for the three methods. In-situ formed nanocomposites at 0.73 weight % organoclay content provided the highest impact strength with an improvement of 27.4% compared to neat resin (Table 4.9). This is again due to the intercalated and partially exfoliated structure observed at low clay contents for the nanocomposites prepared by the in-situ method.

The three methods exhibited maximum values at 0.73wt% clay content. The impact strength decreased dramatically at high clay loadings due to possible agglomerations of clay particles. When the clay agglomerates are present, the stress acting on a small part of the material surface would be much greater than the average stress applied to the test specimen [38]. As a result, the material breaks at a stress which is less than the expected value. The in-situ formed nanocomposite shows a 17.7% reduction in impact strength at 3.36 weight % organoclay compared to neat resin. It is known that the impact strength is a function of the molecular weight of a polymer. In addition to the agglomeration effect, the decrease of the molecular weight of the in-situ formed nanocomposites at high clay contents may be responsible for the decrease in the impact strength.
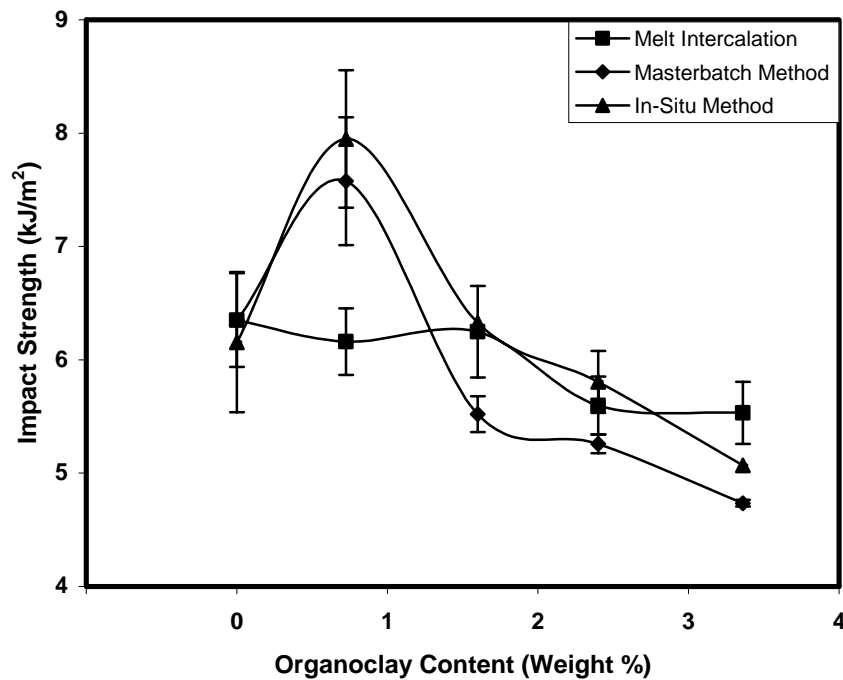
Figure 4.27 Effect of organoclay content on the impact strength of the nanocomposites prepared by the three methods.

Table 4.9 % Change *of impact strength* of the nanocomposites with respect to the method of preparation and organoclay content

MMT (wt. %)	Method 1 MI (kJ/m^2)	% Change wrt to neat resin	Method 2 IS (kJ/m^2)	% Change wrt to neat resin	Method 3 MB (kJ/m^2)	% Change wrt to neat resin
0 (neat resin)	6.3	0	6.2	0	6.3	0
0.73	6.2	-1.6	7.9	27.4	7.6	20.1
1.6	6.2	-1.6	6.3	1.6	5.5	-12.7
2.4	5.6	-11.1	5.8	-6.4	5.3	-15.6
3.36	5.5	-12.7	5.1	-17.7	4.7	-25.4

CHAPTER V

CONCLUSIONS

A series of polystyrene (PS)- Montmorillonite (MMT) nanocomposites were prepared by melt intercalation, in-situ polymerization and masterbatch methods at 0.73, 1.6, 2.4 and 3.36 weight % clay loadings in addition to synthesizing pure polystyrene by free-radical polymerization. SEM analysis elucidated that the crack propagation lines were rather straight and smooth for the neat resins. At low clay contents, the in-situ polymerized materials were clearly distinguishable from the way the cracks propagated within the structure i.e., the crack propagation occurred in a tortuous manner in these materials.

In this study, the insertion of polymer chains caused some intercalation but failed to form completely exfoliated structures. For the in-situ formed materials, the d-spacing increased from 32.94 Å to 36.25 Å and 36.78 Å at 0.73 and 1.6 wt. % clay contents respectively, suggesting the formation of intercalated structures. The increase in d-spacing was not significant relative to pure organoclay since the d-spacing of the pure organoclay was already sufficient to accommodate the polymer chains. The d-spacing of the other materials prepared remained nearly unchanged with respect to pure organoclay.

The results of the melt flow index suggested the decrease of the matrix molecular weight in the in-situ formed materials at high clay loadings. Also, the melt flow index values of the materials prepared by the masterbatch method were in good agreement with this phenomenon i.e., the MFI values increased with increasing clay content. The MFI values of the melt blended nanocomposites decreased with increasing organoclay content as expected.

The in-situ formed nanocomposite at 0.73 wt. % organoclay content exhibited the highest glass transition temperature with an increase from 105.6 ^{o}C to 108.5 ^{o}C, nevertheless, a decrease in T_g values was observed beyond this organoclay content. The trend of the T_g change of the nanocomposites further consolidated the molecular weight effect predicted in the melt flow index test. DSC analysis revealed that clay layers containing well-intercalated polymer chains are responsible for the T_g increase.

For the in-situ formed materials, the optimum organoclay content to yield the best improvements in mechanical properties was 0.73 wt. % organoclay. At this clay content, highest improvement in flexural strength (70.6%), tensile strength (49.8%) and impact strength (27.4%) were observed compared to the corresponding properties of the neat resin. In-situ polymerization did not prove to be efficient at high clay loadings in terms of mechanical properties. In the three methods, Young's modulus increased at all clay contents compared to neat resin but a linear relationship between the amount of organoclay and Young's modulus was not observed. At all clay contents, masterbatch and melt intercalation methods approached each other with regard to the mechanical properties. For the three methods, tensile, flexural and impact strength, as well as the tensile and flexural strain at break increased up to a certain clay content, but decreased beyond this critical point. At high clay loadings, stress-strain response of the three methods converged exhibiting a more brittle structure at high clay contents.

From the results so far obtained, it can be concluded that in the case of polymer/clay nanocomposites, high level of adhesion and well-dispersion of clay platelets play crucial roles in promoting thermal and mechanical properties. In-situ polymerization method at low clay contents seems to end up with satisfying thermal and mechanical properties.

REFERENCES

1.Fischer H., "Polymer nanocomposites: from fundamental research to specific applications", <u>Materials Science & Engineering C</u>, vol.23, 763-772, 2003.

2. Luo J. and Daniel I.M., "Characterization and modeling of mechanical behavior of polymer/clay nanocomposites", <u>Composites Science and Technology</u>, vol.63, 1607-1616, 2003.

3. Rothon R.N., "Particulate-Filled Polymer Composites", 2nd edition, Rapra Technology Limited, United Kingdom, 2003.

4. Akovali G., "Handbook of Composite Fabrication", Rapra Technology Ltd., United Kingdom, 2001.

5. Mazumdar S.K., "Composites Manufacturing Materials Materials, Product and Process Engineering", CRC Press, U.S.A., 2002.

6. "Polymeric Materials Encyclopedia", vol. 9, 6806-6813, CRC Press, New York, 1996.

7. Schwartz M.M., "Composite Materials, Volume II: Processing, Fabrication and Applications", Society of Manufacturing Engineers Publications, New Jersey, 1989.

8. Strong A. B., "Fundamentals of Composites Manufacturing: Materials, Methods and Applications", Society of Manufacturing Engineers, Publications Development Dept., Reference Publications Division, Dearborn, 1989.

9. Muccio E.A., "Plastics Processing Technology", ASM International, U.S.A., 1994.

10. Pinnavaia T.J. and Beall G.W., "Polymer-Clay Nanocomposites", John Wiley and Sons, Ltd., New York, 2000.

11. Zeng Q. H., Wang D.Z., Yu A.B. and Lu G.Q., "Synthesis of polymer-montmorillonite nanocomposites by *in-situ* intercalative polymerization", Nanotechnology, vol.13, 549-553, 2002.

12. Chamley H., "Clay Sedimentology", Springer-Verlag, Berlin,1986.

13. "Ullmann's Encyclopedia of Industrial Chemistry", 5th edition,VCH, vol. A7, 110-119, New York, 1992.

14. "Kirk-Othmer Encyclopedia of Chemical Technology", 4th ed., vol 6, 381-409 John Wiley and Sons, Inc., New York, 1993.

15. Alexandre M. and Dubois P., "Polymer-layered silicate nanocomposites: preparation, properties and uses of a new class of materials", Materials Science and Engineering, vol.28, 1-63, 2000.

16. Kornmann X.,"Synthesis and Characterization of Thermoset-Clay Nanocomposites", Lulea University of Technology, Sweden, 2000.

17. Doh J.G. and Cho I., "Synthesis and properties of polystyrene-organoammonium montmorillonite hybrid", Polymer Bulletin, vol.41, 511-518, 1998.

18. Su S., Jiang D.D. and Wilkie C.A., "Novel polymerically-modified clays permit the preparation of intercalated and exfoliated nanocomposites of styrene and its copolymers by melt blending", Polymer Degradation and Stability ,vol. 83, 333-346, 2004.

19. LeBaron P.C., Wang Z. And Pinnavaia T.J., "Polymer-layerd silicate nanocomposites:an overview", Applied Clay Science, vol.15, 11-29, 1999.

20. Gilman J.W., Jackson C.L., Morgan A.B., Harris R.H., Manias E., Giannelis E.P., Wuthenow M., Hilton D. And Phillips S.H., "Flammability properties of polymer-layered silicate nanocomposites, polypropylene and polystyrene nanocomposites", <u>Chemistry of Materials</u>, vol. 12, 1866-1873, 2000.

21. Krishnamoorti R.and Yürekli K., "Rheology of polymer layered silicate nanocomposites", Current Opinion in Colloid and Interface Science", vol.6, 464-470, 2001.

22. "Ullmann's Encyclopedia of Industrial Chemistry", 5th edition, VCH Publishers, vol. A21, 617-625, New York, 1992.

23. Ebewele R.O., "Polymer Science and Technology", CRC Press LLC, U.S.A., 2000.

24."Polymeric Materials Encyclopedia", vol. 9, 6806-6813, CRC Press, New York, 1996.

25. Carraher C.E.Jr., "Seymour/Carraher's Polymer Chemistry: an Introduction" ,4th edition, Marcel Dekker ,Inc., New York, 1996.

26. Rosen S.L., "Fundamental Principles of Polymeric Materials", 2nd edition, John Wiley and Sons, Inc., New York, 1993.

27. "Encyclopedia of Polymer Science and Technology", vol.13,156-200, John Wiley and Sons, Inc., New York, 1971.

28. Progelhof R.C. and Throne J.L., "Polymer Engineering Principles-Properties, Processes and Tests for Design", Hanser/Gardner Publications, Inc., Cincinatti, 1993.

29. Rauwendaal C., "Understanding Extrusion", Hanser/Gardener Publications, Inc., Cincinatti, 1998.

30. Rodriguez F., "Principles of Polymer Systems", 4th edition, Taylor and Francis Publishers, USA, 1996.

31. www.tut.fi/.../moduuli_6/ hypertext/3/3_2.html

32. Cullity B.D., "Elements of X-Ray Diffraction", 2nd edition, Addison-Wesley Publishing Company, Inc., USA, 1978.

33. Duane M. M. and Reynolds R.C., "X-Ray Diffraction and the Identification and Analysis of Clay Minerals", Oxford University Press, Oxford, 1989.

34. Goldstein J.I., Newbury D.E., Echlin P., Joy D.C., Fiori C., Lifshin E., "Scanning Electron Microscopy and X-Ray Microanalysis", Plenum Press, USA, 1981.

35. "Encyclopedia of Polymer Science and Technology", vol.15, 79-509, John Wiley and Sons, Inc., New York, 1971.

36. http://www.psrc.usm.edu/macrog/dsc.htm

37. 'Annual Book of ASTM Standards', Vol.08.01, American Society for Testing and Materials ASTM D638-91a, Philadelphia, USA, 1993.

38. Nielsen L.E., "Mechanical Properties of Polymers", Reinhold Publishing Corporation, USA, 1962.

39. Shah V., 'Handbook of Plastic Testing Technology', 2nd Edition, Wiley-Interscience Publication, USA, 1998.

40. 'Annual Book of ASTM Standards', Vol.08.01, American Society for Testing and Materials ASTM D790M, Philadelphia, USA, 1993.

41. 'Annual Book of ASTM Standards', Vol.08.01, American Society for Testing and Materials ASTM D256, Philadelphia, USA, 1993.

42. Xie W., Hwu J.M., Jiasng G.J., Buthelezi T.M. and Pan W., "A study of the effect of surfactants on the properties of polystyrene-montmorilllonite nanocomposites", Polymer Engineering and Science, vol.43, 214-222, 2003.

43. Zhang W.A., Chen D.Z., Xu H.Y., Shen X.F., and Fang Y.E., "Influence of four different types of organophilic clay on the morphology and thermal properties of polystyrene/clay nanocomposites prepared by the γ-ray radiation technique", European Polymer Journal, vol.39, 2323-2328, 2003.

44. Lepoittevin B., Pantoustier N., Devalckenaere M., Alexandre M., Calberg C., Jerome R., Henrist C., Rulmont A. And Dubois P., "Polymer/layered silicate nanocomposites by combined intercalative polymerization and melt intercalation: a masterbatch process", Polymer, vol.44, 2033-2040, 2003.

45. Fu X., and Qutubuddin S., "Synthesis of polystyrene-clay nanocomposites", Materials Letters, vol.42, 12-15, 2000.

46. Zhang J., and Wilkie C.A., "A carbocation substituted clay and its styrene nanocomposite", Polymer Degradation and Stability, vol.83, 301-307, 2004.

47. Nielsen L. and Landel R., "Mechanical Properties of Polymers and Composites", 2nd Edition, Marcel Dekker Inc., USA, 1993.

48. Seymour R B., Carraher C E., 'Structure-Property Relationships in Polymers', Plenum Press, New York, 1984.

49. Noh M.W., Lee D.C., "Synthesis and characterization of PS-clay nanocomposite by emulsion polymerization", Polymer Bulletin, vol. 42, 619-626, 1999.

APPENDIX A

A.1 X-RAY DIFFRACTION PATTERNS
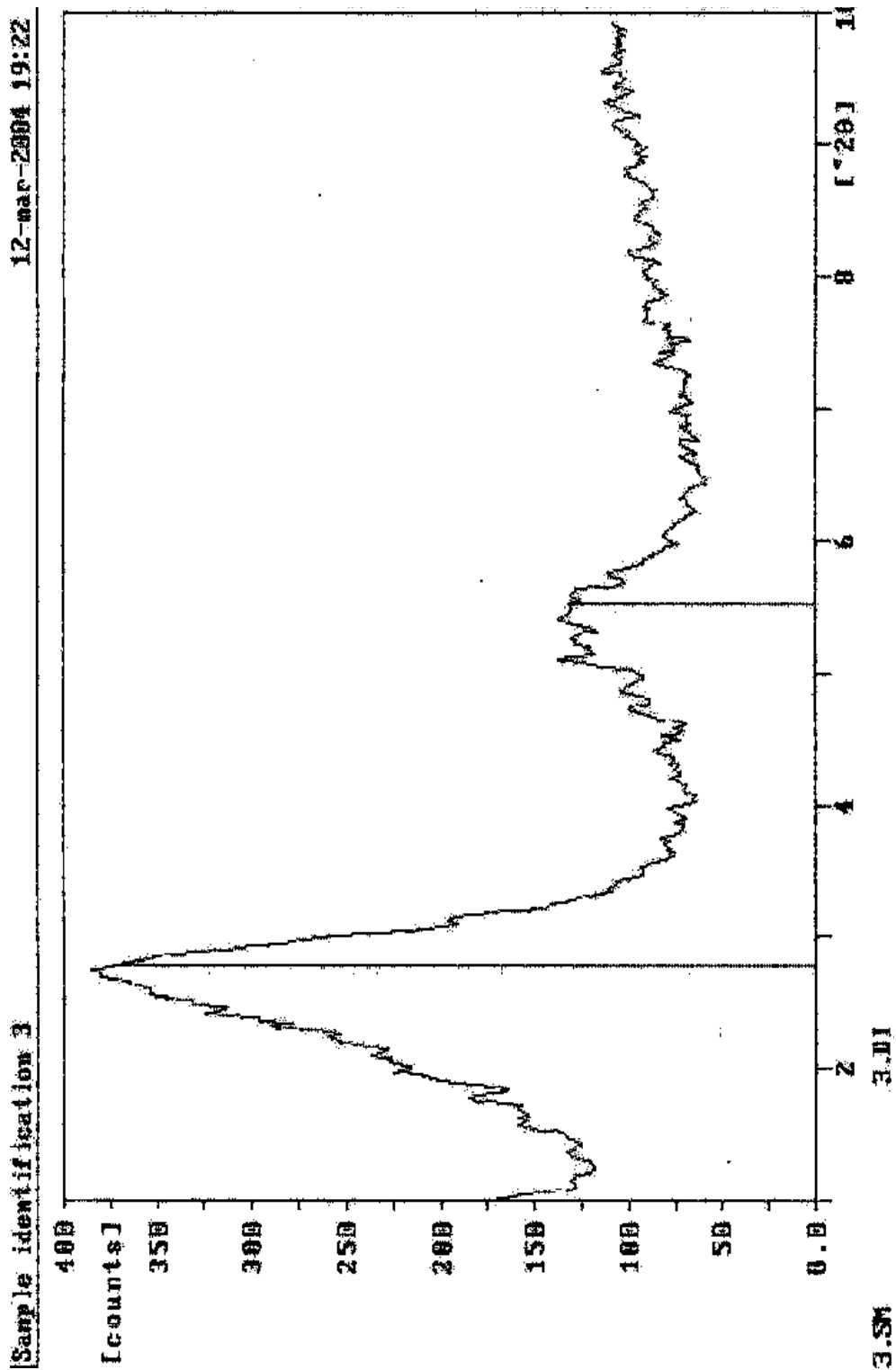
Figure A.1.1 X-ray diffractogram of the sample prepared by melt intercalation method containing 0.73 wt. % organoclay.
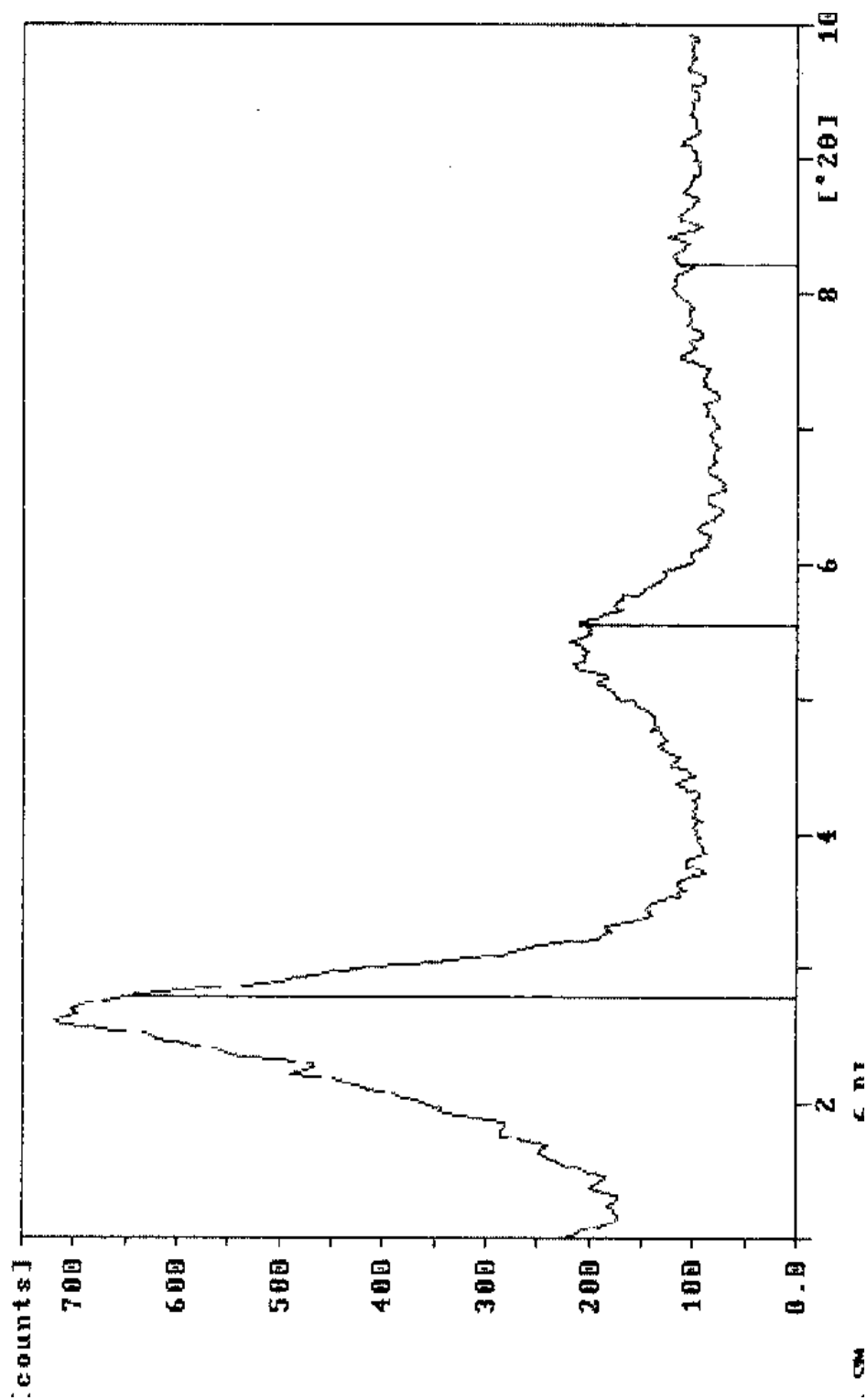
Figure A.1.2 X-ray diffractogram of the sample prepared by melt intercalation method containing 1.6 wt. % organoclay.
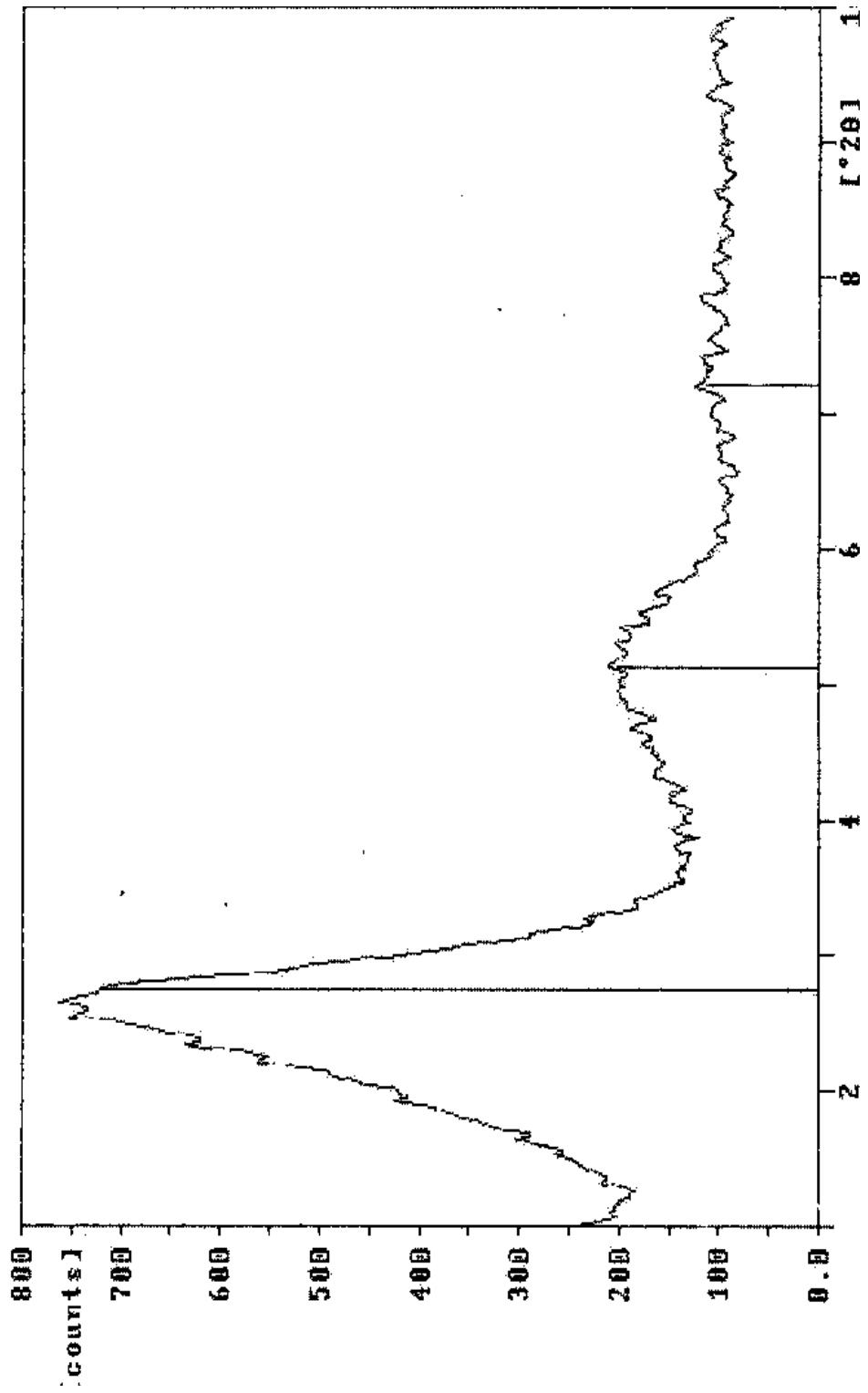
Figure A.1.3 X-ray diffractogram of the sample prepared by melt intercalation method containing 2.4 wt. % organoclay.
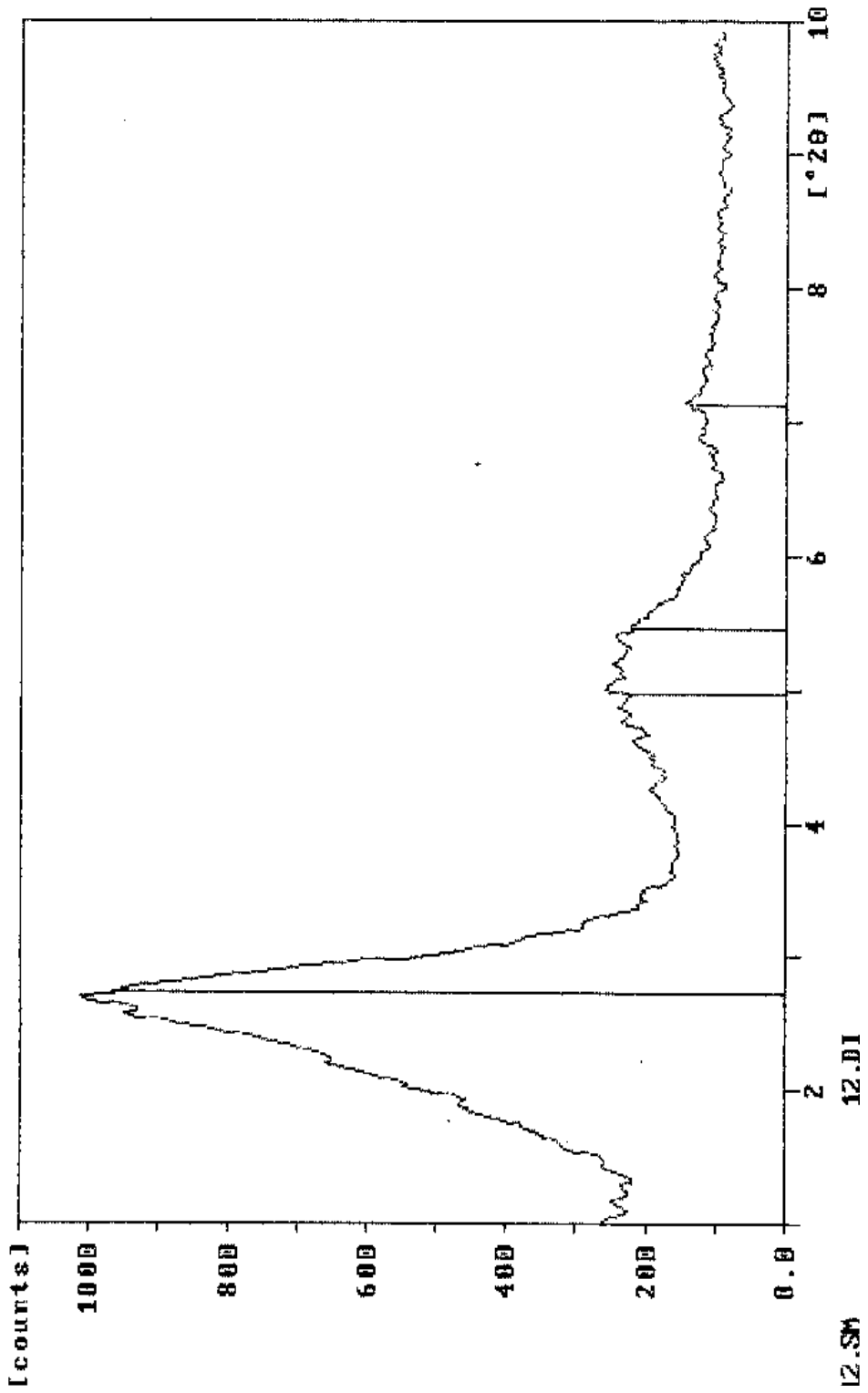
Figure A.1.4 X-ray diffractogram of the sample prepared by melt intercalation method containing 3.36 wt. % organoclay.
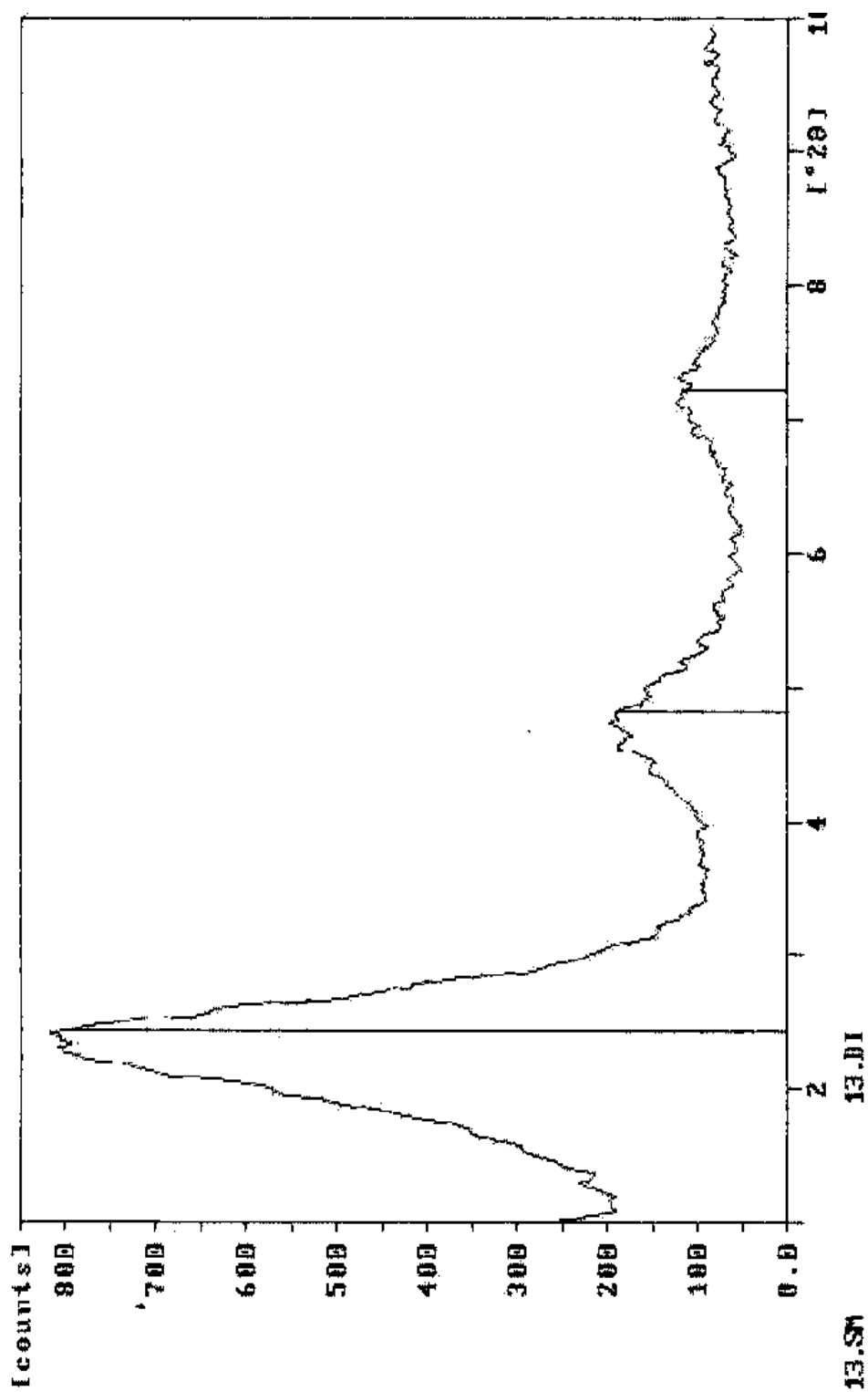
Figure A.1.5 X-ray diffractogram of the sample prepared by in-situ polymerization method containing 0.73 wt. % organoclay.

76
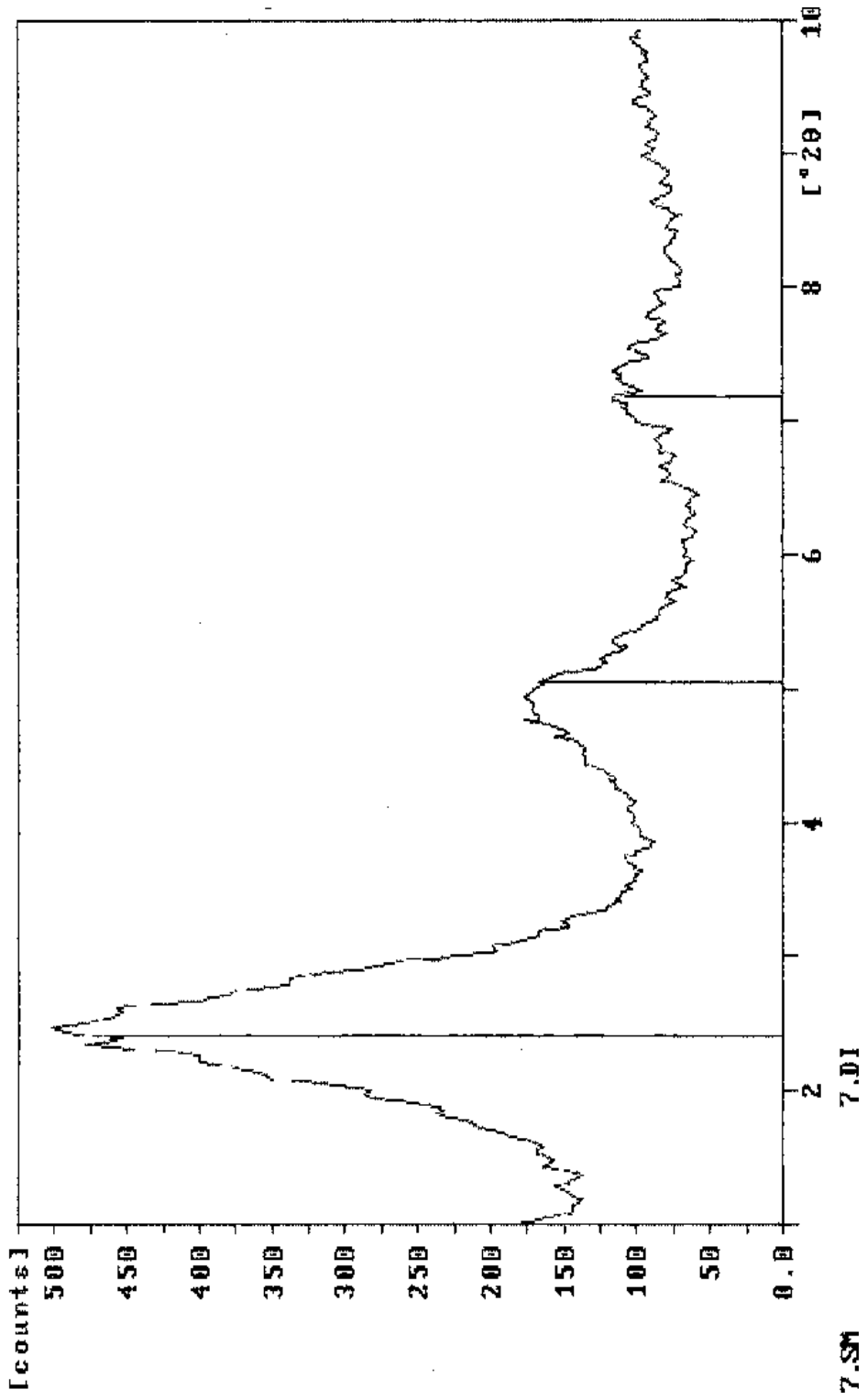
Figure A.1.6 X-ray diffractogram of the sample prepared by in-situ polymerization method containing 1.6 wt. % organoclay.
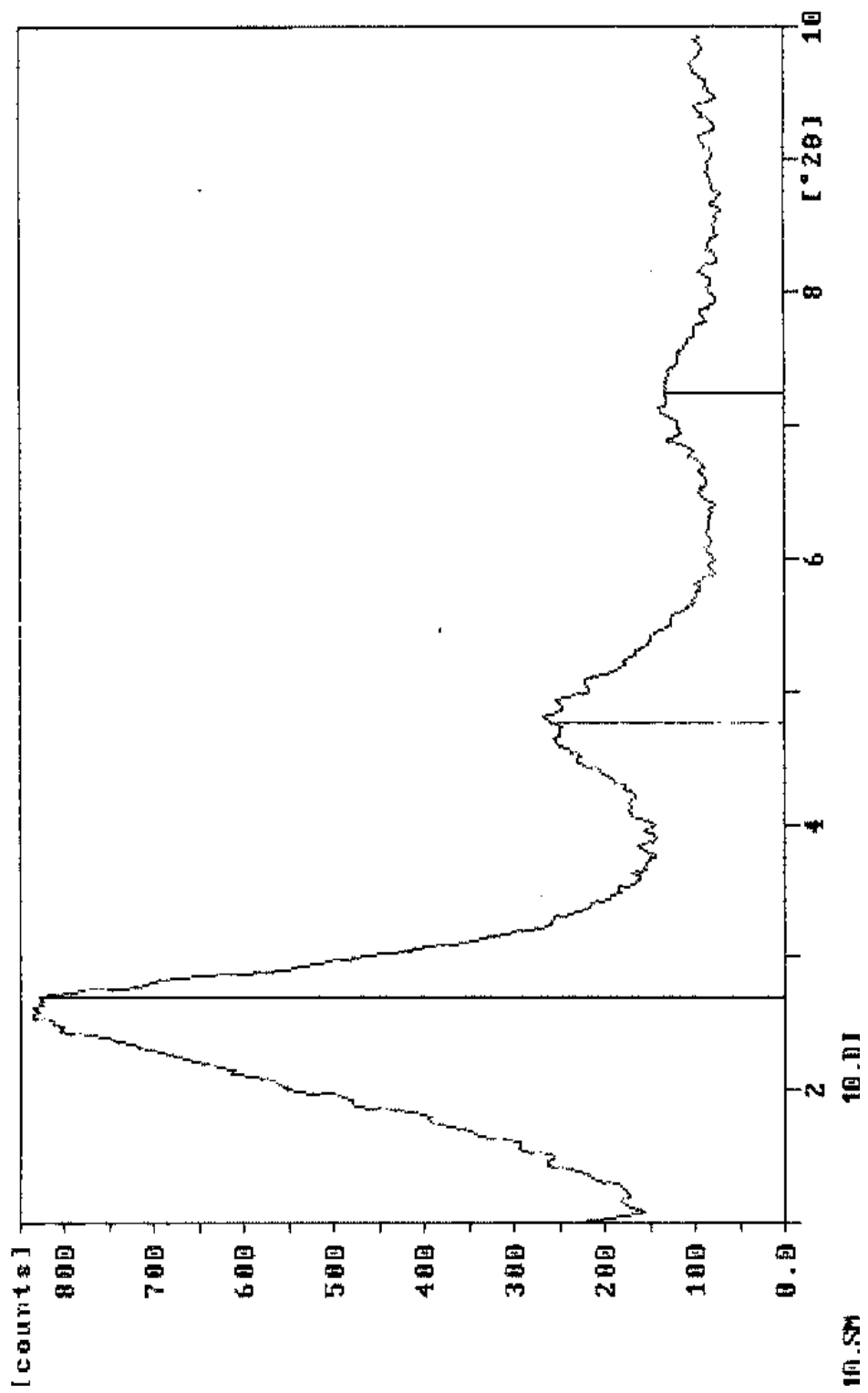
Figure A.1.7 X-ray diffractogram of the sample prepared by in-situ polymerization method containing 2.4 wt. % organoclay.
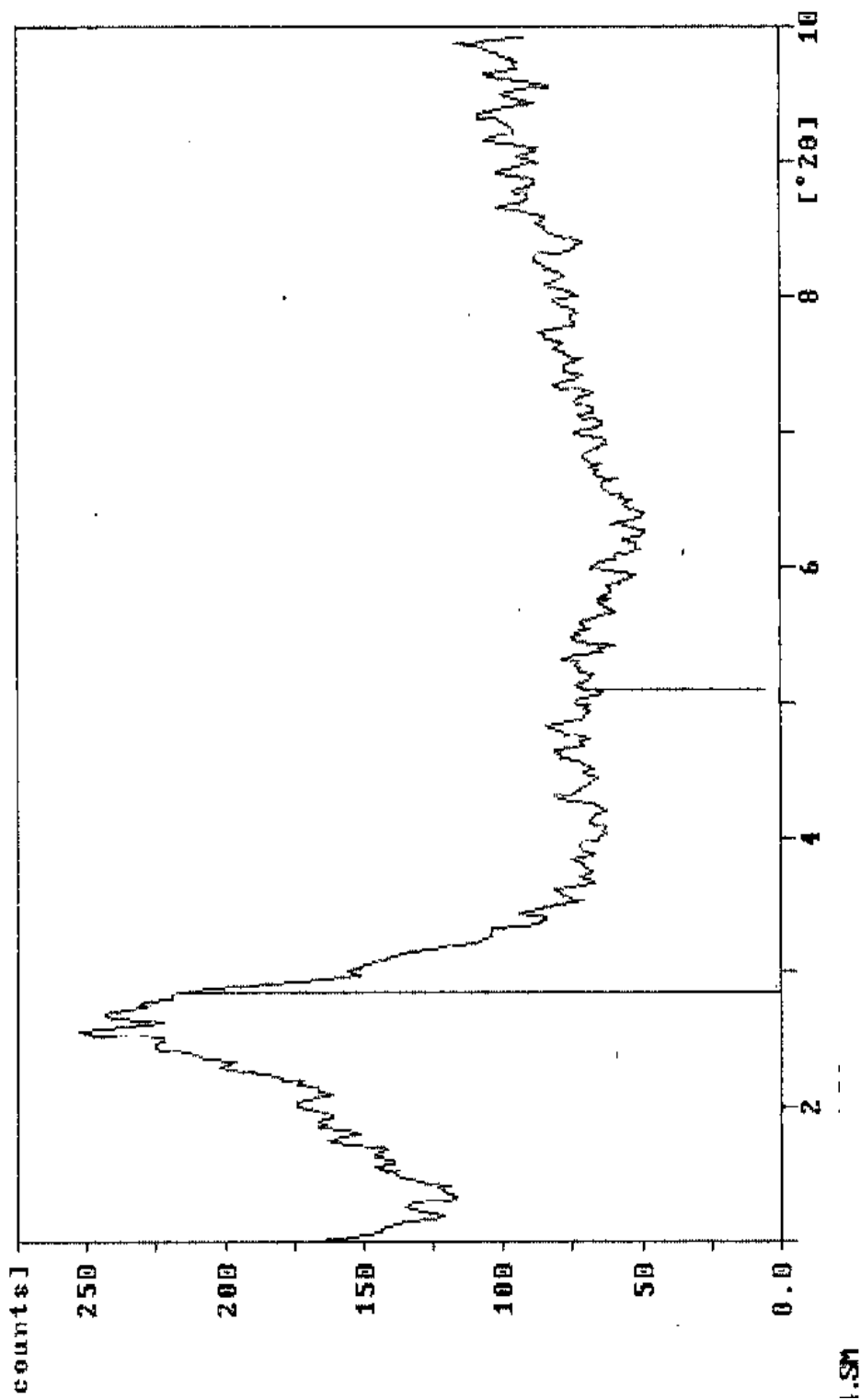
Figure A.1.8 X-ray diffractogram of the sample prepared by in-situ polymerization method containing 3.36 wt. % organoclay.
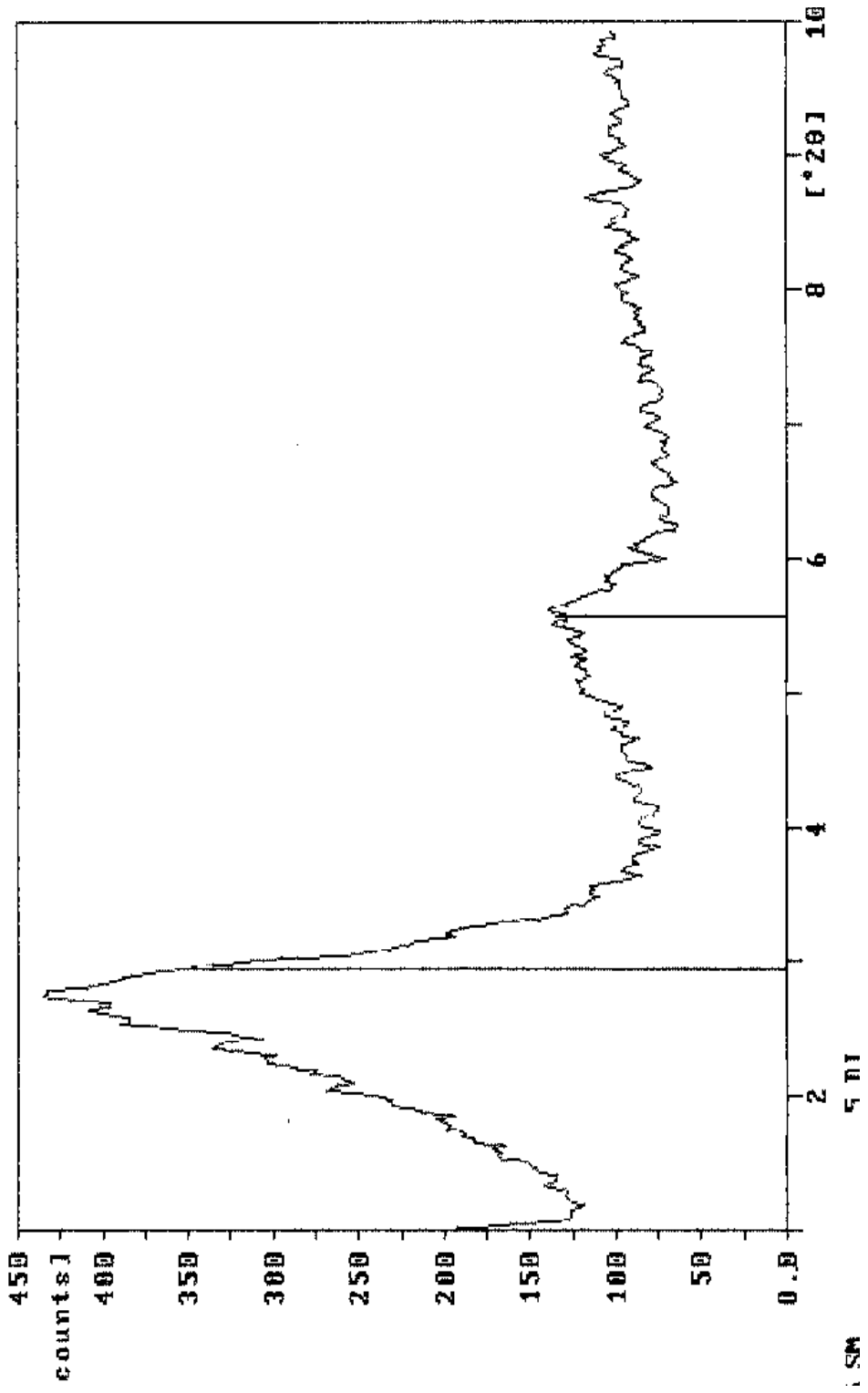
Figure A.1.9 X-ray diffractogram of the sample prepared by masterbatch method containing 0.73 wt. % organoclay.
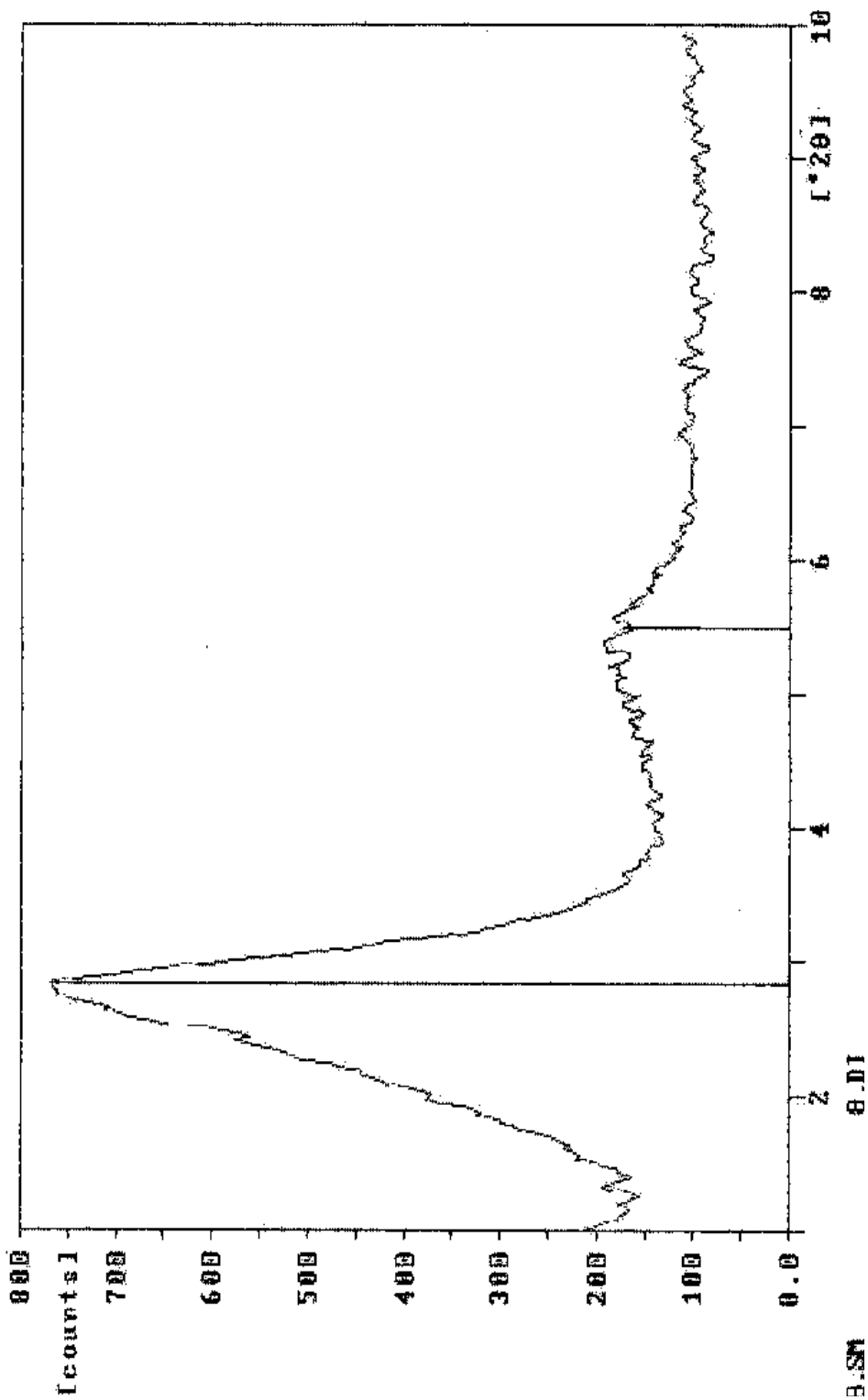
Figure A.1.10 X-ray diffractogram of the sample prepared by masterbatch method containing 1.6 wt. % organoclay.
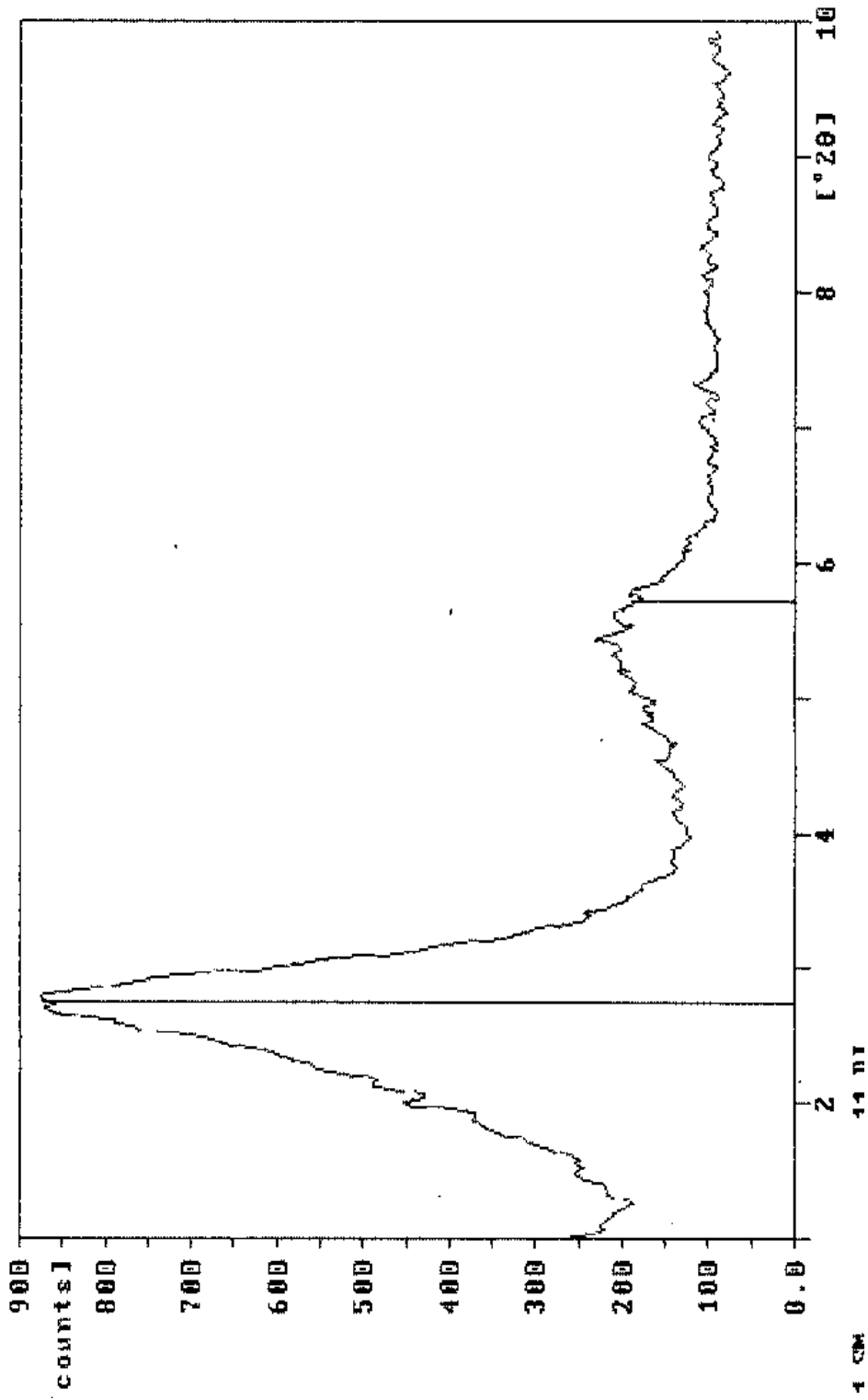
Figure A.1.11 X-ray diffractogram of the sample prepared by masterbatch method containing 2.4 wt. % organoclay.
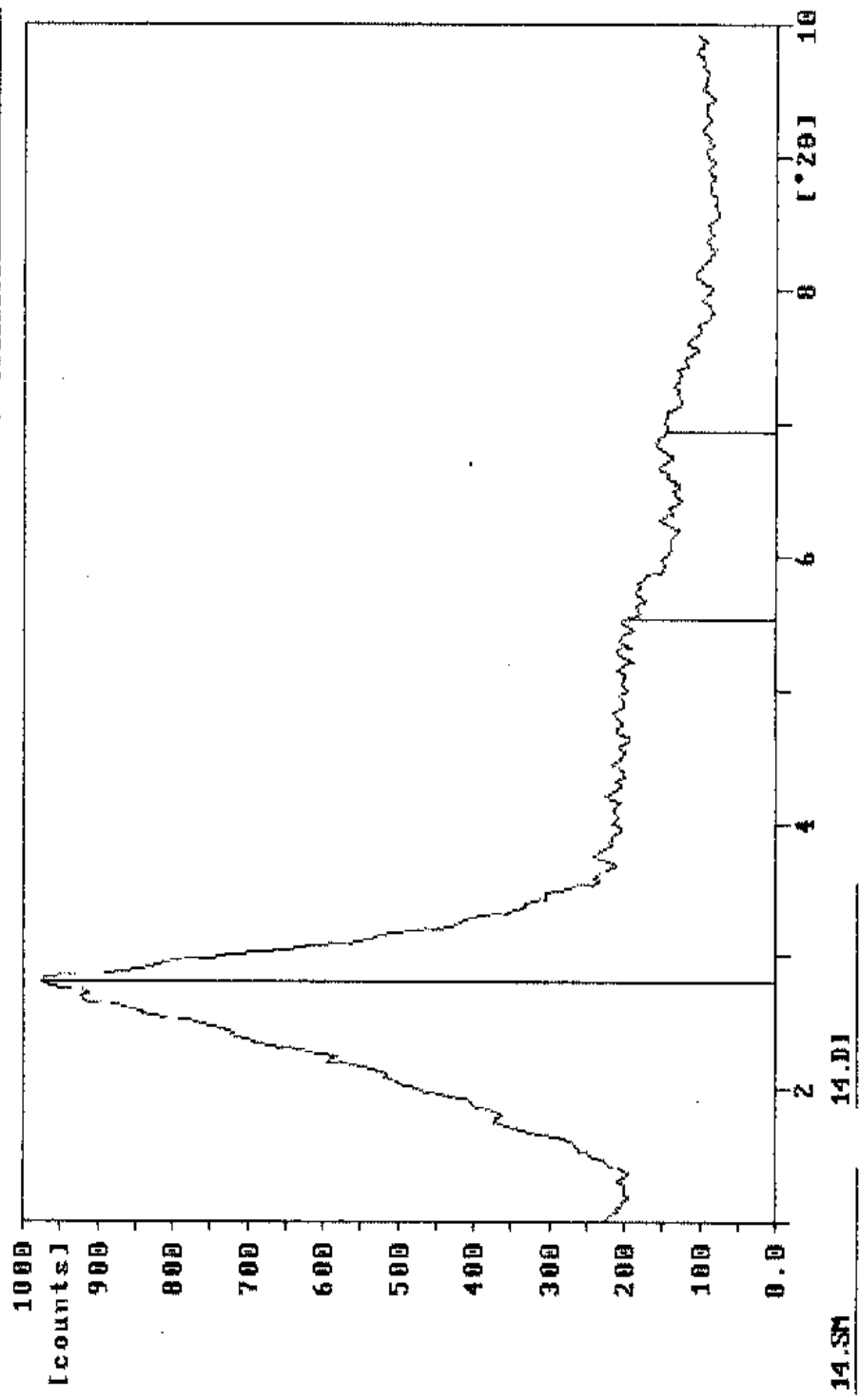
Figure A.1.12 X-ray diffractogram of the sample prepared by masterbatch method containing 3.36 wt. % organoclay.
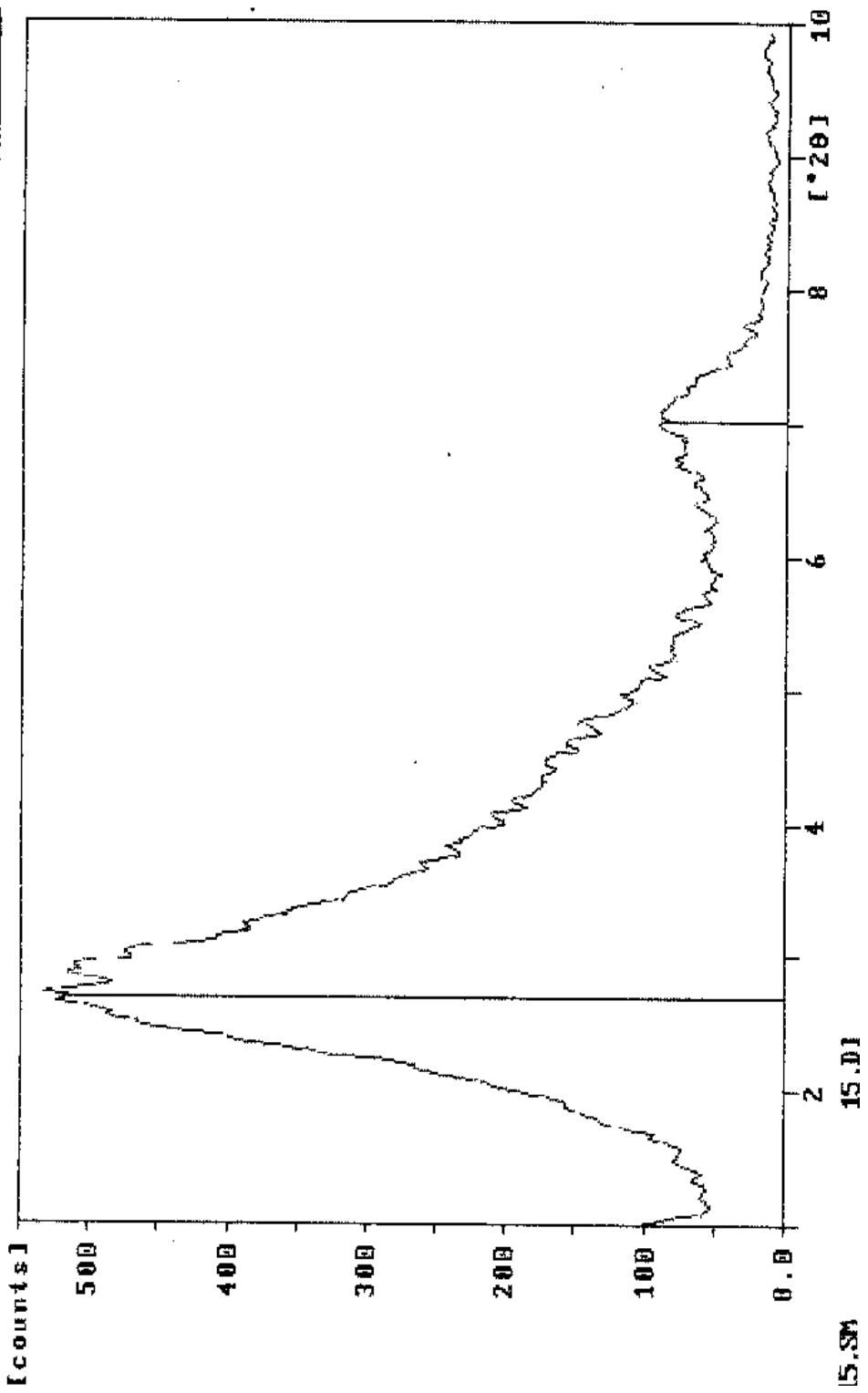
Figure A.1.13 X-ray diffractogram of Cloisite 15A

APPENDIX B

B.1 DIFFERENTIAL SCANNING CALORIMETRY THERMOGRAMS
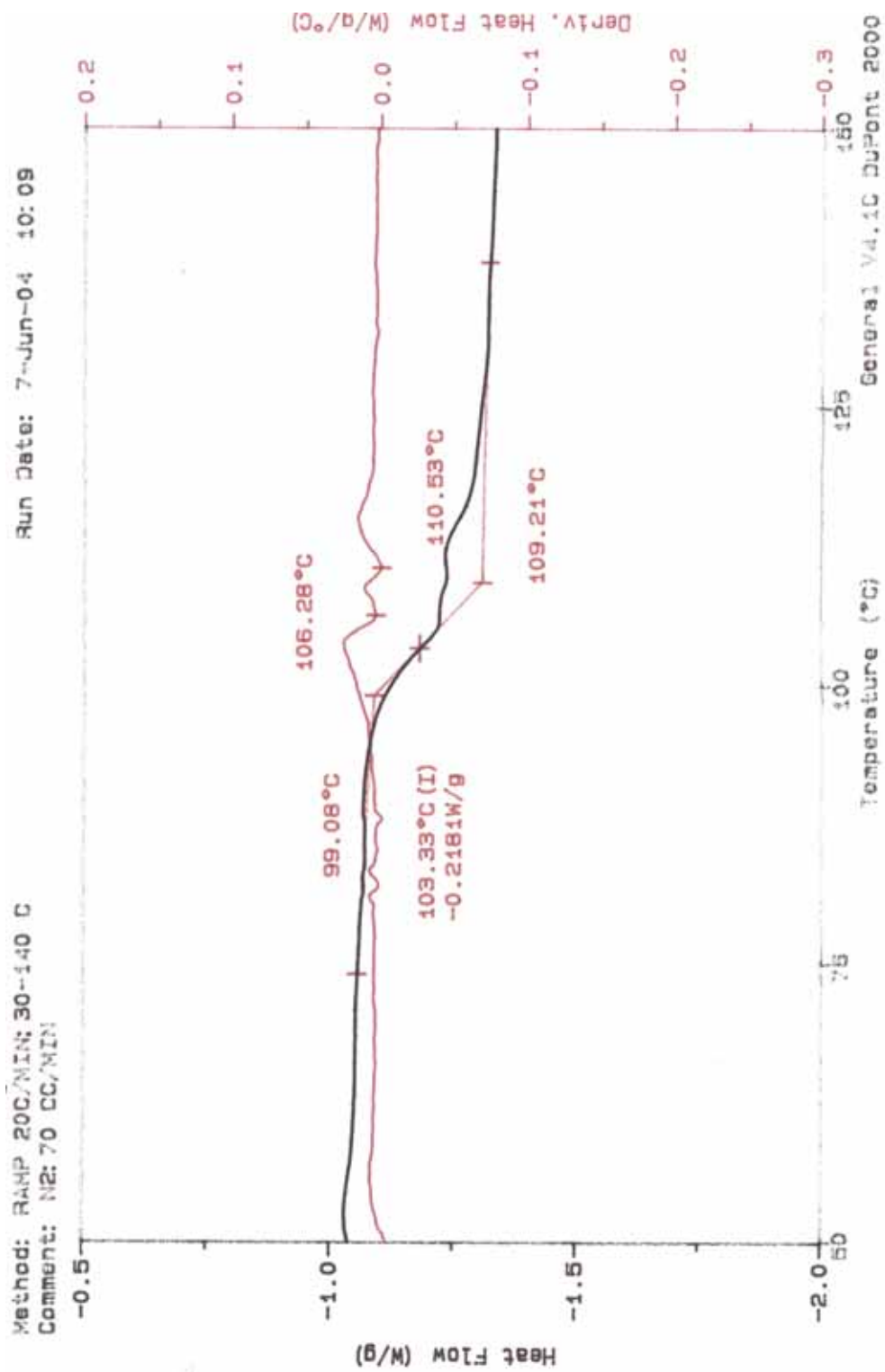
Figure B.1.1 DSC Diagram of commercial polystyrene
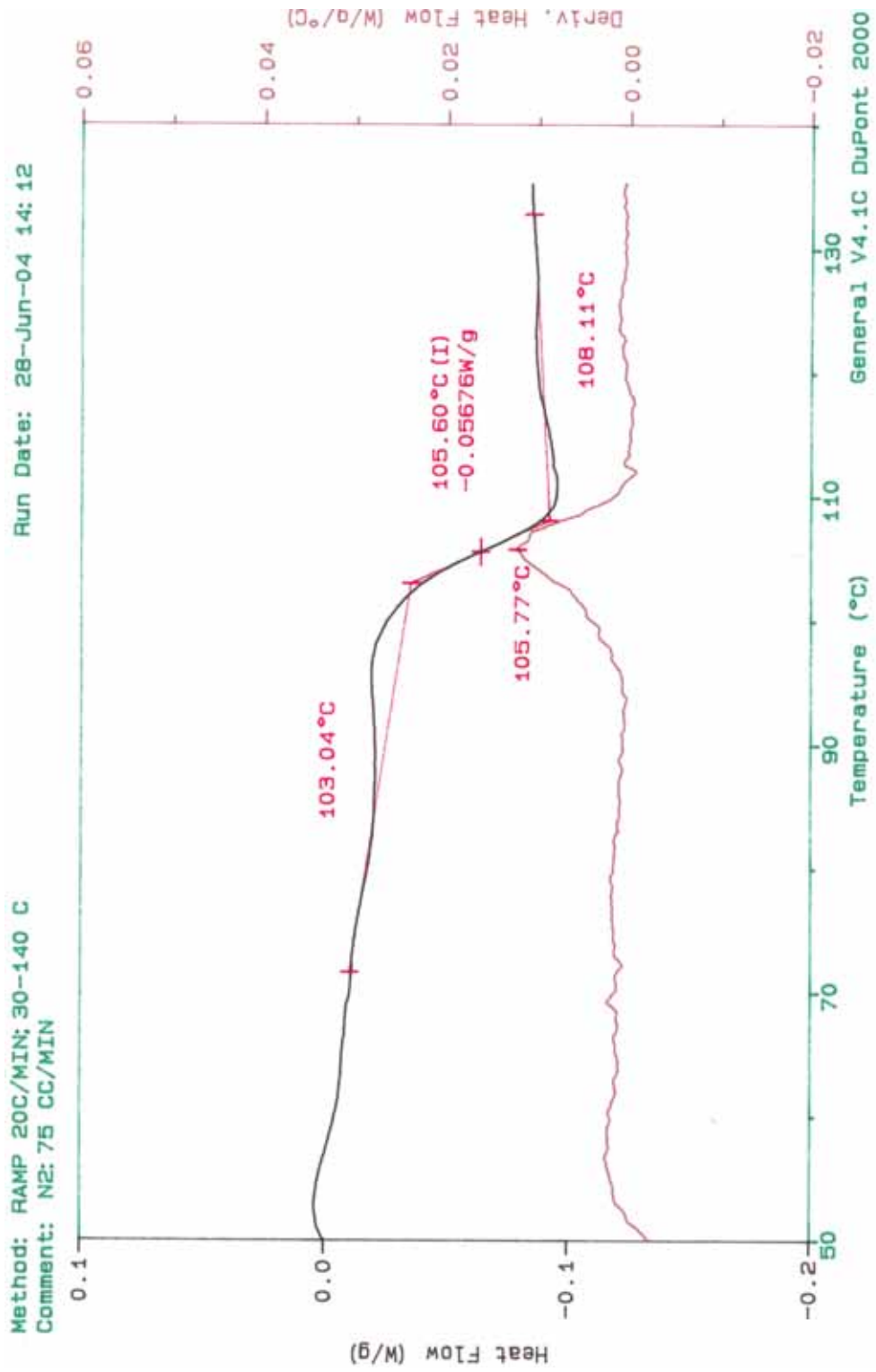
Figure B.1.2 DSC Diagram of synthesized polystyrene
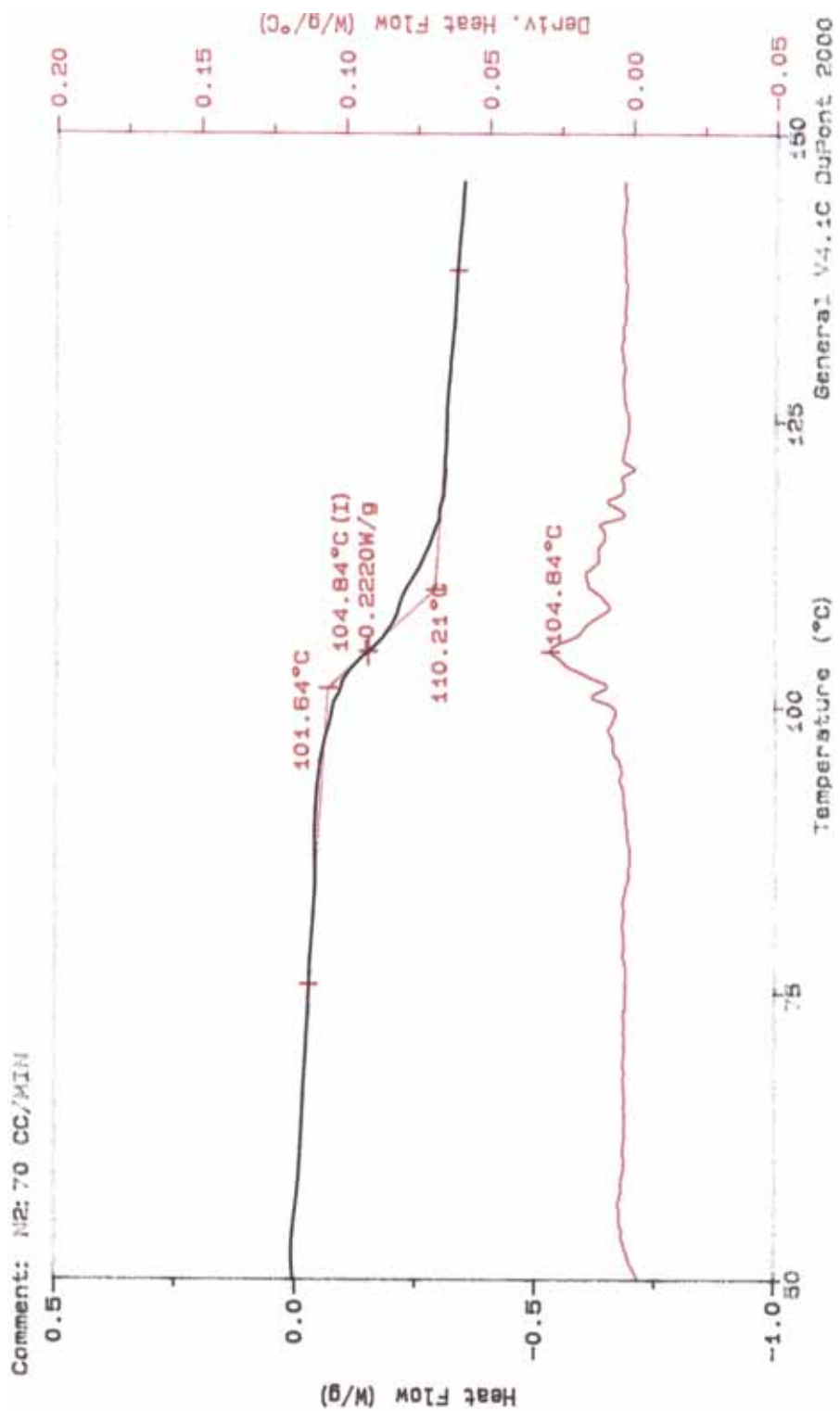
Figure B.1.3 DSC Diagram of nanocomposite prepared by melt intercalation containing 0.73 wt. % MMT
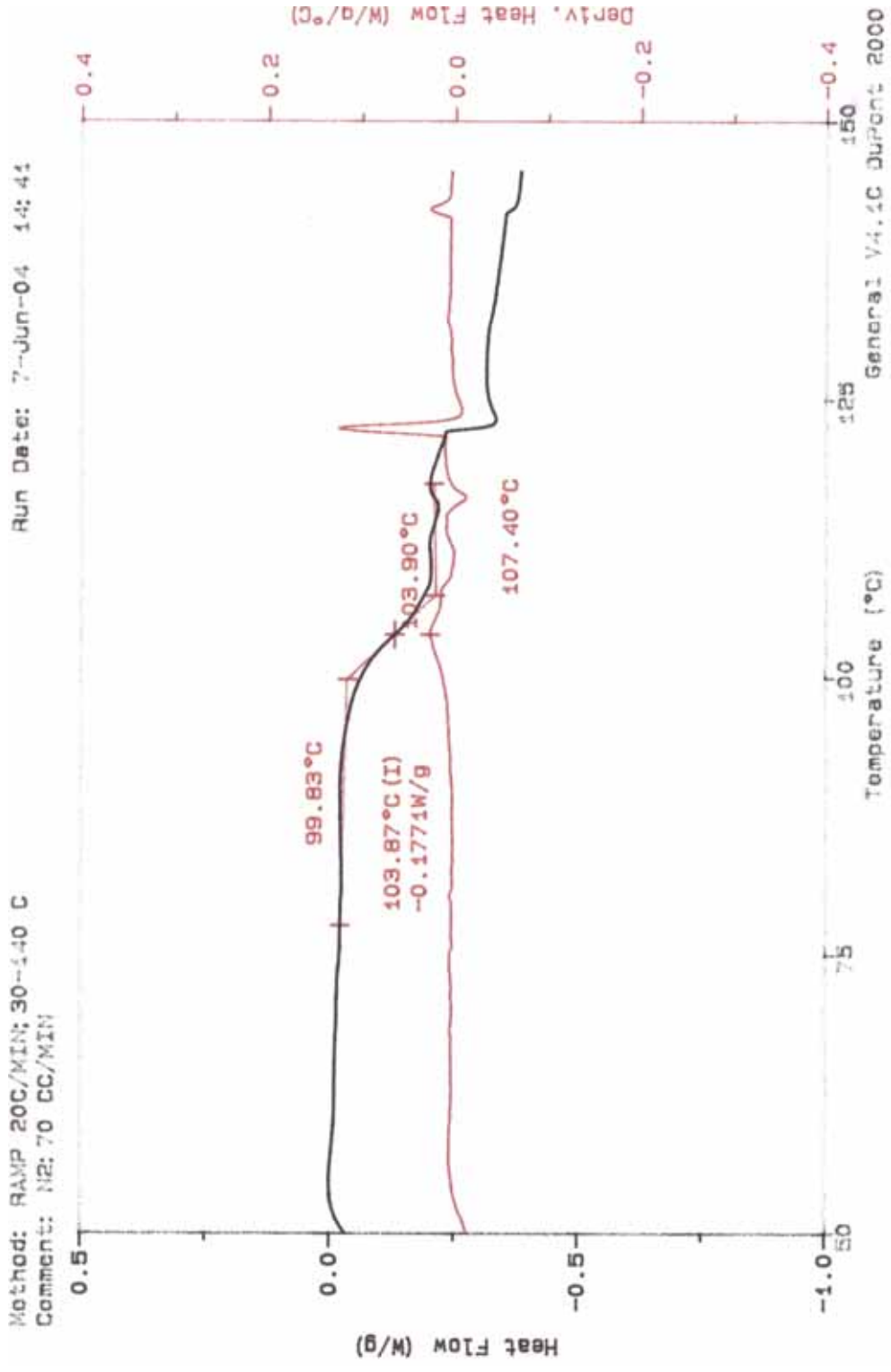
Figure B.1.4 DSC Diagram of nanocomposite prepared by melt intercalation containing 1.6 wt. % MMT
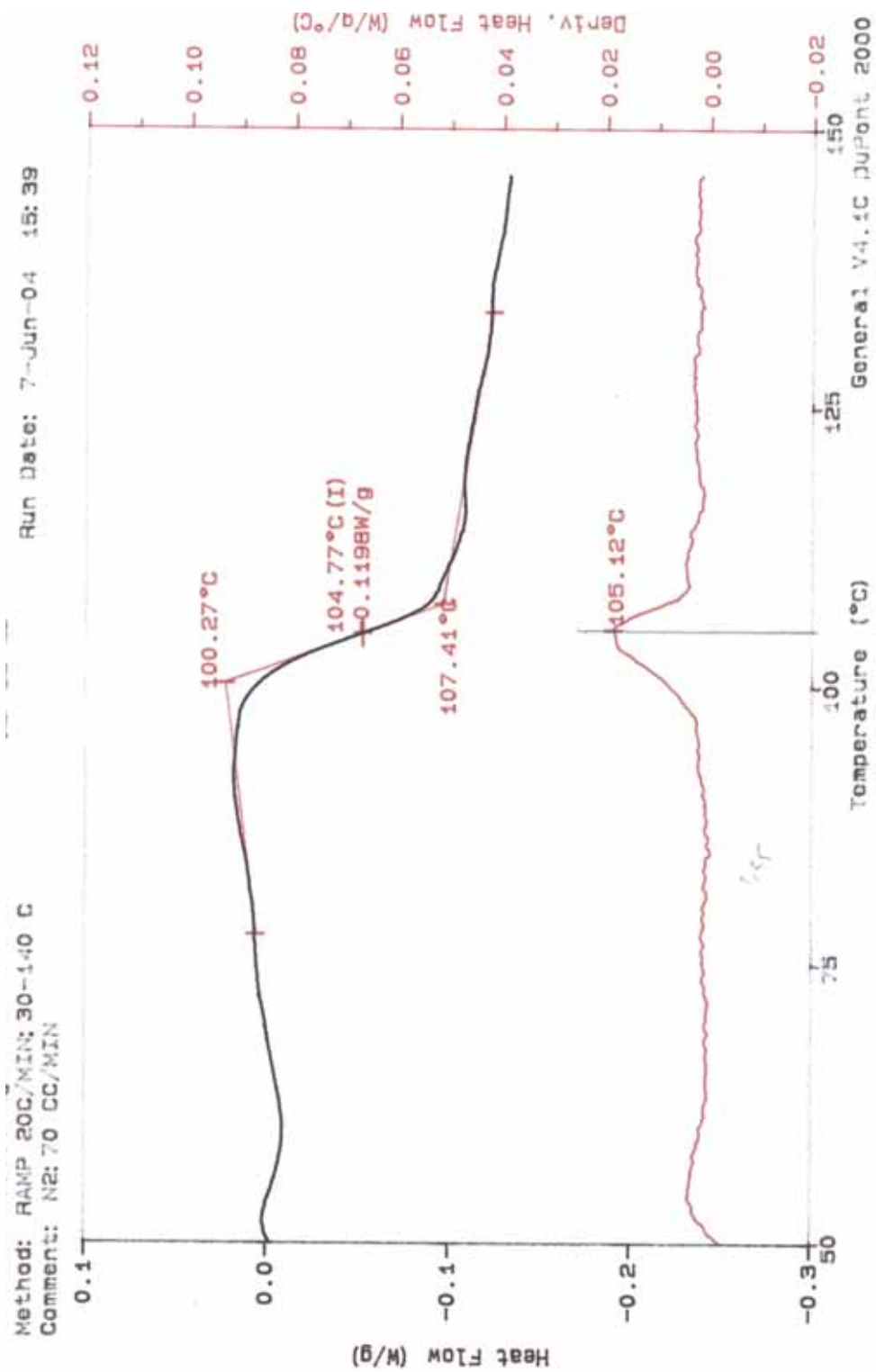
Figure B.1.5 DSC Diagram of nanocomposite prepared by melt intercalation containing 2.4 wt. % MMT

89
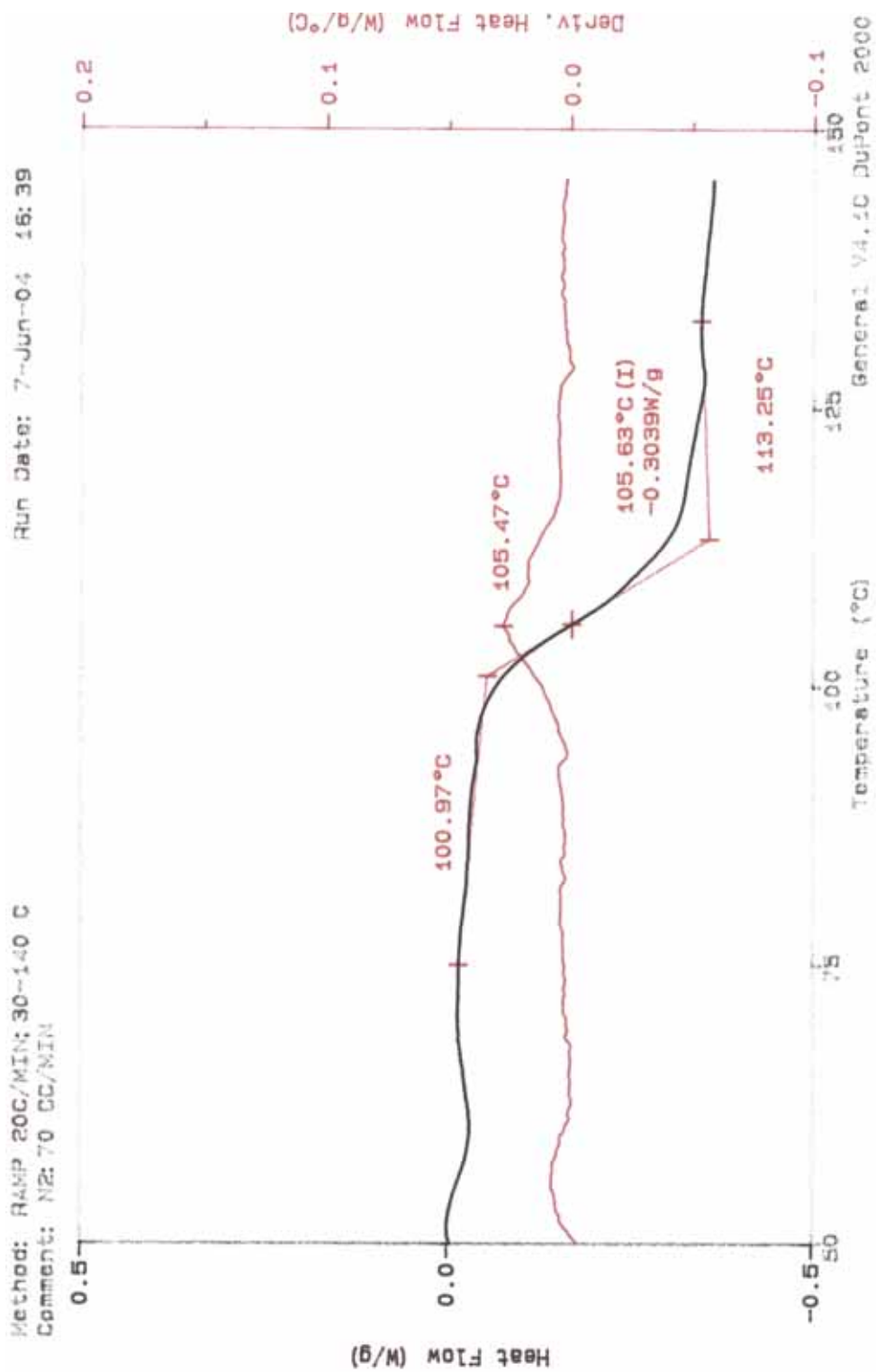
Figure B.1.6 DSC Diagram of nanocomposite prepared by melt intercalation containing 3.36 wt. % MMT
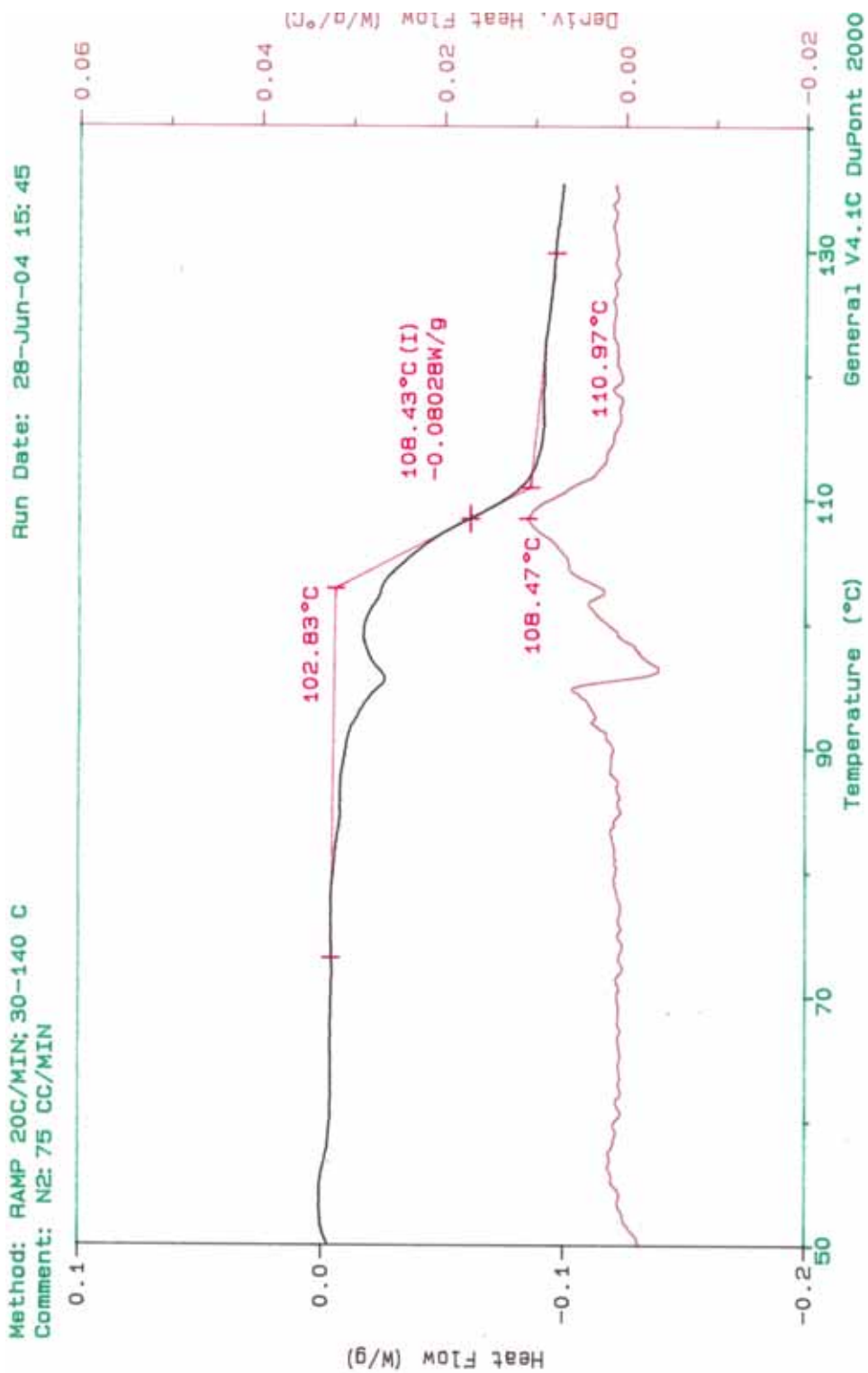
Figure B.1.7 DSC Diagram of nanocomposite prepared by in-situ polymerization containing 0.73 wt. % MMT

T
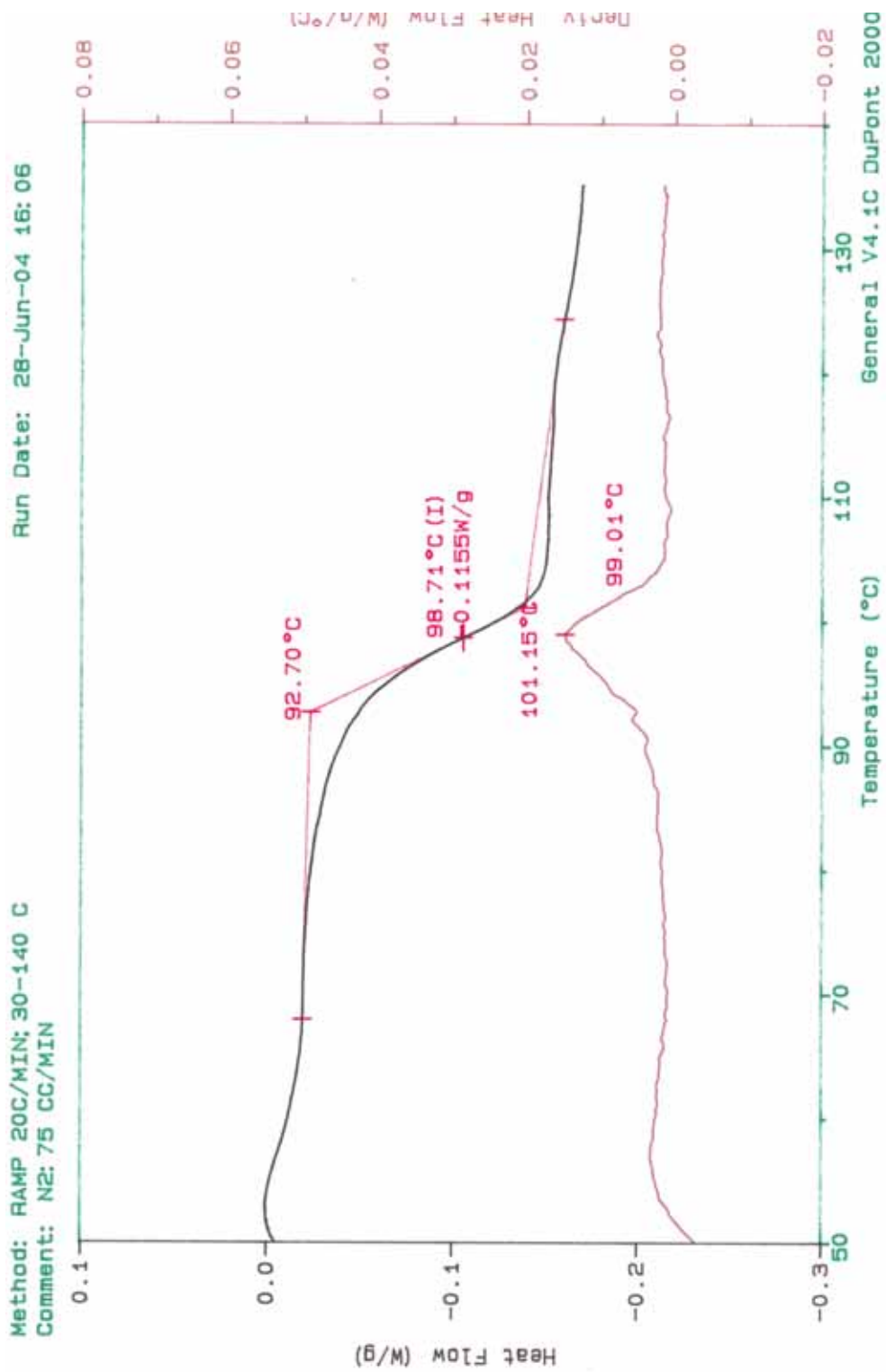
Figure B.1.8 DSC Diagram of nanocomposite prepared by in-situ polymerization containing 1.6 wt. % MMT
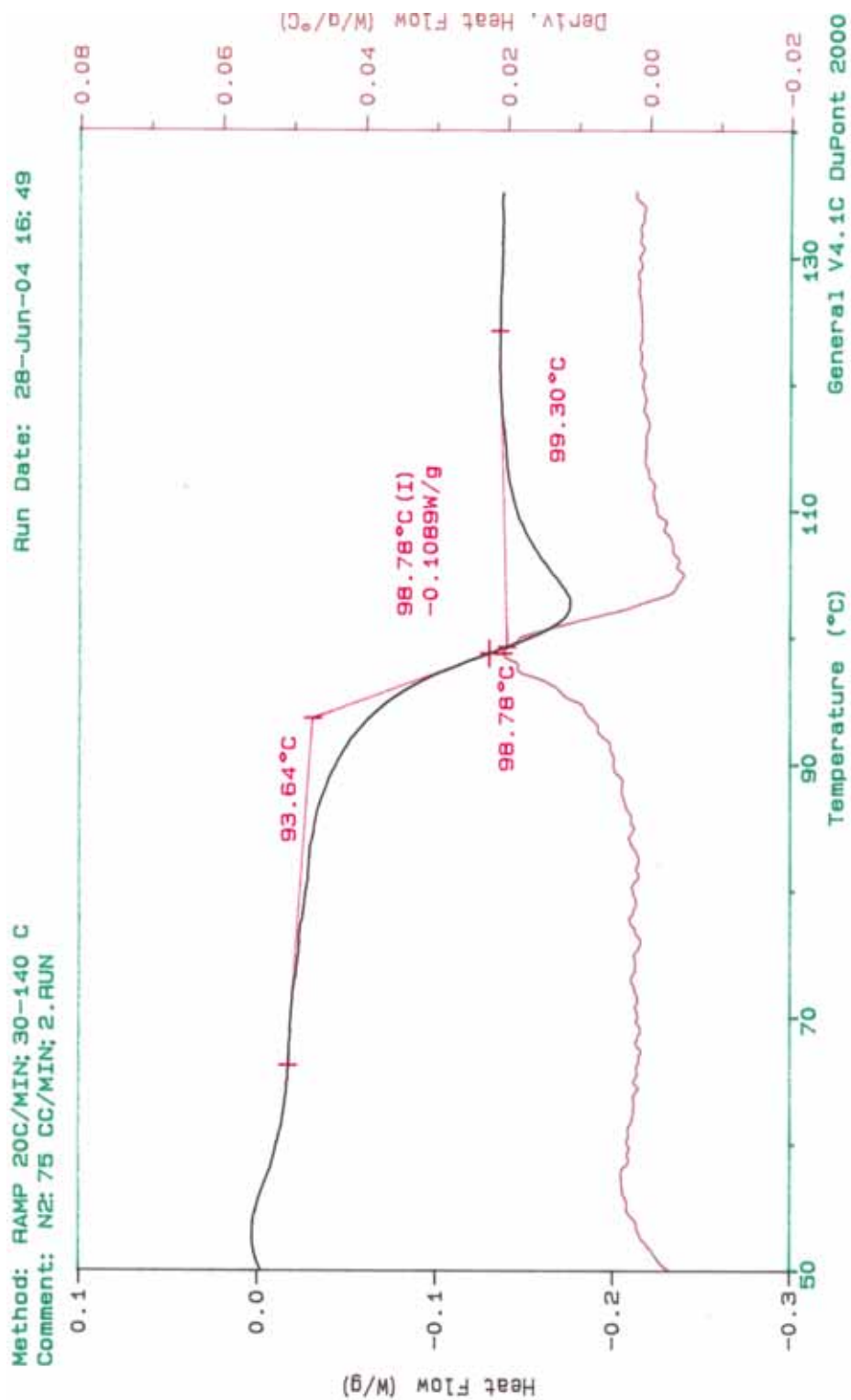
Figure B.1.9 DSC Diagram of nanocomposite prepared by in-situ polymerization containing 1.6 wt. % MMT (2.Run)
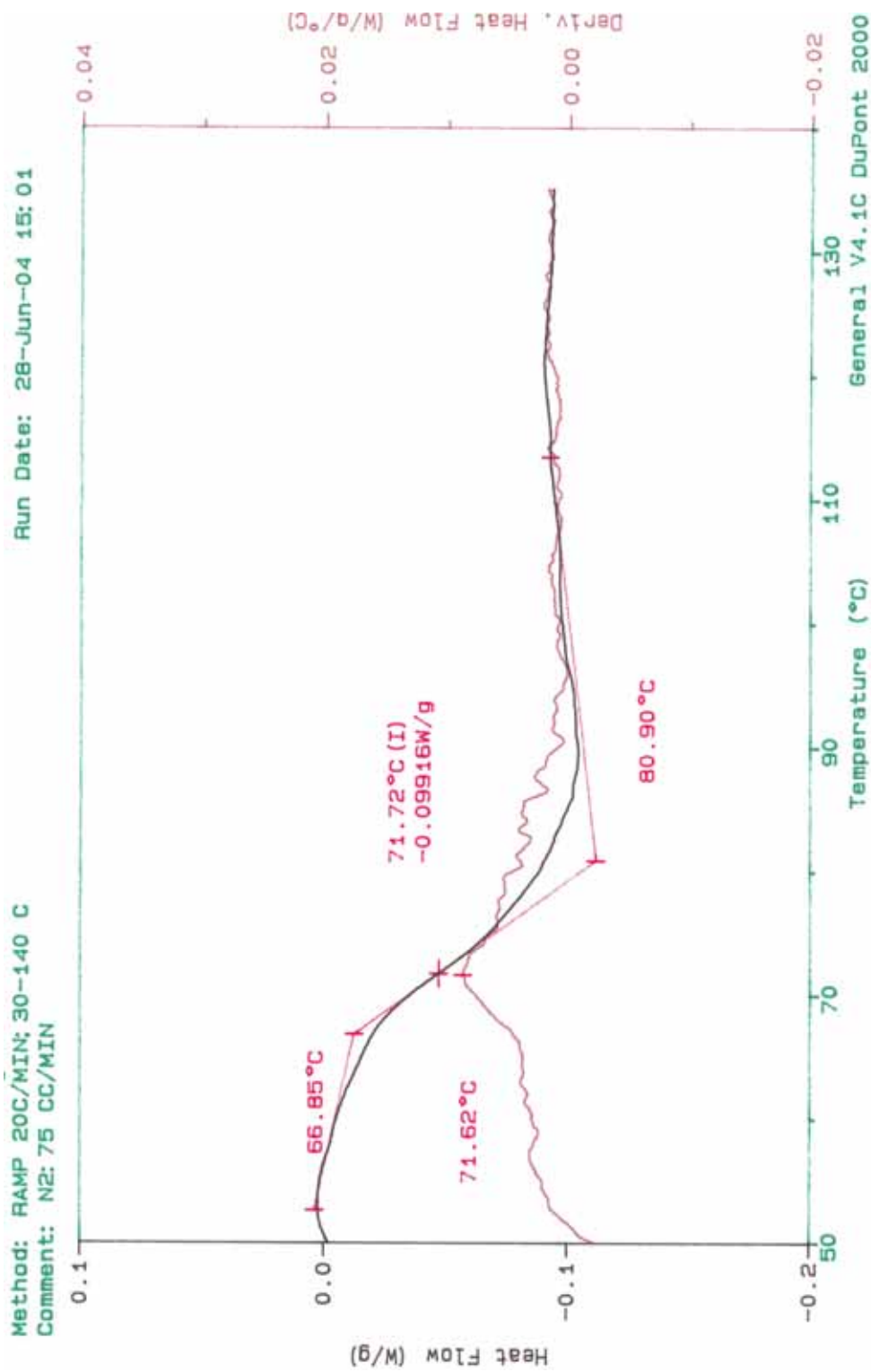
Figure B.1.10 DSC Diagram of nanocomposite prepared by in-situ polymerization containing 2.4 wt. % MMT
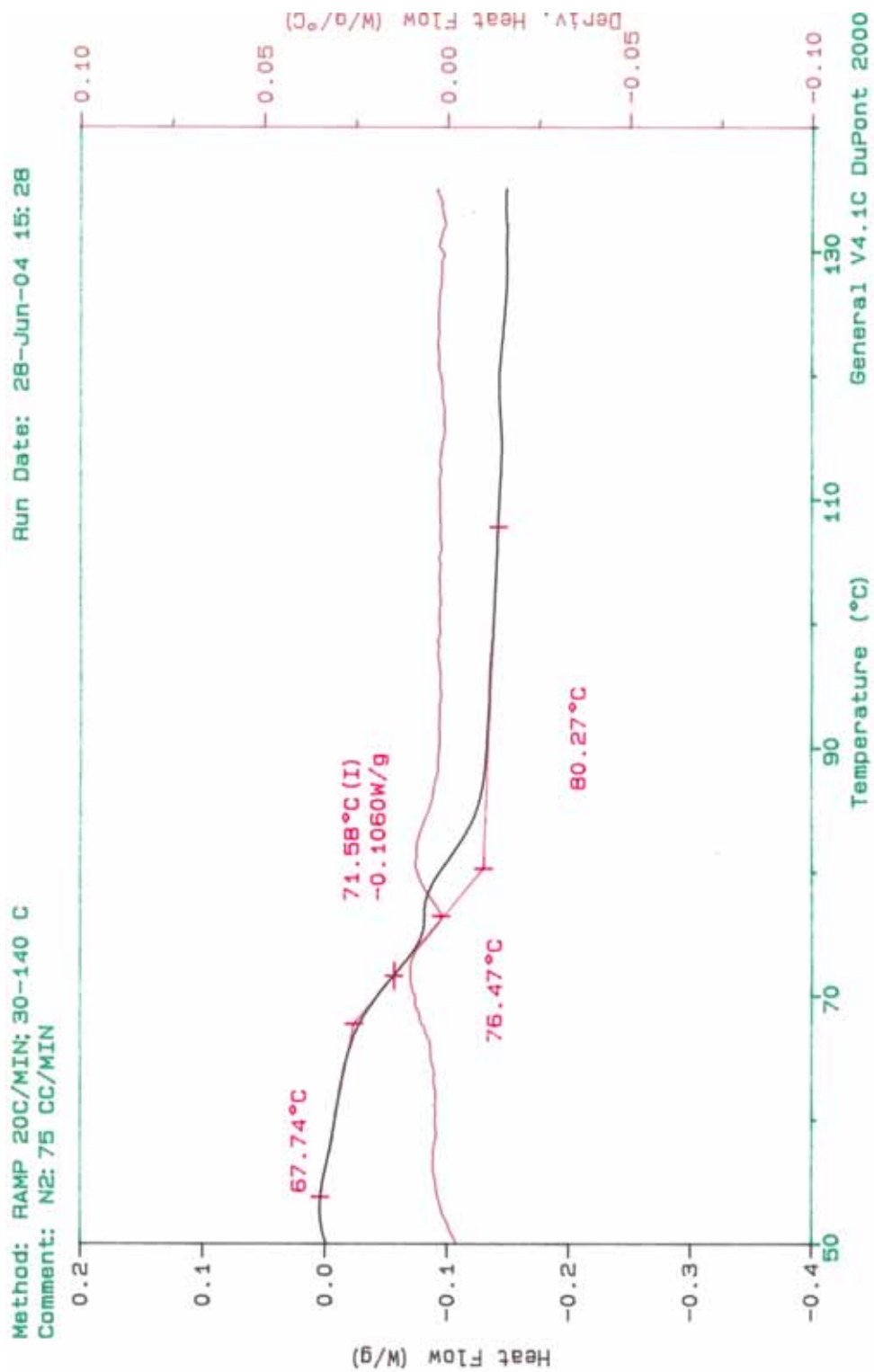
Figure B.1.11 DSC Diagram of nanocomposite prepared by in-situ polymerization containing 3.36 wt. % MMT
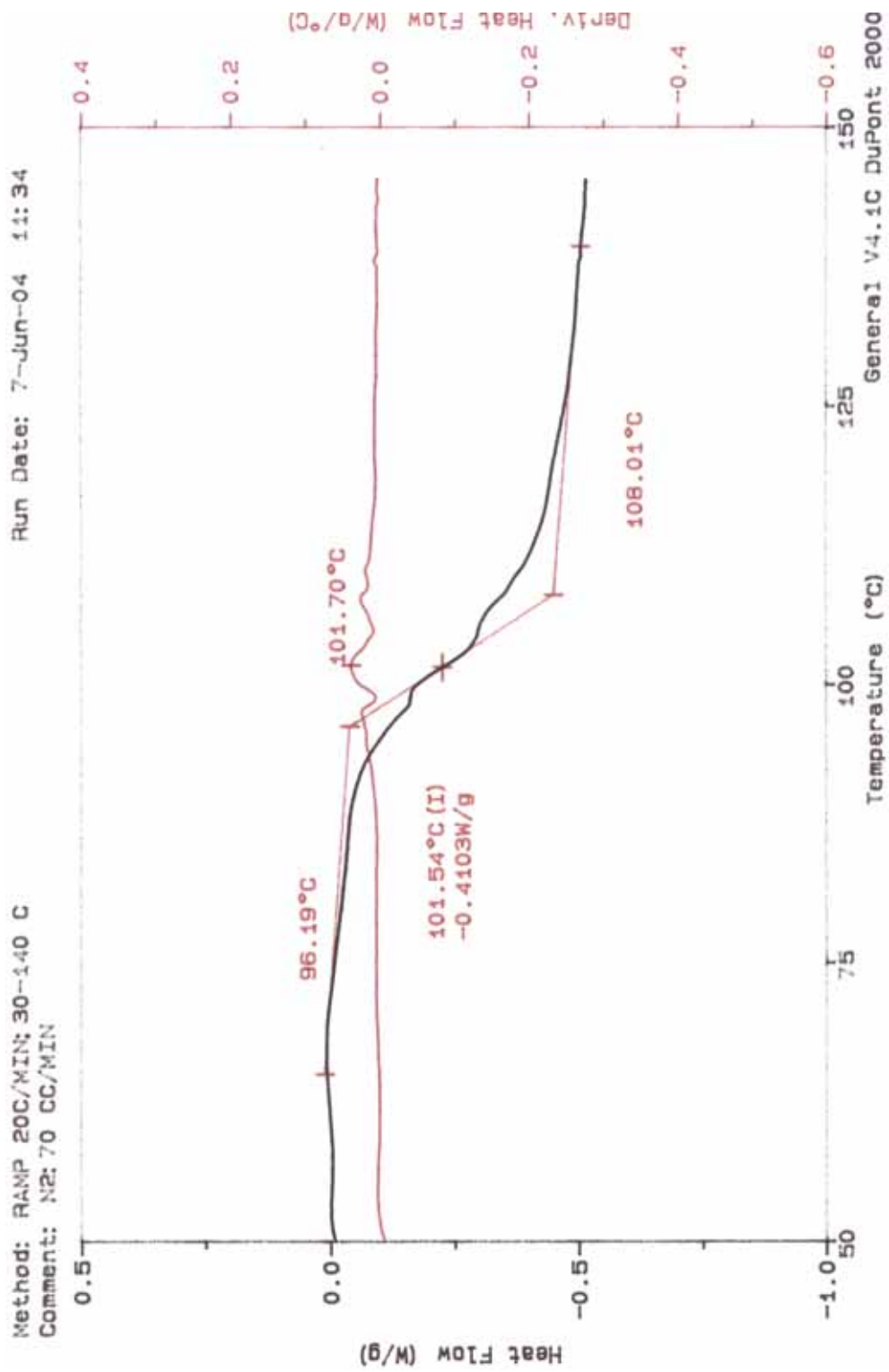
Figure B.1.12 DSC Diagram of nanocomposite prepared by masterbatch containing 0.73 wt. % MMT
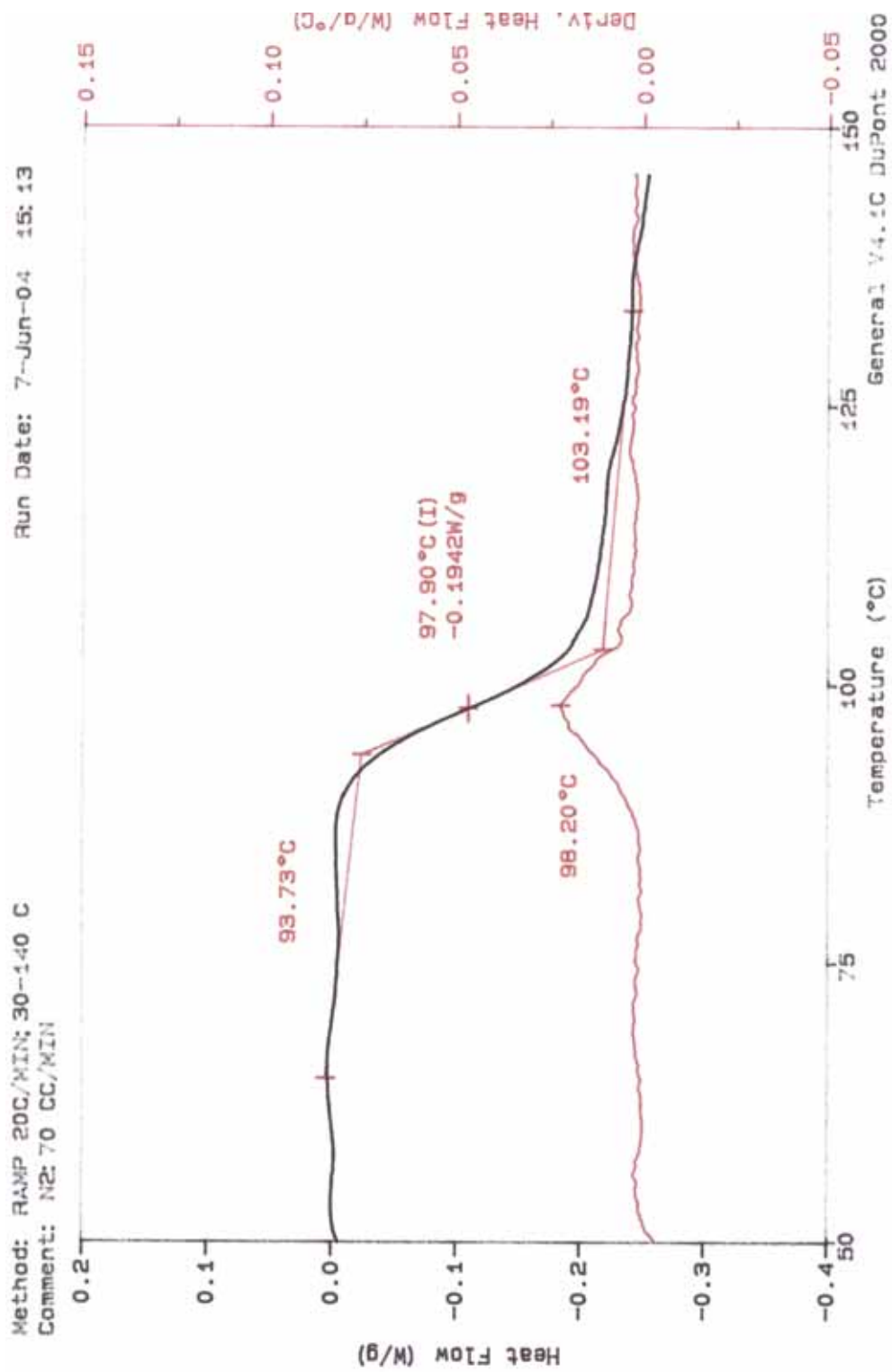
Figure B.1.13 DSC Diagram of nanocomposite prepared by masterbatch containing 1.6 wt. % MMT
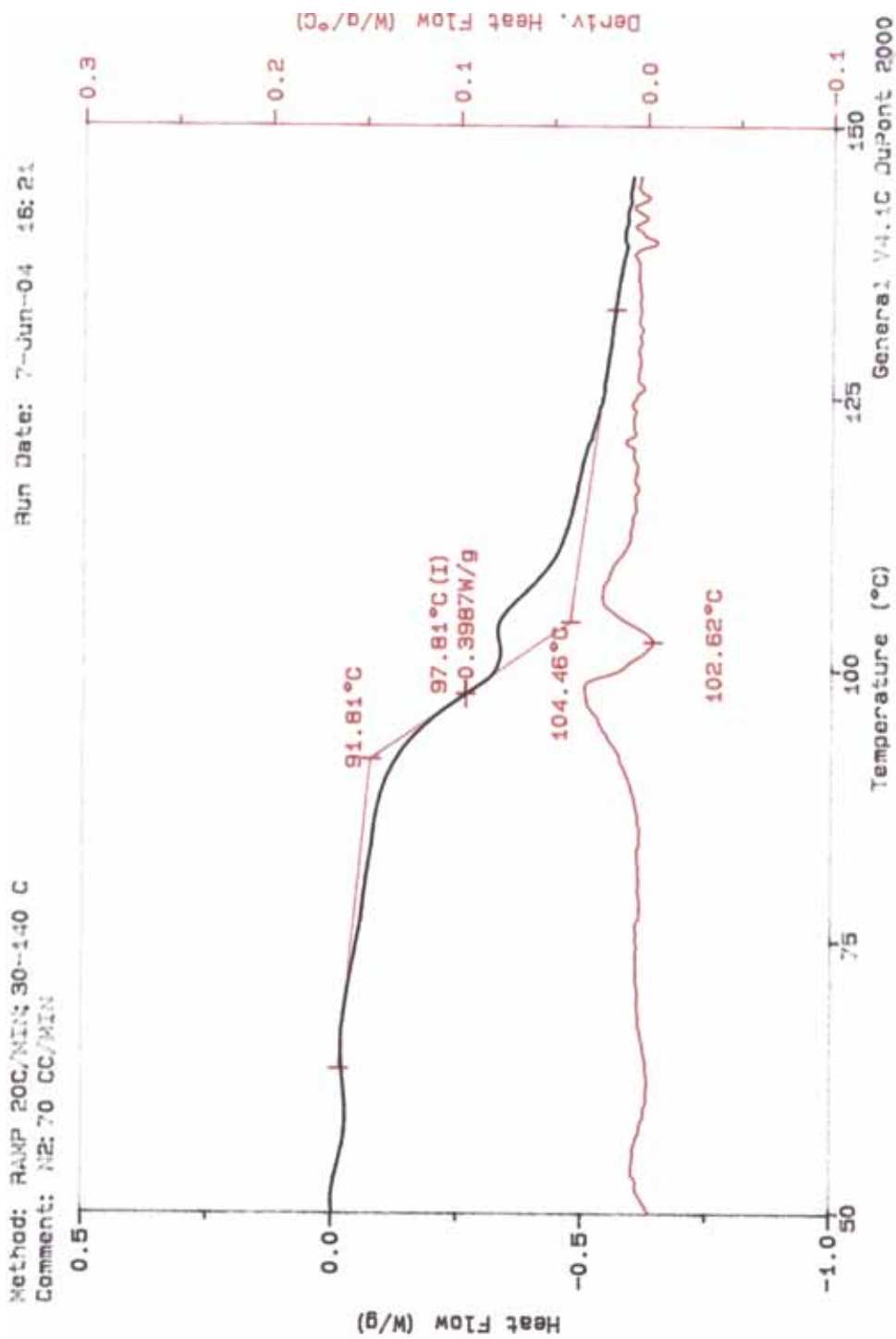
Figure B.1.14 DSC Diagram of nanocomposite prepared by masterbatch containing 2.4 wt. % MMT
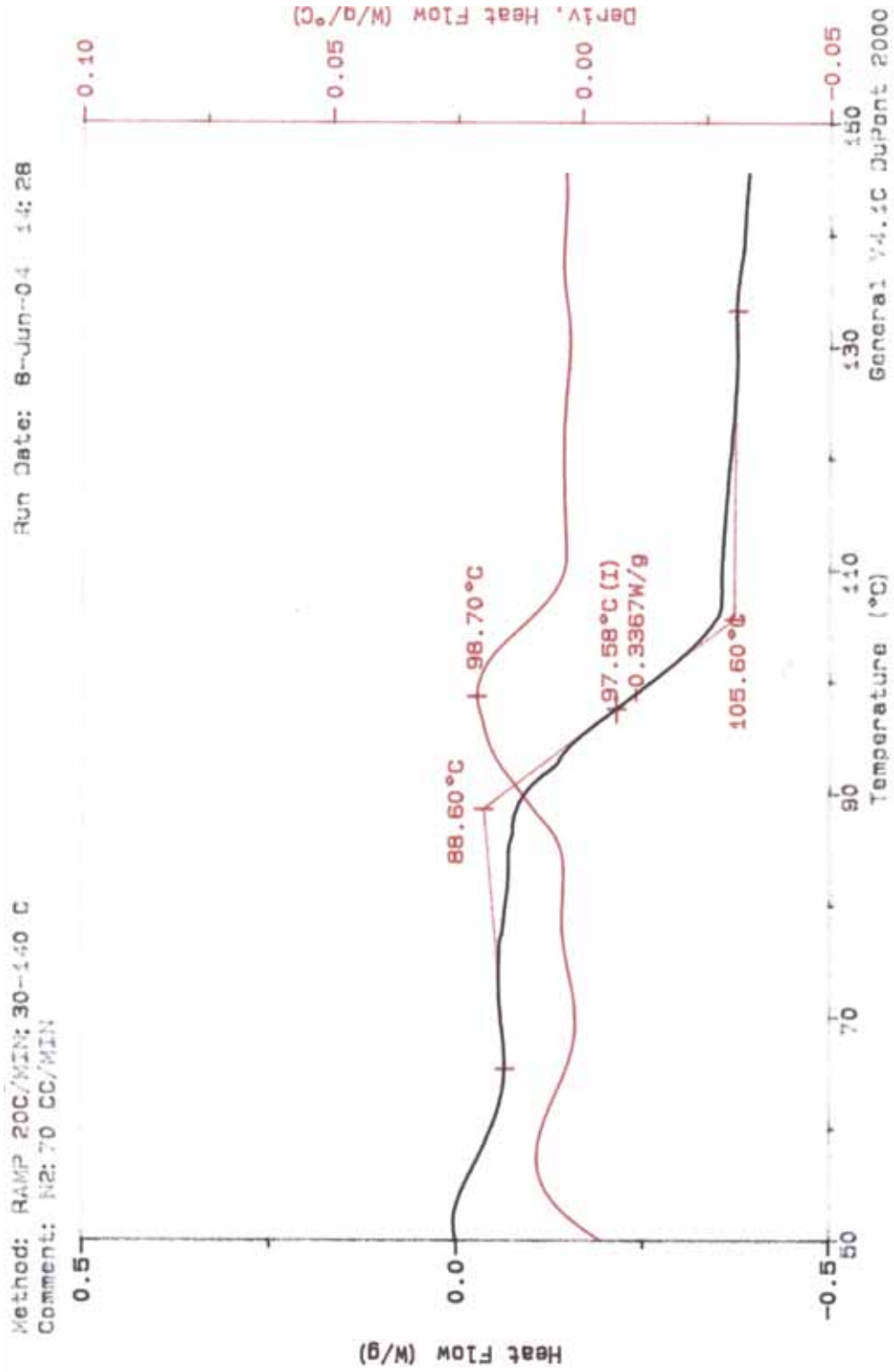
Figure B.1.15 DSC Diagram of nanocomposite prepared by masterbatch containing 3.36 wt. % MMT

99

APPENDIX C

C.1. MECHANICAL TEST DATA

Table C.1.1 Tensile strength data of the samples with respect to the method of preparation and organoclay content.

MMT (wt. %)	AVG. Method 1 MI (MPa)	Standard Deviation	AVG. Method 2 IS (MPa)	Standard Deviation	AVG. Method 3 MB (MPa)	Standard Deviation
0	19.9	0.6	23.9	2.9	19.9	0.6
0.73	23.0	0.9	35.8	1.6	20.8	1.7
1.6	23.0	2.8	29.8	1.3	19.1	1.0
2.4	22.9	1.4	27.6	1.2	21.3	1.7
3.36	22.2	1.2	26.6	0.8	21.5	1.8

Table C.1.2 Tensile modulus data of the samples with respect to the method of preparation and organoclay content.

MMT (wt. %)	AVG. Method 1 MI (MPa)	Standard Deviation	AVG. Method 2 IS (MPa)	Standard Deviation	AVG. Method 3 MB (MPa)	Standard Deviation
0	1424	67	1320	17	1424	67
0.73	1595	73	1991	139	1717	115
1.6	2621	130	2488	128	2607	210
2.4	2501	236	2345	173	2508	104
3.36	2513	155	2439	78	2577	134

Table C.1.3 Tensile Strain (%) data of the samples with respect to the method of preparation and organoclay content.

MMT (wt. %)	AVG. Method 1 MI (%)	Standard Deviation	AVG. Method 2 IS (%)	Standard Deviation	AVG. Method 3 MB (%)	Standard Deviation
0	2	0.1	2.1	0.1	2	0.1
0.73	2.1	0.3	2.8	0.2	2.2	0.1
1.6	1.9	0.2	2.6	0.3	1.6	0.3
2.4	1.7	0.2	1.7	0.1	1.1	0.1
3.36	1.6	0.2	1.7	0.1	1.2	0.1

Table C.1.4 Flexural strength data of the samples with respect to the method of preparation and organoclay content.

MMT (wt. %)	AVG. Method 1 MI (MPa)	Standard Deviation	AVG. Method 2 IS (MPa)	Standard Deviation	AVG. Method 3 MB (MPa)	Standard Deviation
0	40.4	2.7	44.7	2.1	40.4	2.7
0.73	47.3	1.4	76.1	2.5	46.6	2.8
1.6	41.4	0.2	66.1	1.1	46.3	1.6
2.4	48.1	1.2	50.7	1.3	45.1	2.7
3.36	35.0	1.8	48.8	0.8	38.2	2.1

Table C.1.5 Flexural modulus data of the samples with respect to the method of preparation and organoclay content.

MMT (wt. %)	AVG. Method 1 MI (MPa)	Standard Deviation	AVG. Method 2 IS (MPa)	Standard Deviation	AVG. Method 3 MB (MPa)	Standard Deviation
0	2800	41	2703	46	2800	41
0.73	3242	55	3176	80	3123	63
1.6	3205	11	3125	26	3184	7
2.4	3060	51	2763	54	3052	51
3.36	3129	17	2606	60	3130	94

Table C.1.6 Flexural Strain (%) data of the samples with respect to the method of preparation and organoclay content.

MMT (wt. %)	AVG. Method 1 MI (%)	Standard Deviation	AVG. Method 2 IS (%)	Standard Deviation	AVG. Method 3 MB (%)	Standard Deviation
0	1.5	0.1	2.1	0.05	1.5	0.1
0.73	1.9	0.3	3.1	0.2	1.7	0.1
1.6	1.6	0.05	2.7	0.2	1.7	0.05
2.4	1.9	0.05	2.8	0.1	1.8	0.05
3.36	1.3	0.05	2.3	0.05	1.4	0.1

Table C.1.8 Impact strength data of the samples with respect to the method of preparation and organoclay content

MMT (wt. %)	Method 1 MI (kj/m^2)	Standard Deviation	Method 2 IS (kj/m^2)	Standard Deviation	Method 3 MB (kj/m^2)	Standard Deviation
0	6.3	0.4	6.2	0.6	6.3	0.4
0.73	6.2	0.3	7.9	0.6	7.6	0.6
1.6	6.2	0.4	6.3	0.3	5.5	0.2
2.4	5.6	0.2	5.8	0.3	5.3	0.1
3.36	5.5	0.3	5.1	0.2	4.7	0.1

D.1 MOLECULAR WEIGHT DISTRIBUTION CURVES
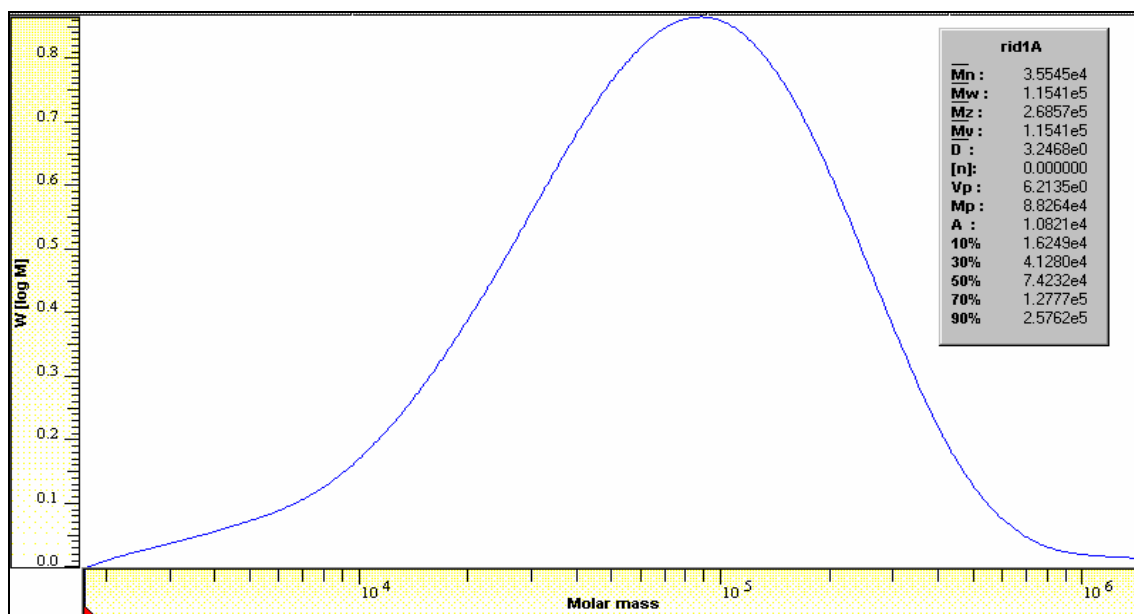
D.1.1 Molecular weight distribution curve of commercial polystyrene
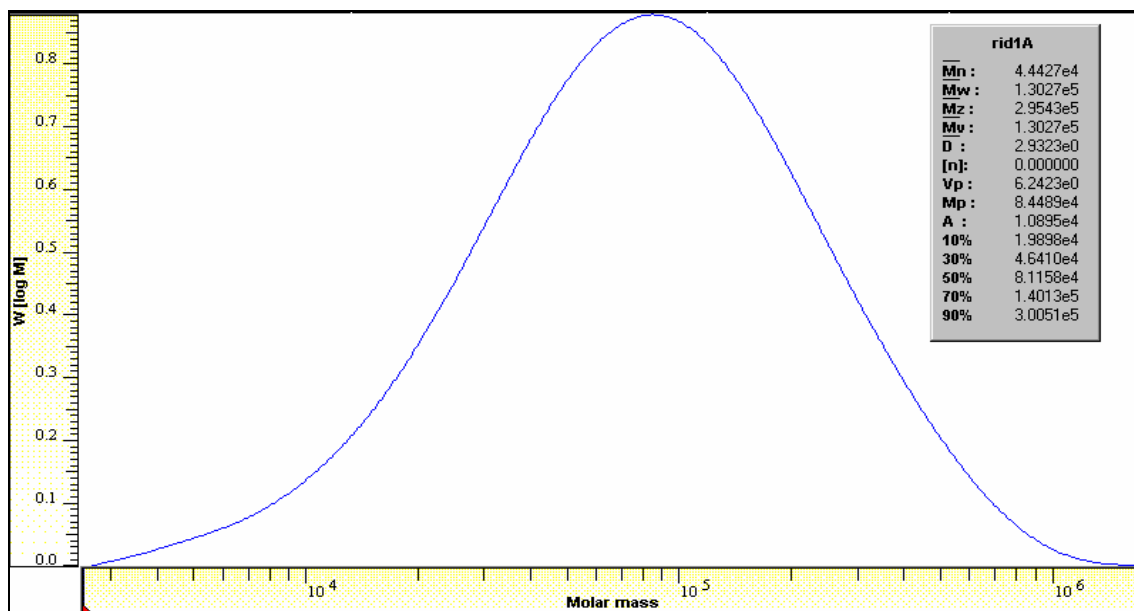
D.1.2 Molecular weight distribution curve of synthesized polystyrene